AD-A064 972 SRI INTERNATIONAL MENLO PARK CA F/G 4/2
TRACKING AND MONITORING HURRICANES BY HF SKYWAVE RADAR OVER THE--ETC(U)
NOV 78 J W MARESCA, C T CARLSON F49620-76-C-0023
UNCLASSIFIED AFOSR-TR-79-0042 NL

1 OF 2
AD
A064972

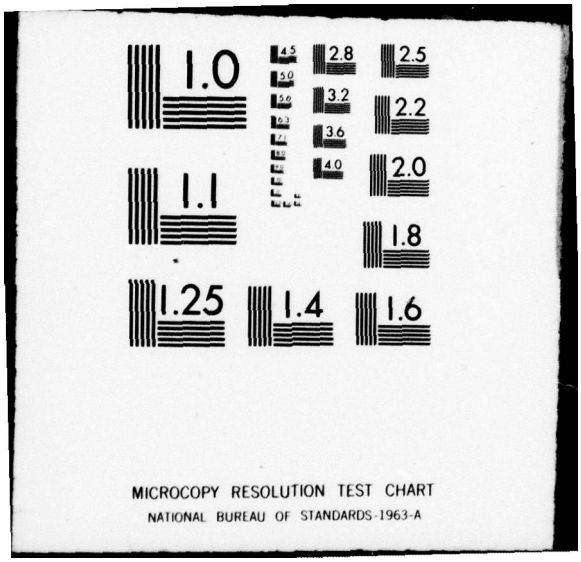
1.0
1.1
1.25
1.4
1.6
1.8
2.0
2.2
2.5
2.8
3.2
3.6
4.0
4.5
5.0
5.6
MICROCOPY RESOLUTION TEST CHART
NATIONAL BUREAU OF STANDARDS-1963-A

AFOSR-TR- 79-0042



*Final Report*

LEVEL II



*November 1978*

12

# TRACKING AND MONITORING HURRICANES BY HF SKYWAVE RADAR OVER THE GULF OF MEXICO

*By:* J. W. MARESCA, JR. C. T. CARLSON

*Prepared for:*

AIR FORCE OFFICE OF SCIENTIFIC RESEARCH
BOLLING AIR FORCE BASE
WASHINGTON, D.C. 20332

CONTRACT F49620-76-C-0023

Approved for public release; distribution unlimited.





333 Ravenswood Avenue
Menlo Park, California 94025 U.S.A.
(415) 326-6200
Cable: SRI INTL MNP
TWX: 910-373-1246

SRI International

UNCLASSIFIED

SECURITY CLASSIFICATION OF THIS PAGE (When Data Entered)

# REPORT DOCUMENTATION PAGE

READ INSTRUCTIONS BEFORE COMPLETING FORM

1. REPORT NUMBER: AFOSR-TR-79-0042
2. GOVT ACCESSION NO.
3. RECIPIENT'S CATALOG NUMBER

4. TITLE (and Subtitle): TRACKING AND MONITORING HURRICANES BY HF SKYWAVE RADAR OVER THE GULF OF MEXICO.

5. TYPE OF REPORT & PERIOD COVERED: Final Report. 14 July 1976 - 30 November 1978

6. PERFORMING ORG. REPORT NUMBER: SRI Project 5630

7. AUTHOR(s): Joseph W. Maresca, Jr. Christopher T. Carlson

8. CONTRACT OR GRANT NUMBER(s): F49620-76-C-0023

9. PERFORMING ORGANIZATION NAME AND ADDRESS
SRI International
333 Ravenswood Avenue
Menlo Park, California 94025

10. PROGRAM ELEMENT, PROJECT, TASK AREA & WORK UNIT NUMBERS
61102F
2310 A1
A1

11. CONTROLLING OFFICE NAME AND ADDRESS
Air Force Office of Scientific Research/NC
Bolling Air Force Base
Washington, D. C. 20332

12. REPORT DATE: November 1978
13. NO. OF PAGES: 109

14. MONITORING AGENCY NAME & ADDRESS (if diff. from Controlling Office)
111 p.

15. SECURITY CLASS. (of this report): UNCLASSIFIED

15a. DECLASSIFICATION/DOWNGRADING SCHEDULE

16. DISTRIBUTION STATEMENT (of this report)

Approved for public release; distribution unlimited.

17. DISTRIBUTION STATEMENT (of the abstract entered in Block 20, if different from report)

18. SUPPLEMENTARY NOTES

19. KEY WORDS (Continue on reverse side if necessary and identify by block number)

| | |
|---|---|
| Hurricane tracking | Hurricane wave spectra |
| Hurricane monitoring | Hurricane surface currents |
| Hurricane wind speed | HF radar |
| Hurricane surface wind circulation | Skywave radar |
| Remote sensing | OTH radar |

deg

20. ABSTRACT (Continue on reverse side if necessary and identify by block number)

This report describes the results of a study to evaluate the effectiveness of a high-frequency (HF) skywave radar used to determine (1) the track of a hurricane, and (2) hurricane wind velocity and wave height throughout all regions of a storm. Experimental data were collected using the SRI-operated Wide Aperture Research Facility (WARF) located in central California. The WARF radar is a high-resolution skywave radar capable of forming a 0.5° beam at 15 MHz. HF skywave radar sea-echo Doppler spectra were recorded for: Hurricanes Anita (1977), Caroline (1975), and Eloise (1975); tropical storms Babe (1977) and Debra (1978), in the Gulf of Mexico;

(over)

DD FORM 1 JAN 73 1473 410 281

EDITION OF 1 NOV 65 IS OBSOLETE

UNCLASSIFIED

SECURITY CLASSIFICATION OF THIS PAGE (When Data Entered)

19. KEY WORDS (Continued)

(abs cont)

six hurricane/tropical storms in the Gulf of Mexico and Pacific Ocean between 1975 and 1978.

20 ABSTRACT (Continued)

and Hurricane Kate (1976) in the Pacific Ocean. Both day and night measurements were made, as well as one- and two-ionospheric-hop measurements ranging out from 2800 to 4000 km.

Surface wind direction maps were computed for all 6 tropical storms. In situ measurements were available for two storms, ~~Anita and Eloise~~ for comparison to the WARF radar wind maps. The radar-derived wind directions coincident in time and space with National Data Buoy Office ~~(NDBO)~~ moored buoys ~~for Anita and Eloise~~ showed agreement to within 10 deg. The spatial distribution of the wind directions within the hurricane were computed from NDBO buoys during Eloise and Anita using the buoy data compiled over 22 hours and 36 hours, respectively, and were compared to the WARF radar wind maps. Agreement to within 10° for Eloise and 20° for Anita was found despite the different time and space scales.

The center of the hurricane was estimated from each WARF wind map for Hurricane Anita 1977, and was compared to the official track compiled by the National Hurricane Center (NHC). A track was developed for hurricane Anita from 17 ~~wind maps~~ compiled over a 5-day period. The mean difference between the WARF radar positions and the interpolated positions along the NHC track was 19 km. A track for tropical storm Debra was similarly developed from 7 wind maps computed during a two-day tracking experiment. The WARF position fixes for Debra were compared to the reconnaissance aircraft position fixes and agreement was within 25 km.

WARF measurements of ocean wind speed and wave height were made during hurricanes Anita and Babe. A parametric wave prediction model developed previously was used to compute wind speeds from rms wave height and the radial fetch. The wind speeds and significant wave heights measured at NDBO EB71 during Anita were also plotted with respect to the radar measured center, and were compared to the radar estimates and a wave prediction model forecast. Significant wave-height and wind speed estimates made at WARF were within 0.5 m and 2 m/s, respectively, of the buoy-derived measurements.

SRI International

*Final Report* *November 1978*

# TRACKING AND MONITORING HURRICANES BY HF SKYWAVE RADAR OVER THE GULF OF MEXICO

*By:* J. W. MARESCA, JR. C. T. CARLSON

*Prepared for:*

AIR FORCE OFFICE OF SCIENTIFIC RESEARCH
BOLLING AIR FORCE BASE
WASHINGTON, D.C. 20332

CONTRACT F49620-76-C-0023

SRI Project 5630



*Approved by:*

L. E. SWEENEY, JR., *Director*
*Remote Measurements Laboratory*

DAVID A. JOHNSON, *Executive Director*
*Technology and Systems Development Division*

333 Ravenswood Avenue • Menlo Park, California 94025 • U.S.A.

SRI International

CONTENTS

## ACKNOWLEDGMENTS

We wish to acknowledge the contributions of a number of SRI staff members in this research effort. Clair Powell, James Lomasney, William Preuss, Gary Glassmeyer, and Glenn Tomlin contributed significantly to the scheduling and operation of the radar system and in data collection. Douglas Westover and William Weir developed the hurricane tracking and monitoring, collection and analysis computer software. Mr. Sidney M. Serebreny and Russell Trudeau of the Atmospheric Sciences Laboratory of SRI significantly contributed to satellite cloud photographic analysis and comparisons to the radar data. Helpful suggestions and comments were made by Drs. Lawrence E. Sweeney, James R. Barnum, Walter B. Zavoli and Taylor W. Washburn. Barbara Richards, Jane King and Patti Holys assisted in preparation and typing of this report.

We are grateful for assistance obtained outside SRI. Mr. and Mrs. Paul Duhon, Cameron, Louisiana and Mr. Andy Andrews, Miami, Florida have provided and maintained temporary field sites for the hurricane experiments. We are also grateful for data received from the National Hurricane Center, National Hurricane Environmental Research Laboratory, the National Weather Service in Honolulu, Hawaii and Redwood City, California, and the National Data Buoy office. We acknowledge the helpful discussions and computer programs supplied to us by Drs. Donald Barrick and Thomas Georges of the Wave Propagation Laboratory, NOAA.

We are grateful for the financial support by the Air Force Office of Scientific Research.

# I INTRODUCTION

The objectives of the SRI hurricane tracking and monitoring research program for the U.S. Air Force Office of Scientific Research were to collect and analyze at the Wide Aperture Research Facility (WARF) the HF skywave sea backscatter for Gulf of Mexico tropical storms and hurricanes, and to determine the feasibility of:

- Tracking tropical storms and hurricanes from a long distance.
- Estimating the ocean surface-wind direction field.
- Estimating the significant wave height.
- Estimating the ocean surface-wind speed.

This final report briefly summarizes the research program and results from 14 July 1976 to 30 November 1978.

The principal results of this research are summarized in more detail in the technical papers submitted or accepted for publication. These papers are given in Appendices A through E. In Appendix A we describe the results of the Eloise experiments in which we demonstrated that we could map the surface wind direction field around a hurricane and determine the hurricane position from this map. In Appendices B and C we describe the results of the tracking experiments conducted for hurricane Anita and tropical storm Debra. In Appendix D we describe the method and results of estimating wind speed and significant wave height for hurricane Anita and tropical storm Babe. In Appendix E we describe the method and results of measuring significant wave height and the wave frequency spectrum for low, moderate and high wind speed cases. We have or will be presenting the results of this research at technical sessions of several professional society meetings.[1-7]

Technical Report Number One[8] is a summary of preliminary interpretation of the WARF hurricane measurements, theoretical simulations of the sea-echo Doppler spectra, methods of computing wind velocity and wave height from the sea-echo, theoretical simulations of the effect of scattering patch size on the measurements, and the effects of the ionosphere on the interpretation of the data.

In September 1975, we mapped the surface wind direction field and estimated the storm center of Gulf of Mexico hurricane Eloise[9] using the WARF high-frequency (HF) skywave radar.[10] We compared the radar wind directions to available in situ wind directions measured at the National Oceanic and Atmospheric Administration (NOAA) National Data Buoy Office (NDBO) data buoys EB10 and EB04[11] and found agreement to within $10^{o}$. We compared the WARF radar position estimate to the official National Hurricane Center (NHC) track and found agreement to within 35 km. These early experiments suggested that the WARF HF skywave radar might provide a new, independent source of surface hurricane data that were not routinely available through the use of more conventional sensors. In addition, the radar was capable of continuously recording data at locations specified in real-time by the radar operator. Our subsequent work has demonstrated the feasibility of estimating the ocean wave frequency spectrum, ocean surface current velocity, and surface wind velocity from the WARF measured sea backscatter from ocean gravity waves. In Sections II-V we summarize the principal results of research, the WARF HF skywave radar, the sea-echo Doppler spectrum, and the radar measurements, respectively.

## II WARF MEASUREMENT CAPABILITY

During the past 26 months, we collected and analyzed data for hurricanes Anita (1977), Babe (1977), Kate (1976), tropical storm Debra (1978), and further analyzed the data for Eloise (1975). We developed tracks for Anita[12] (Appendix B), an intense hurricane, and for Debra[13] (Appendix C), a weak tropical storm, from the WARF-derived surface-wind direction maps. The mean difference between the WARF-determined positions and the National Hurricane Center (NHC) interpolated positions along the NHC track was less than 20 km.

The WARF surface-wind direction maps made for hurricanes Anita[12] (Appendix B) and Eloise[9] (Appendix A) were compared to wind direction maps computed from NDBO buoy measurements. For Anita, the buoy-derived wind field represented conditions during a 36-hour period; for Eloise the buoy-derived wind field represented conditions during a 22-hour period. The radar data, however, in both cases were collected in less than 45 minutes. The relative agreement between the buoy- and WARF-derived wind-direction data was better than $5^{o}$ for Eloise and $20^{o}$ for Anita. Comparison of the WARF and the buoy measurements of the wind direction, coincident in both time and space, agreed to within $10^{o}$. Estimates of wind speed were derived from a parametric wave prediction model,[14-17] which required a WARF measurement of wave height and radial distance from the center of the storm. Only a few in situ wave height and surface wind speed measurements were available at the NDBO buoys to compare with the WARF estimates.

The WARF measurements of significant wave height and wind speed made during hurricane Anita (Appendix D) were compared to those made simultaneously at NDBO buoy EB71 ($26.0^{o}$N, $93.5^{o}$W); agreement was within 0.5 m, 0.4 m/s and $9^{o}$[18] (Appendix D). The methods used to interpret rms wave height from the sea-echo Doppler spectrum are accurate to approximately 10%.[19] The accuracy of the wind speed estimates are a function of the accuracy of the parametric wave prediction model, and

the WARF estimates of rms wave height and the radial distance. We determined that the WARF measurements of significant wave height and radial distance are accurate to within 0.5 m and 20 km, respectively. For a significant wave height of 5.5 m and radial distances ranging from 30 km to 300 km, the potential errors are less than 2 m/s.[18] This estimate is consistent with the parametric wave prediction model verification tests of Ross and Cardone.[17]

## III WARF SKYWAVE RADAR

The WARF[10] is a high-resolution experimental high frequency (HF) skywave radar located in central California. The radar is bistatic and operates in the HF band between 6 and 30 MHz. Ocean areas are illuminated by a 20 kW swept-frequency continuous-wave (SFCW) signal from a transmitter site located at Lost Hills, California. The energy reflected from the ocean surface is received 185 km north of the transmitting site at the Los Banos, California receiving site. The receiving antenna array is 2.5-km long and consists of a double linear array of 256 whip antennas producing a nominal $0.5^{\circ}$ azimuthal beamwidth at 15 MHz. The signal propagates to and from remote ocean patches up to 3000 km from the radar by means of a single reflection from one or more layers in the ionosphere. These layers are defined by peaks in the electron density height profile and occur at different heights between 100 and 500 km.

The WARF coverage area is shown in Figure 1 of Appendix B. The radar can be directed either east or west, and can be electronically steered in azimuth $\pm 32^{\circ}$ from boresight anywhere within the coverage area in $0.25^{\circ}$ increments. Position accuracy is a function of ionospheric height estimates where uncertainties in the midpath height result in a nominal position accuracy of approximately 20 km. However, at any one location, the accuracy between consecutive measurements in range and azimuth is an order of magnitude better. WARF has multiple-beam capability. For hurricane monitoring, sea backscatter is simultaneously received at four adjacent ocean areas from four different beams separated by $0.25^{\circ}$. The size of the ocean scattering patch is a function of the radar beamwidth and the range cell separation. The size of the minimum scattering patch is 3 km in range by 15 km in azimuth.

## IV THE SEA ECHO DOPPLER SPECTRUM

The sea backscatter received at the WARF is coherently processed in range and Doppler to produce a sea-echo Doppler spectrum. The typical sea-echo Doppler spectrum is characterized by two dominant first-order echoes surrounded by a second-order continuum. Crombie[20] interpreted the first-order echoes in terms of simple Bragg scattering that represented a resonant response between radio waves of wavenumber $k_o$ and ocean waves of wavenumber $k = 2k_o$. The radar measures the relative power and Doppler of the ocean waves traveling radially toward or away from the radar. The power ratio of the two first-order echoes representing the upwind and downwind conditions, relative to the radar look direction, are indicative of the wave direction of the waves with wavenumber k. Because k is usually large ($k > 0.5$), it is assumed that the predominant wind direction is identical to the predominant direction of these ocean waves.

Barrick[21,22] derived theoretical expressions that accurately describe the HF scattering process to second-order. For a specified directional wave spectrum, his model accurately predicts the sea-echo Doppler spectrum. Using Barrick's second-order model, we have studied the effects of the wind direction, wave directionality, and the wave frequency spectrum on the Doppler spectrum.[1] The wave height spectrum is derived from the second-order structure surrounding the first-order echoes. As wave energy increases, the amplitude of the second-order structure increases. Barrick and Lipa[23] have reviewed numerous inversion techniques used to compute rms wave height, the wave spectrum, and the directional wave spectrum. Agreement between ground-wave radar measurements and in situ observations is within 10%.

## V THE RADAR MEASUREMENTS

For each coherent radar measurement, we processed 21 independent Doppler spectra spaced contiguously at 3-km range intervals. These spectra were obtained simultaneously at each of the four adjacent radar beams. The size of the ocean patch monitored by the WARF was specified by the radar operator. The size was consistent with ionospheric propagation conditions and the characteristic length scales of the ocean wave and wind fields being measured. For hurricane sampling, the data could, therefore, be averaged over a large number of adjacent range and azimuth cells.

To obtain wind direction estimates with WARF, we used a coherent integration time of 12.8 s and averaged the sea-echo Doppler spectra obtained from five contiguous range cells at each azimuth. For each 12.8 s we obtained 16 wind direction estimates. At a range of 3000 km, the typical distance of our hurricane measurements, the size of the scattering patch is approximately 15 km in range and 25 km in azimuth. To estimate wave height and wind speed with WARF, we used a coherent integration of 102.4 s and averaged the sea-echo Doppler spectra obtained from 21 range cells and 3 azimuths. At a range of 3000 km, the size of the scattering patch is approximately 60 km in range and 50 km in azimuth. We conducted some simple simulations to determine the effect of the scattering patch size on the radar measurement of wind speed and direction. We only found significant discrepancies between the simulated spatial estimate and the midpoint value when the scattering patch was centered directly in the hurricane eye. From the region of the maximum winds radially outward, we found the relative agreement between the space average and the point measurement was within approximately 10%.

The accuracy of the skywave radar estimates of wave height and wind velocity is not only dependent on the accuracy of the theoretical models, but on the quality of the measured sea-echo Doppler spectrum.

The quality of the recorded sea backscatter depends on the ionospheric conditions over fairly short periods (tens of seconds). If the radio waves propagate through a strong, single, stable, coherent ionospheric layer, than high-quality sea backscatter similar to ground-wave radar is obtained. However, if the signals are received at the same time from two or more different paths (multipath), the backscatter from one ocean patch, generally shifted in Doppler and amplitude, will be reflected from a different part of the ocean and a different part of the ionosphere. The backscatter from the first ocean patch will be contaminated by the backscatter from the other ocean patches. If the ionosphere is also changing in time or space during a coherent sampling period, smearing of the data will occur. The ability to predict the ionospheric conditions over these short time periods would enhance the quality of sea backscatter and reduce the sampling time. Both vertical and oblique incidence ionospheric soundings are used to provide some data quality information. More time is required to complete an ionospheric sounding than is required to take the data; thus, assessment of the data quality is difficult for rapidly changing ionospheres. Therefore, real-time output of the data from the WARF site minicomputer is required and is used to verify the data quality.

The wind direction measurement is not extremely sensitive to ionospheric contamination caused by ionospheric smearing and multipath because only the amplitude of the two strong first-order echoes must be measured, and the coherent integration time is short (12.8 s). Mapping the wind-direction field in a hurricane can be routinely accomplished under most ionospheric conditions in 10 minutes or less. Once the surface-wind-direction map is made, the storm center can be identified and more extensive monitoring of the wind speed and wave height anywhere within the storm can be accomplished.

The wave height and wind speed estimates, dependent on extracting spectral information from the weak second-order echoes surrounding the first-order echoes, are more sensitive to ionospheric contamination than the wind direction measurements. This contamination is the largest source of error in the measurements.

The net effect of the multipath and smearing is to increase the calculated wave height and wind speed because power is added in an unknown way to the sea-echo Doppler spectrum. Fortunately, for the large sea-state conditions normally encountered during hurricanes, the power of the second-order echoes is large and is frequently stronger than the contamination. Under these conditions, wave height and wind speed estimates can still be made. The effects of contamination are variable in time and space. Often a small portion of the data may not be contamintated while the remainder of the data will be contaminated. We have developed several techniques to filter the contaminated sea-echo spectra out of the sample to improve data quality. On-going work at SRI and NOAA to develop better ways of collecting and processing skywave data has improved the skywave estimates of wave height.[24] Because of the longer integration times and special data sampling and processing, the time required to make an estimate of the wave height and wind speed is longer than that necessary to estimate wind direction. However, the radar operator can selectively steer the radar beams to specific regions of the storm to make the desired measurements.

## VI SUMMARY

We have demonstrated that high-resolution HF skywave radar can be used to track and to monitor remotely wind direction and speed and wave height throughout all regions of hurricanes and tropical storms. The radar position fixes are accurate to 20 km; the wind and wave estimates are accurate to within 10%. Skywave radar can be steered by the operator in real-time to specific regions of the storm located over 3000 km from the radar, or the radar can be used to scan across the entire storm. The skywave radar surface measurements can be combined with the upper level satellite measurements to improve the quality and reliability of hurricane and tropical storm observations.



## REFERENCES


1 J. W. Maresca, Jr., "Interpretation and Collection of HF Skywave Radar Sea Backscatter Obtained During Hurricanes," (Abstract), American Geophysical Union, 1976 Fall Annual Meeting, San Francisco, California (December 8-12, 1976).

2 J. W. Maresca, Jr., "High-Frequency Skywave Radar Measurements of Waves and Currents Associated with Tropical and Extra-Tropical Storms," (Abstract), National Oceanic and Atmospheric Administration Ocean Wave Climate Symposium, Herdon, Virginia (July 12-14, 1977).

3 J. W. Maresca, Jr. and C. T. Carlson, "HF Skywave Radar Measurement of Hurricane Generated Ocean Wave Spectra," (Abstract), Sixteenth International Conference on Coastal Engineering, Hamburg, Germany (August 27-September 3, 1978).

4 C. T. Carlson and J. W. Maresca, Jr., "HF Skywave Radar Measured Track of Hurricane Anita," (Abstract), International Union of Radio Science, National Radio Science Meeting, Boulder, Colorado (November 6-9, 1978).

5 C. T. Carlson, J. W. Maresca, Jr. and T. M. Georges, "HF Skywave Radar Measurement of Significant Wave Height During Hurricane Anita," (Abstract), American Geophysical Union 1978 Fall Annual Meeting, San Francisco, California (December 4-8, 1978).

6 J. W. Maresca, Jr. and C. T. Carlson, "HF Skywave Radar Estimates of the Track and Wind Velocity During Hurricane Anita," (Abstract) American Geophysical Union 1978 Fall Annual Meeting, San Francisco, California (December 4-8, 1978).

7 J. W. Maresca, Jr. and C. T. Carlson, "HF Skywave Radar Estimates of the Track, Surface Wind and Waves of Hurricane Anita," (Abstract) Advisory Group Aerospace Research and Development Technical Meeting of the Electromagnetic Wave Propagation Panel, Lisbon, Portugal (May 28-June 1, 1979).

8 J. W. Maresca, Jr. and C. T. Carlson, "Tracking and Monitoring Hurricanes by HF Skywave Radar over the Gulf of Mexico," Technical Report 1, SRI International, Menlo Park, California (1977).

9 J. W. Maresca, Jr. and J. R. Barnum, "Remote Measurements of the Position and Surface Circulation of Hurricane Eloise by Skywave Radar," accepted by Monthly Weather Review.




10 "SRI Remote Measurements Laboratory Research Capabilities," brochure, Stanford Research Institute, Menlo Park, California (1977).

11 G. W. Whithee and A. Johnson, Jr., "Data Report: Buoy Observations During Hurricane Eloise, September 19-October 11, 1975," Environmental Sciences Division, Data Buoy Office, National Oceanic and Atmospheric Administration, Bay St. Louis, Mississippi (1975).

12 J. W. Maresca, Jr. and C. T. Carlson, "Tracking Hurricane Anita by HF Skywave Radar," to be submitted to J. Geophys. Res.

13 J. W. Maresca, Jr. and C. T. Carlson, "HF Skywave Radar Track of Tropical Storm Debra," to be submitted to Monthly Weather Review.

14 D. B. Ross, "A Simplified Model for Forecasting Hurricane Generated Waves" (Abstract), Bull. Am. Meteorol. Soc., presented at Conference on Atmospheric and Oceanic Waves, Seattle, Washington, March 29-April 2, 1976 American Meteorological Society (1976).

15 V. J. Cardone and D. B. Ross, "State of Art Wave Predictions and Data Requirements," Ocean Wave Climate, eds. M. D. Earle and A. Malahoff, Plenum Publishing Company, New York (1978).

16 D. B. Ross and V. J. Cardone, "A Comparison of Parametric and Spectral Hurricane Wave Prediction Products," to be published in the Proceedings of "NATO Symposium on Turbulent Fluxes Through the Sea Surface, Wave Dynamics and Prediction," Marseille, France, September 12-16, 1977, Plenum Publishing Company, New York (1978).

17 V. J. Cardone, D. B. Ross, and M. R. Ahrens, "An Experiment in Forecasting Hurricane Generated Sea States," Proceedings of the 11th Technical Conference on Hurricanes and Tropical Meteorology, Miami, Florida (December 13-16, 1977).

18 J. W. Maresca, Jr. and C. T. Carlson, "HF Skywave Estimates of Hurricane Winds and Waves," Proceedings of the Sixteenth Conference on Coastal Engineering, Hamburg, Germany (August 1978).

19 J. W. Maresca, Jr. and T. M. Georges, "HF Skywave Radar Measurement of the Ocean Wave Spectrum," submitted to J. Geophys. Res.

20 D. D. Crombie, "Doppler Spectrum of Sea Echo at 13.56 mc/s," Nature, Vol. 175, pp. 681-682 (1955).

21 D. E. Barrick, "First-Order Theory and Analysis of MF/HF/VHF Scatter From the Sea," IEEE Trans. on Antennas and Propagation, AP-20, pp. 2-10 (1972).

22 D. E. Barrick, "Remote Sensing of Sea State by Radar," Remote Sensing of the Troposphere, V. E. Derr, Ed., U.S. Government Printing Office, Washington, D. C. (1972).

23 D. E. Barrick and B. J. Lipa, "Ocean Surface Features Observed by HF Coastal Ground-wave Radars: A Progress Review, Ocean Wave Climate, eds. M. D. Earle and A. Malahoff, Plenum Publishing Company, New York (1978).

24 T. M. Georges and J. W. Maresca, Jr., "The Effect of Radar Beamwidth on the Quality of Sea Echo Doppler Spectra Measured with HF Skywave Radar," accepted by Radio Science.

APPENDIX A

# REMOTE MEASUREMENT OF THE POSITION AND SURFACE CIRCULATION OF HURRICANE ELOISE BY HF SKYWAVE RADAR

by

J. W. Maresca, Jr.
J. R. Barnum

Accepted for Publication in
Monthly Weather Review

This work was performed by SRI International, Menlo Park, California, and was sponsored in part by the Air Force Office of Scientific Research and SRI Internal Research and Development funds.

# REMOTE MEASUREMENT OF THE POSITION AND SURFACE CIRCULATION OF HURRICANE ELOISE BY HF SKYWAVE RADAR

Joseph W. Maresca, Jr. and James R. Barnum

SRI International
Menlo Park, California 94025

## ABSTRACT

The position and surface wind direction field of hurricane Eloise was observed by measuring sea backscatter from the Gulf of Mexico through the use of an HF skywave radar situated in central California. A radar map of the surface wind direction field was compiled from the direction of the ocean gravity waves 8-m long, and compared to the surface wind directions measured at National Data Buoy Office (NDBO) open ocean moored buoys EB10 and EB04. Agreement to within 10% was found. The radar position fix was determined from the radar-derived surface wind map and showed agreement to within 35 km of the position estimated from the official National Hurricane Center track.

## I INTRODUCTION

The position of a hurricane in open water often can be determined remotely by the cloud cover in satellite photographs and by reconnaissance aircraft flights directly through the center of the hurricane. Measurements of surface wind directions are sparse. We discuss a new technique to estimate the surface wind directions and position of a hurricane through the use of high-frequency (HF) skywave radar sea backscatter measurements. The position and surface wind direction field of hurricane Eloise was determined remotely (at a distance of 3000 km) at approximately 2030Z on 22 September 1975 from a detailed description of the ocean gravity wave field.

## II THEORY RELATING WIND DIRECTION TO RADAR SPECTRA

Backscatter measurements obtained from the skywave radar measurements are coherently range and Doppler processed to obtain a Doppler spectrum. The sea-echo Doppler spectrum shown in Figure 1 is characterized by two dominant first-order echoes. These strong echoes were first explained by Crombie (1955), and are caused by the resonant interaction of ocean waves of length L equal to one half the electromagnetic wave of length $\lambda$. Only ocean waves traveling directly toward or away from the radar are detected by this means. The principle direction of ocean gravity waves (8 to 9 meters long) is inferred from the power ratio of the approaching and receding waves. Because the waves are short it is assumed that they are coincident with the mean wind direction. Techniques to calculate direction have been described in the literature by Long and Trizna (1973), Ahearn et al. (1974), Tyler et al. (1974), Stewart and Barnum (1975), and Barnum et al. (1975). Stewart and Barnum (1975) derived an expression for the direction of the ocean gravity waves based on ocean wave directional distribution, $G(\theta)$, of the form

$$G(\theta) = \cos^{s}\left[\frac{\theta}{2}\right] \qquad (1)$$

suggested by Longuet-Higgins, Cartwright, and Smith (1963) and Cartwright (1963). The wave direction, $\theta$, relative to the radar bearing is

$$\theta = 2 \arctan (r^{1/s}) \qquad (2)$$

where $r = \frac{G(\theta)}{G(\theta+\pi)}$ is the power ratio computed from the first-order echoes, and s is a parameter in Equation (1) which describes the spreading envelope of the ocean gravity wave field. Stewart and Barnum (1975) found that the standard deviation of the measurement was ±16 degrees for open ocean conditions. Equation (2) was used for the data to be described herein.

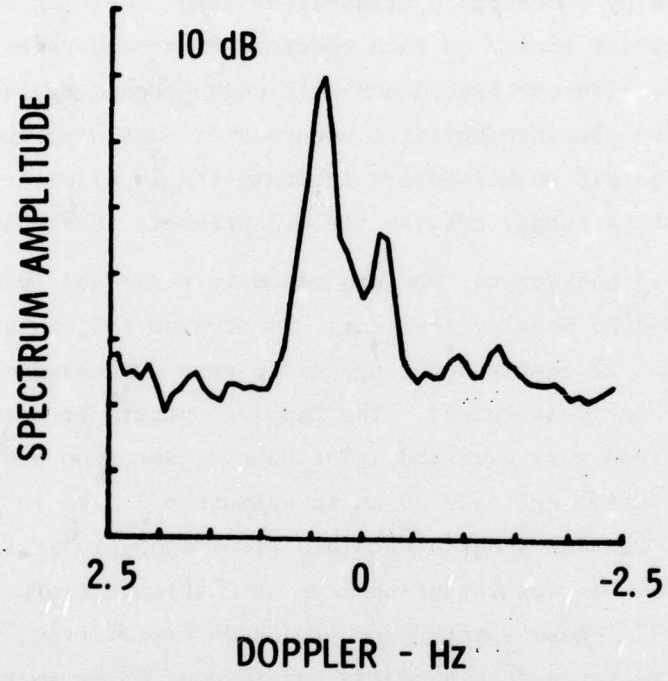


FIGURE 1 AN EXAMPLE OF A DOPPLER SPECTRUM OBTAINED FROM PROCESSING 12.8 s OF HF SKYWAVE RADAR BACKSCATTER DATA. The first-order Bragg lines are the two maxima.

## III BACKSCATTER SPECTRUM RECORDING AND INTERPRETATION

The Wide Aperture Research Facility (WARF) HF skywave radar was used to collect the hurricane data as Eloise moved northward through the Gulf of Mexico. The WARF radar is located in central California (Figure 2) approximately 3000 km west of the hurricane. The receiving array is 2.55 km long and forms a $0.5^{o}$ beam at 15 MHz. The area was illuminated by a 30-degree transmitter beam* centered on the hurricane, and backscatter energy on each coherent 26-second radar measurement was received at five contiguous one-half degree beams spaced by one-quarter degree. The absolute position accuracy of each WARF dwell observation is approximately 20 kilometers in range and 20 kilometers in azimuth. The relative accuracy between two measurements is significantly better.

The sea backscatter was processed in range and in Doppler to produce a sea-echo Doppler spectrum. Twenty-one indivudual Doppler spectra processed at 21 contiguous range cells were processed for each 12.8 s coherent radar measurement. The Doppler spectra from two consecutive 12.8 s periods were averaged. The Doppler spectrum processed for each range resolution cell was 26 km in azimuth and 3 km in range. An example of Doppler spectra obtained simultaneously at five different azimuths in the vicinity of the eye of hurricane Eloise is presented in Figure 3. These spectra are produced in real time, and each of the five spectra represents a spatial average of 63 km in range and 25 km in azimuth. The abrupt change in the first-order echoes and, therefore, wind direction occurs over less than 100 km, the typical diameter of a hurricane eye. At each azimuth, we averaged the Doppler spectra from 5 contiguous range cells (instead of 21). Wind direction was estimated from the Doppler spectrum averaged over five range cells and two time periods. This procedure involved a spatial average of the wave direction over only 390 $km^2$ of ocean (15 km in range by 26 km in azimuth). Each such measurement was centered at grid points spaced by 13 km in

* Normally, the transmitter beam is $6^{o}$. Because one of the transmitters was under repair during the experiment, only the center four elements of the eighteen element transmitting array were used.

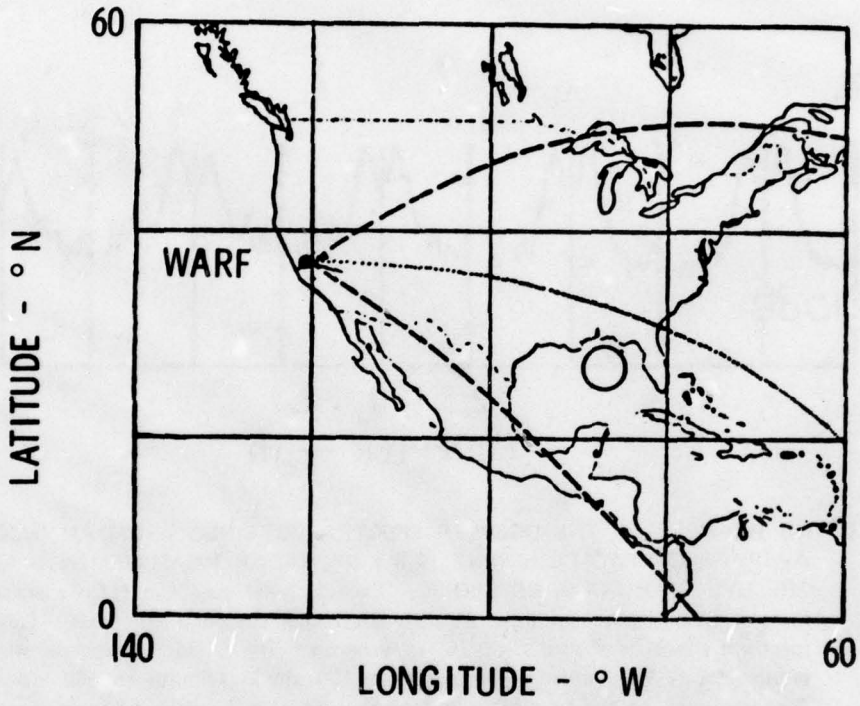


FIGURE 2 THE AREA SCANNED BY THE WIDE APERTURE RESEARCH FACILITY (WARF), SKYWAVE RADAR TO LOCATE HURRICANE ELOISE IN THE GULF OF MEXICO AT 2100Z ON SEPTEMBER 22, 1975

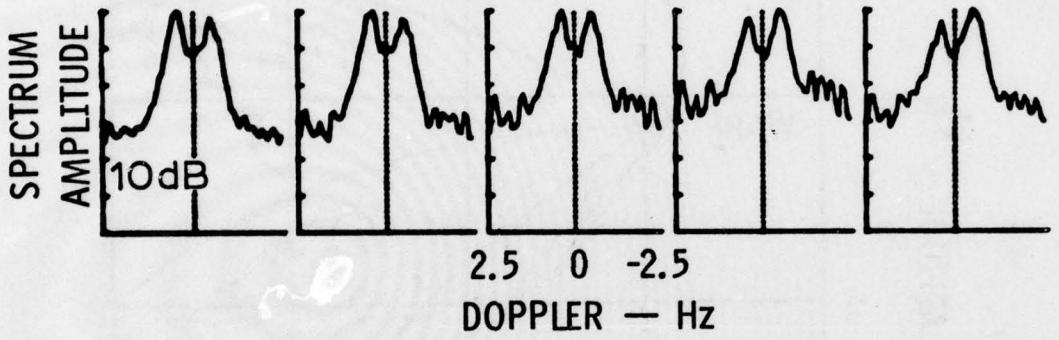


FIGURE 3 AN EXAMPLE OF THE DOPPLER SPECTRA OBTAINED FROM AN INCOHERENT AVERAGE OF TWO COHERENT 12.8 s HF RADAR MEASUREMENTS ACROSS THE EYE OF HURRICANE ELOISE. Each Doppler spectrum is an average of the Doppler spectra obtained from 21 different ranges spaced 3 km apart. Each Doppler spectrum shown is spaced by 0.25° in azimuth. The 5 Doppler spectra were obtained simultaneously over an area approximately 100 km in azimuth and 60 km in range. The amplitude of the first-order echoes changes as a function of wave direction from approaching to receding directions in less than 100 km.

azimuth and 15 km in range. A total of 20 wind direction estimates are obtained every 26 s. The total time required to complete a scan of the entire hurricane was 33 min.

We used Equations (1) and (2) to derive the ocean gravity wave field measured by the skywave radar for ocean wave lengths ranging from 8 m to 9 m for three values of s. For hurricane waves, the value of s is not well known. The value of s is inversely proportional to wave frequency and wind speed as shown by Ewing (1969), Tyler et al. (1974) and others. Stewart and Barnum (1975) derived an expression for s as a function of wind speed and wave number. Using their model for hurricane wind speeds resulted in values of s less than 1.0. This would imply a highly nondirectional wave field. We calculated three wind direction maps using s equal to 1.0, 2.0, and 4.0.

The left-right ambiguity in direction was resolved from the general circulation of a hurricane in the following manner. First, we assumed that the directional properties of the wind field and the wave field for the higher wave numbers were similar. Then, we assumed that the winds are directed counterclockwise and flow inward, and resolved the left/right ambiguity. Only in cases in which the winds were approximately radial to the radar beam direction with no clear inflow angle discernable was the choice arbitrary. In this case, the possible direction error was inconsequential because the difference in total direction between the left/right direction vectors was less than the expected error of the measurement (±16 degrees). The three wind direction maps were compared to the NWS surface analyses for 1800Z on 22 September 1975, the two wind observations at NOAA buoys EB10 and EB04, and cloud patterns obtained from the NASA SMS1 Synchronous Meteorological Satellite photographs. The best agreement was found for the wave pattern derived from a value of s equal to 1.0. This value of s was thus assumed correct for all radar measures of direction in the hurricane.

## IV HURRICANE WIND AND WAVE FIELD

The directional ocean wave field derived from the radar measurements during Hurricane Eloise is shown in Figure 4. During the period 22-23 September 1975, Hurricane Eloise moved northeasterly across the Gulf of Mexico, passing within 56 km of NDBO buoy EB04 and within 46 km of buoy EB10. We computed a wind direction field from the buoy-measured wind directions over a 22-hr period to compare to the WARF-derived wind directions. We plotted the buoy-measured wind directions with respect to one center. We superimposed the buoy-derived wind field on the WARF-derived wind map. The buoy data overlaps the WARF measurements taken at approximately 2030Z and spans the period 1000Z on 22 September 1975 through 0800Z on 23 September 1975. The agreement between the WARF and buoy wind direction measurements was dependent on the assumptions that the hurricane surface wind circulation and storm motion remained uniform during the period when Eloise passed between the two buoys. However, Eloise stalled for a period of approximately 5 hours, so some error in both the position and wind direction was expected. Nevertheless, the radar measured wind directions agreed to within $10^{o}$ overall with the buoy-derived spatial wind field, and they verified in a qualitative sense the observed surface circulation inferred for the radar measurements. The difference between the wind directions measured at the NOAA buoys EB10 and EB04 (Withee and Johnson, 1975) coincident in time and space with the radar-derived mean wind directions at those locations was less than 10 degrees.

We considered several possible sources of error in the radar measurements. First, the full transmitting array was not used during the experiment, which resulted in a 30 degree beam instead of the usual 6 degree beam. Hence the combined radar antenna sidelobes were higher, and could have received measurable backscatter energy from other areas of the Gulf. Serious sidelobe contamination was unlikely since the sidelobe gain of the narrow receive beam should have been at least

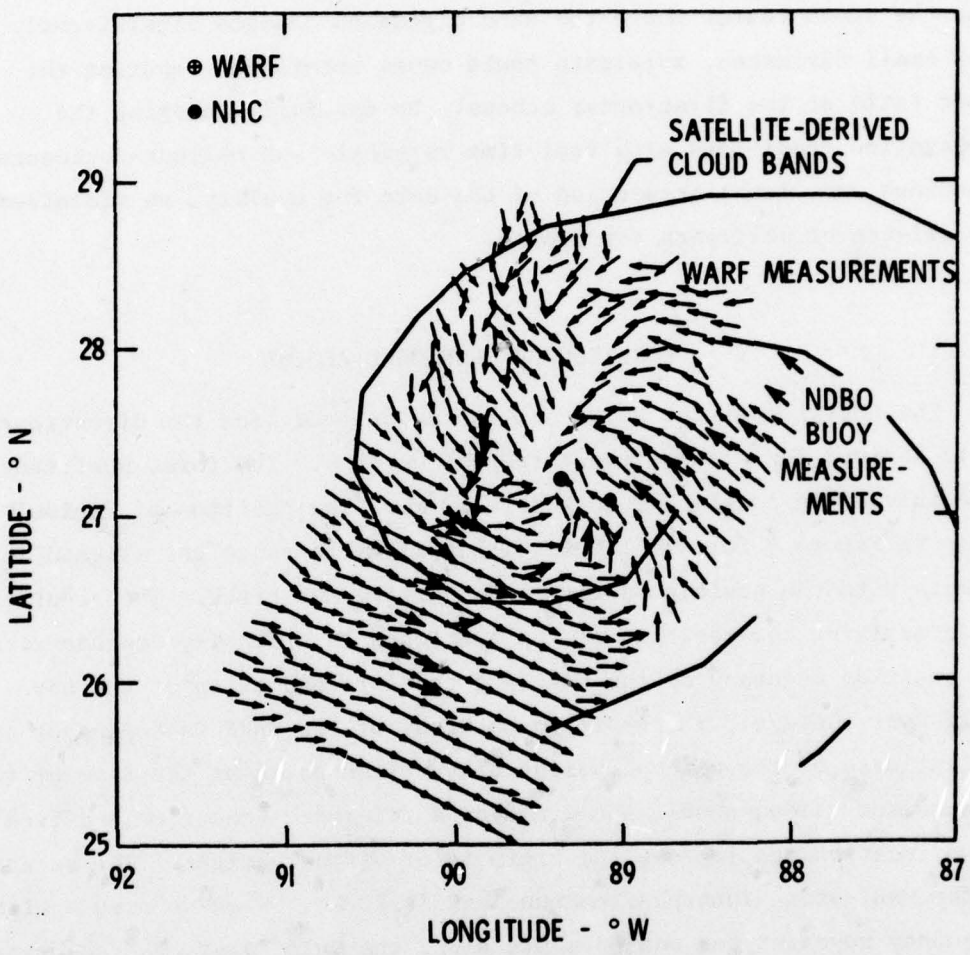


FIGURE 4 COMPARISON OF WARF-MEASURED SURFACE CIRCULATION WITH NDBO DATA BUOY AND SATELLITE CLOUD WIND DIRECTIONS FOR HURRICANE ELOISE

20 dB down. Backlobe reception of scatter from the Pacific Ocean was also measured by reversing the transmitter steer, and it was found to be negligible during the experiment. Second, ionospheric multipath, the simultaneous reception of signals from two different patches of the ocean could contaminate the sea-echo Doppler spectrum. Especially, near the storm center where the wind direction changes significantly over small distances, multipath could cause errors in computing the power ratio of the first-order echoes. By carefully managing the propagation conditions with real-time vertical- and oblique-incidence soundings and visual inspection of the data for quality, we minimized the effects of multipath for Eloise.

## V POSITION OF HURRICANE ELOISE

The position of the hurricane was determined from the direction field derived for each of the three values of s. The three positions were internally consistent to within 10 km. The position of Eloise, shown in Figure 4 for s = 1.0 is within 35 km in range and aligned in azimuth with the position determined from the NHC track. The accuracy of determining the position of the hurricane is primarily dependent on the position accuracy of the WARF and the interpretation of the wave field near the eye. The position accuracy of the WARF is dependent on the estimate of the virtual height of the ionosphere at the time of the measurement. Ionospheric soundings or a reference echo received from a known location can improve the estimate of virtual height. The accuracy of the WARF using ionospheric soundings is 20 km. When we used a high-frequency repeater for measurements along the Gulf coast, the accuracy of the observations could be increased to 5 km or better. The left/right ambiguity in the direction of the wave field near the eye of the hurricane is difficult to resolve without prior knowledge of the position of the eye. This center position is determined from scans similar to Figure 3. The left/right ambiguity is then resolved. For the Eloise data, this ambiguity could cause a 10 to 30 km error in our position of the hurricane.

## V CONCLUSION

The position and surface circulation of the wind field was determined remotely by HF skywave radar for Hurricane Eloise from backscatter measurements of the direction of the short ocean gravity waves. The position of the hurricane agreed to within 35 km of the reported position of the hurricane. The circulation agreed with that estimated using NWS surface charts, SMS1 satellite cloud photographs, and two NOAA buoy measurements. The ability to infer detailed wind direction in the vicinity of the eye of the hurricane and in the region of maximum winds was demonstrated and suggests a potential for measuring the waves, currents, and winds at the surface level in this region.

## ACKNOWLEDGMENTS

This work was performed by the Remote Measurements Laboratory under Internal Research and Development funds at Stanford Research Institute. The computation of the buoy-derived wind field and comparison to the WARF wind directions was accomplished under the sponsorship of the Air Force Office of Scientific Research under Contract No. 49620-76-C-0023. The invaluable assistance of Bill Preuss and Gary Glassmeyer in taking the radar data and Christopher T. Carlson in analyzing the data is gratefully acknowledged.

## REFERENCES


J. L. Ahearn, S. R. Curley, J. M. Headrick, and D. B. Trizna, 1974, "Tests of Remote Skywave Measurement of Ocean Surface Conditions," Proc. of the IEEE, Vol. 62, No. 6, pp. 681-687.

J. R. Barnum, J. W. Maresca, Jr., and S. M. Serebreny, 1977, "High-Resolution Mapping of Oceanic Wind Fields with Skywave Radar," IEEE Trans. on Antennas and Propagation, Vol. AP-25, No. 1.

D. E. Cartwright, 1963, "The Use of Directional Spectra in Studying the Output of a Wave Recorder on a Moving Ship," Ocean Wave Spectra, Prentice-Hall, Englewood Cliffs, N.J., pp. 203-218.

D. D. Crombie, 1955, "Doppler Spectrum of Sea Echo at 13.56 Mc/s," Nature, Vol. 175, pp. 681-682.

J. A. Ewing, 1969, "Some Measurements of the Directional Wave Spectrum," J. Mar. Res., Vol. 25, pp. 795-816.

A. E. Long and D. B. Trizna, 1973, "Mapping of North Atlantic Winds by HF Radar Sea Backscatter Interpretation," IEEE Trans. on Antennas and Propagation, Vol. AP-21, No. 5, pp. 680-685.

M. S. Longuet-Higgins, D. E. Cartwright, and N. D. Smith, 1963, "Observations of the Directional Spectrum of Sea Waves Using Motions of a Floating Buoy," Ocean Wave Spectra, Prentice-Hall, Englewood Cliffs, N.J., pp. 111-136.

R. H. Stewart and J. R. Barnum, 1975, "Radio Measurements of Oceanic Winds at Long Ranges: An Evaluation," Radio Science, Vol. 10, No. 10, pp. 853-857.

G. L. Tyler, C. C. Teague, R. H. Stewart, A. M. Peterson, W. H. Munk, and J. W. Joy, 1974, "Wave Directional Spectra from Synthetic Aperture Observations of Radio Scatter," Deep-Sea Research, Vol. 21, pp. 989-1016, Pergamon Press, New York.

G. W. Withee and A. Johnson, Jr., 1975, "Data Report: Buoy Observations During Hurricane Eloise, September 19 to October 11, 1975," Environmental Sciences Division, Data Buoy Office, National Oceanic and Atmospheric Administration, Bay St. Louis, Mississippi, 39520.

APPENDIX B

# TRACKING HURRICANE ANITA BY HF SKYWAVE RADAR

by

J. W. Maresca, Jr.
C. T. Carlson

To be submitted to
Journal of Geophysical Research
1978

This work was performed by SRI International, Menlo Park, California, and was sponsored by the Air Force Office of Scientific Research.

# TRACKING HURRICANE ANITA BY HF SKYWAVE RADAR

Joseph W. Maresca, Jr. and Christopher T. Carlson
SRI International, Menlo Park, CA

Hurricane Anita was tracked across the Gulf of Mexico from 29 August 1977 to 2 September 1977 by using an HF skywave radar. The radar position estimates were made from California, 3 to 5 times per day, at the SRI-operated Wide Aperture Research Facility (WARF). The storm center was located using the WARF-derived ocean surface wind direction maps. Seventeen independent wind maps were used to develop the WARF-derived track. The WARF-derived positions were compared to coincident temporal positions on the official track produced by the National Hurricane Center (NHC), and the relative agreement was 19 km.

# TRACKING HURRICANE ANITA BY HF SKYWAVE RADAR

Joseph W. Maresca, Jr. and Christopher T. Carlson

SRI International
Menlo Park, California 94025

## INTRODUCTION

This note describes a new method for tracking hurricanes using an HF skywave radar. Hurricane Anita, the first Atlantic hurricane of the 1977 season, formed as a tropical depression in the Gulf of Mexico at about 1200Z on 29 August 1977. Anita developed into a tropical storm at approximately 0600Z on 30 August 1977 and intensified into a hurricane about 12 hours later. As the storm moved west across the Gulf, maximum winds in excess of 75 m/s were recorded prior to landfall approximately 48 km south of Brownsville, Texas.

The skywave radar measurements of Anita were made at the California-based Wide Aperture Research Facility (WARF) [SRI, 1977], an SRI-operated high-resolution HF skywave radar. Seventeen independent position estimates were computed for Hurricane Anita from WARF at ranges between 2400 km and 3200 km, beginning on 29 August 1977 and continuing through landfall on 2 September 1977. The hurricane position estimates were derived from skywave radar maps of the areal distribution of the surface wind directions generated using techniques similar to those used for Hurricanes Caroline [Maresca and Barnum, 1975], Eloise [Maresca, 1976 and Maresca and Barnum, 1978], Kate [Maresca and Carlson, 1977], and Babe [Maresca and Carlson, 1977, 1978]. The Anita maps were updated 3 to 5 times per day at arbitrary times including nighttime periods. The WARF radar position estimates cluster around the corresponding interpolated temporal positions on the National Hurricane Center (NHC) official smooth track. The NHC track was obtained from satellite imagery, reconnaissance aircraft, shore-based microwave Doppler radar,

and open ocean moored buoys. The mean deviation of the WARF positions from corresponding temporal positions along the NHC track is 19 km. WARF skywave radar position estimates for Hurricanes Caroline, Eloise, Kate, and Babe show agreement with NHC positions ranging from 25 to 40 km. The number of WARF position estimates for each of these hurricanes was limited to only one or two. We attribute the improved agreement between the WARF- and NHC-derived tracks to the increased number of WARF wind maps that showed the evolving wind circulation with time. The accuracy of the skywave radar position estimates is similar to the accuracy of the satellite position estimates [Sheets and Grieman, 1975]. One can more reliably track hurricanes remotely by combining both skywave radar and satellite cloud measurements, thus reducing the frequency of aircraft reconnaissance flights required principally for identification of the hurricane center.

Skywave measurements of significant wave height, ocean wave spectra [Maresca and Carlson, 1978; Maresca, 1978; Maresca and Georges, 1978], and the mean surface wind velocity [Maresca and Carlson, 1977, 1978] were also made for Hurricanes Anita and Babe and were compared to measurements made at NOAA Data Buoy Office (NDBO) data buoy EB71. Agreement between the radar- and buoy-measured wind speeds was within ±2 m/s (10%), and agreement between the wind direction measurements was within $10^{\circ}$. The radar estimates of significant wave height were within 0.5 m (10%) of the buoy measurements.

## WARF SKYWAVE RADAR

WARF is an SRI-operated experimental bistatic HF skywave radar located in Central California. The radar is operated in the high-frequency (HF) band between 6 and 30 MHz. A 20-kW swept-frequency continuous-wave (SFCW) signal is transmitted from the transmitter site at Lost Hills, California, and after round-trip ionospheric propagation, is received at a site 185 km to the north at Los Banos, California. The receiving array is 2.5 km long and forms a beam of $0.5^{\circ}$ at 15 MHz.

The WARF radar can be electronically steered in $0.25^{\circ}$ increments anywhere within the coverage area shown in Figure 1. The radio waves propagate over long distances to an ocean scattering patch via one or more ionospheric "reflections". Remote ocean patches illuminated by only one ionospheric reflection are typically within the minimum radar range of 1000 km and the maximum range for one-hop propagation of more than 3000 km. The nominal absolute position accuracy is about 20 km without any surface position references, but at any one location the accuracy between consecutive measurements in range and azimuth is an order of magnitude better.

The size of the ocean patch monitored by the WARF radar is a function of the sampling parameters specified by the radar operator. The operator considers the characteristic length scales of the ocean wave features before selecting the size of the ocean patch illuminated by the radar. For example, in a hurricane where sea conditions may change rapidly over short distances, the monitored ocean patch would be smaller than the one monitored for large ocean storms. We usually sample 21 contiguous range cells spaced at 3 km. The azimuthal or cross-range resolution is a function of the radar beamwidth. For a one-hop range of 3000 km, the $0.5^{\circ}$ beam would produce a cross-range distance of about 25 km. We have found from simulation experiments [Maresca and Carlson, 1977] that a scattering patch 15 km in range by 25 km in azimuth is sufficiently small to accurately determine the wind and wave parameters of the storm.

## RADAR-MEASURED WIND-DIRECTION MAPS

The HF skywave radar-measured surface wind directions are derived from the predominant direction of decameter ocean gravity waves about 10 m long, which are assumed to be tightly coupled to the wind over a period of tens of minutes. Measurements of the directional wave spectrum are generally sparse, but available measurements [Longuet-Higgins et al., 1963; Ewing, 1969; Mitsuyasu et al., 1975] support the computation of wind direction from the wave direction. The WARF radar measures the

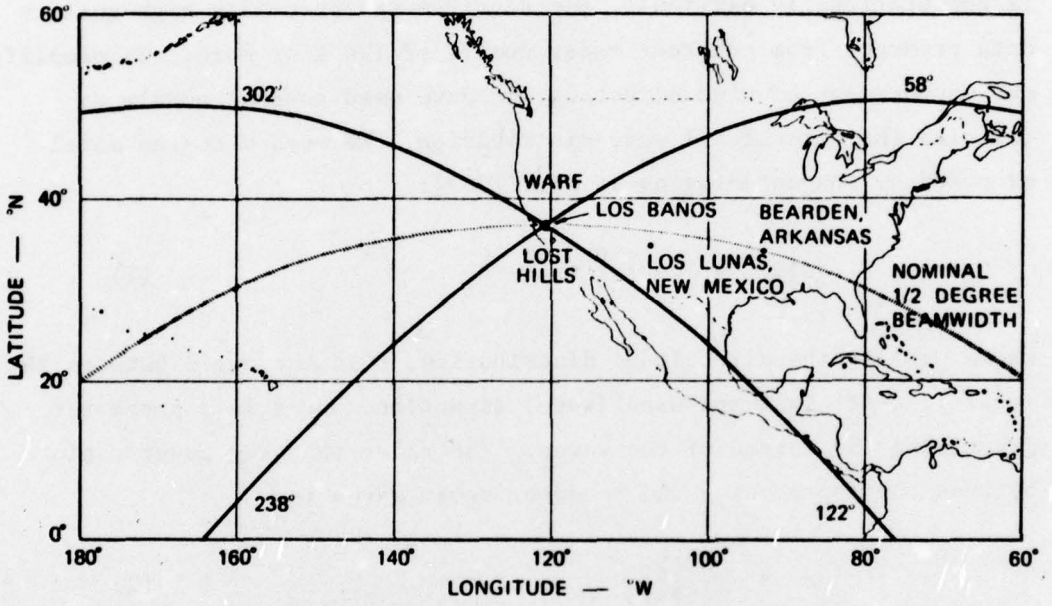


FIGURE 1. COVERAGE AREA OF THE WARF HF SKYWAVE RADAR. All Anita measurements were made west of 88°W in the Gulf of Mexico.

relative power of the approaching and receding ocean waves that satisfy the resonance condition with the radio waves $k = 2k_o$, where $k_o$ is the radio wave number and k the ocean wave number. An example of the radar-measured sea-echo Doppler spectrum is shown in Figure 2. This figure shows approximately 13 dB more energy in the waves receding from the radar than in those approaching the radar. If the directional distribution of the ocean waves were known precisely, the predominant wind direction could be determined directly from the radar measurement. It is possible to compute the directional distribution directly from the radar data using Lipa's [1977a,b] inversion model. However, this method is computationally difficult, and requires exceptionally high-quality data produced from coherent radar dwells of 100 s or more. To simplify our measurement of wind direction, we have used several models to describe the directional wave distribution. We used a cosine model proposed by Longuet-Higgins et al. [1963]:

$$G(\theta) = \cos^s \frac{\theta}{2} \tag{1}$$

where $G(\theta)$ is the directional distribution, $\theta$ is the angle between the radar line-of-sight and wind (wave) direction, and s is a parameter describing the spread of the waves. The radar-measured power ratio between the approaching and receding ocean waves is

$$r = \frac{G(\theta)}{G(\theta+\pi)} \tag{2}$$

Solving for $\theta$ and substituting Eq. (1) into Eq. (2) gives

$$\theta = 2 \arctan r^{1/s} \tag{3}$$

Several models have been proposed to calculate $\theta$ from the radar data [Long and Trizna, 1973; Ahearn et al., 1974; Tyler et al., 1974; Stewart and Barnum, 1975; Barnum et al., 1977; Maresca and Carlson, 1977]. The accuracy of the $\theta$ estimate is dependent on the validity of the directional model and the value of s. For nonhurricane winds, estimates of the mean radar-derived wind direction agree to within $\pm 16^\circ$

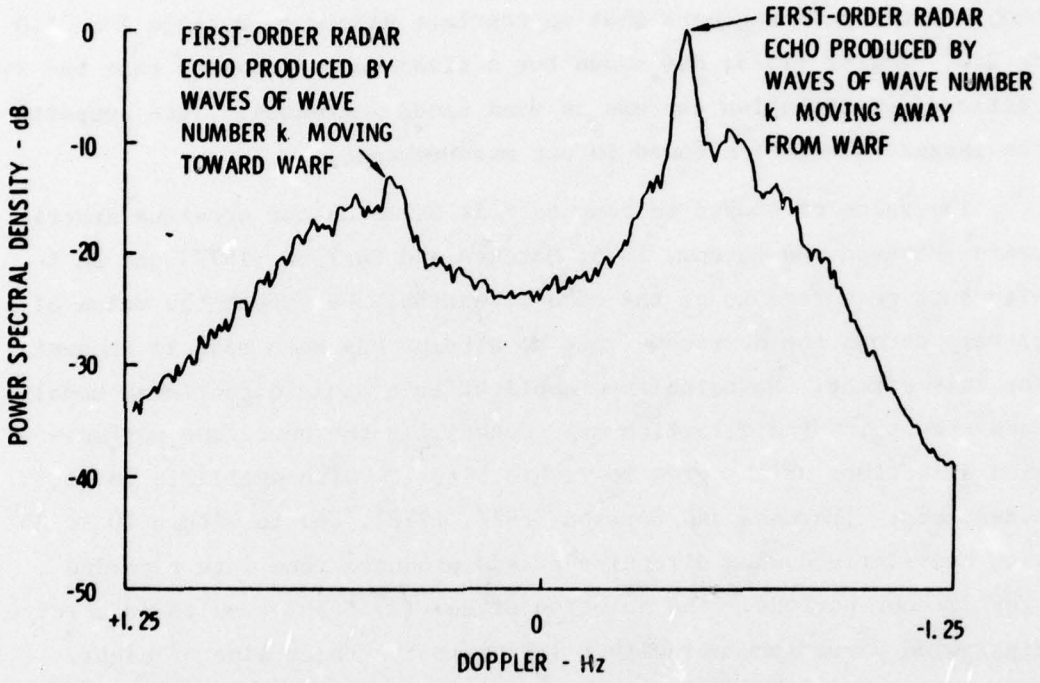


FIGURE 2 AVERAGE SEA-ECHO DOPPLER SPECTRUM RECORDED WITHIN 35 km OF THE CENTER OF HURRICANE ANITA AT 2343Z ON AUGUST 31, 1977

of the wind direction measured on research vessels and ships of opportunity [Stewart and Barnum, 1975]. We have used the methods derived by Stewart and Barnum [1975] and Mitsuyasu et al. [1975] to calculate s and $\theta$ Both methods are based on the wind-speed to wave-speed scaling where $G(\theta)$ is broad at high frequencies and narrow at low frequencies. For hurricane winds, both methods predict values of s considerably less than 1.0 which results in a directional spread which is too broad. Comparison of the radar measurements with coincident offshore NDBO data buoy measurements suggests that appropriate values of s range from 1.0 to 2.0. Regier [1975] has shown for a fixed-wave frequency that the directional distribution narrows as wind speed increases. This supports the larger values of s found in our measurements.

The value of s used to compute $\theta$ is based on our previous experiments [Maresca and Barnum, 1975; Maresca and Carlson, 1977] and on in situ spot measurements of the wind direction. We expect the value of s to vary across the hurricane, but no attempt has been made to account for this effect. Nevertheless, application of this directional model does result in wind direction maps describing the hurricane surface-wind directions which agree to within 5 to $10^{\circ}$ with available in situ measurements [Maresca and Carlson, 1977, 1978], and to within 10 to $20^{\circ}$ with buoy-derived wind direction fields produced from data recorded over 20-hour periods. The solution of Eq. (3) for $\theta$ results in a left-right wind direction ambiguity relative to the radar line of sight. This ambiguity can be resolved from well-known cyclonic patterns of a tropical storm.

## SKYWAVE RADAR-DERIVED TRACK OF HURRICANE ANITA

Twenty-one independent position estimates were made for Hurricane Anita over a 5-day period. The first 4 radar position estimates were not used in the WARF track because the storm had two centers during this early period as we observed in both the satellite cloud photographs and WARF wind maps. For the remaining 17 estimates, we updated the position estimates 3 to 5 times per 24-hour period. The radar

position estimates are based solely on the surface-wind circulation maps. Examples of the radar-derived surface wind circulation maps made over 4 days are shown in Figure 3. In Figure 4 a surface wind direction field derived from data recorded by NDBO buoy EB71 is compared to one of the WARF maps. These buoy-measured wind directions were recorded at 2-hour intervals during the period ±18 hours of Anita's passing EB71. We used a time-space conversion to compute the buoy-derived wind field by assuming uniform wind direction and lateral storm motion during this period. We compared the buoy-derived wind directions to the WARF-derived wind directions; agreement was within $19^{\circ}$. Agreement between the WARF-derived wind direction estimate coincident in time and space with the buoy wind direction estimate was $1^{\circ}$. Each map took between 30 and 60 minutes to complete although the measurements near the center used for positioning took less than 10 minutes. A single radar measurement of wind direction producing 16 direction arrows requires an integration time of only 12.8 s; therefore, the entire wind map could be produced in a 10-min period. Our maps took longer to complete because we took 60-s radar dwells to allow postexperiment analysis of wave height and wind speed.

Using maps similar to the ones in Figure 3, we developed a smooth skywave radar track for Anita. The WARF position estimates were compared to the interpolated positions estimated on the official smooth track of the NHC shown in Figure 5. The NHC track was derived from an integration of individual position estimates obtained from satellite photographs, periodic aircraft reconnaissance, shore-based microwave radar and NDBO buoys. The mean displacement between the WARF position estimates and the interpolated temporal position estimates along the NHC smooth track is ±19 km.

## MEASUREMENT ERRORS

The precision of the radar-tracking measurements is dependent on the absolute position accuracy of the WARF radar, the accuracies associated with techniques used to produce the surface wind maps by radar, and the uncertainties in determining a storm center based on the surface-wind circulation field.

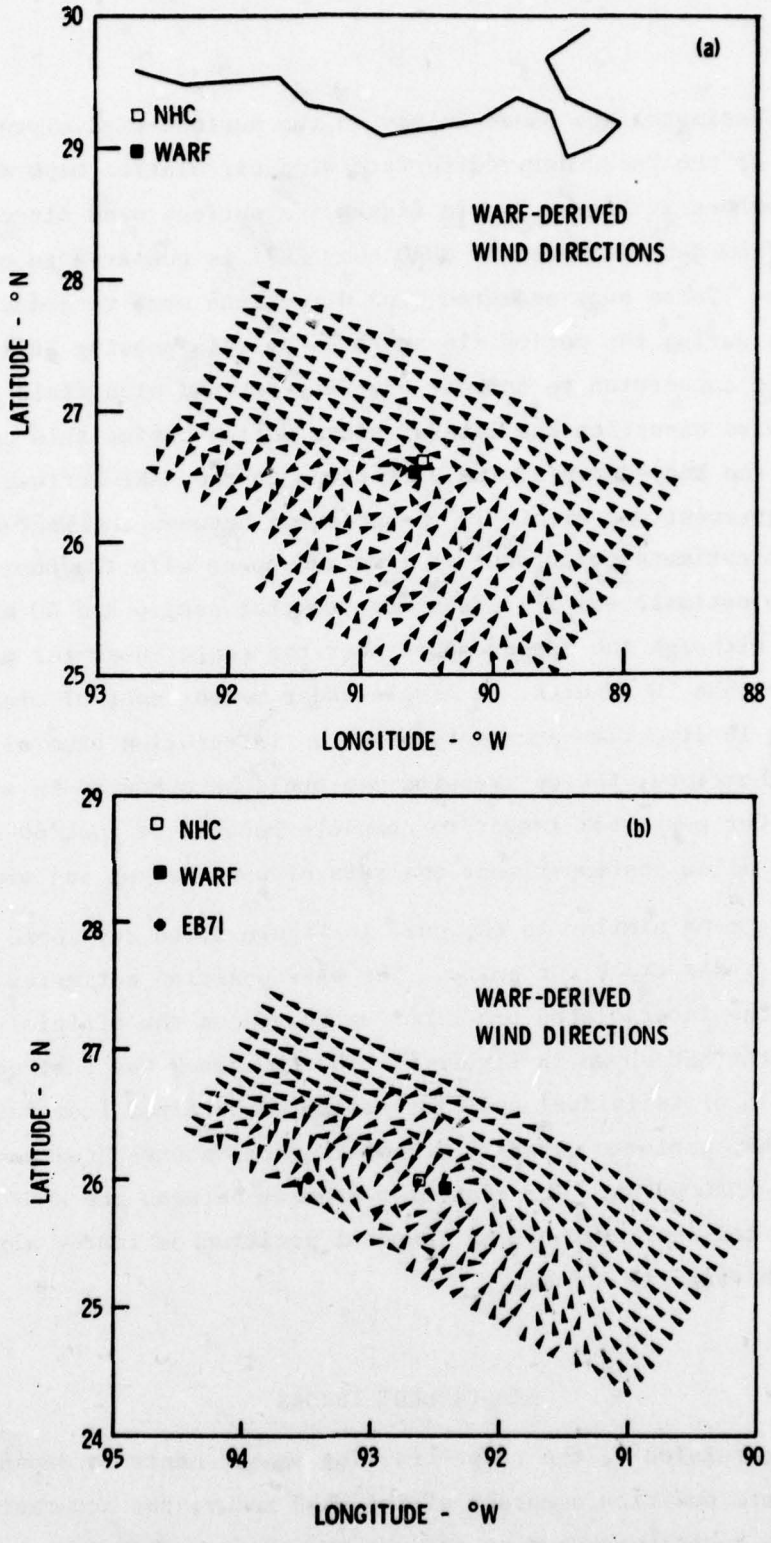


FIGURE 3 WARF-DERIVED SURFACE WIND MAPS FOR ANITA MADE AT (a) 1700Z ON AUGUST 30, 1977, (b) 2140Z ON AUGUST 31, 1977, (c) 1934Z ON SEPTEMBER 1, 1977, AND (d) 0456Z ON SEPTEMBER 2, 1977

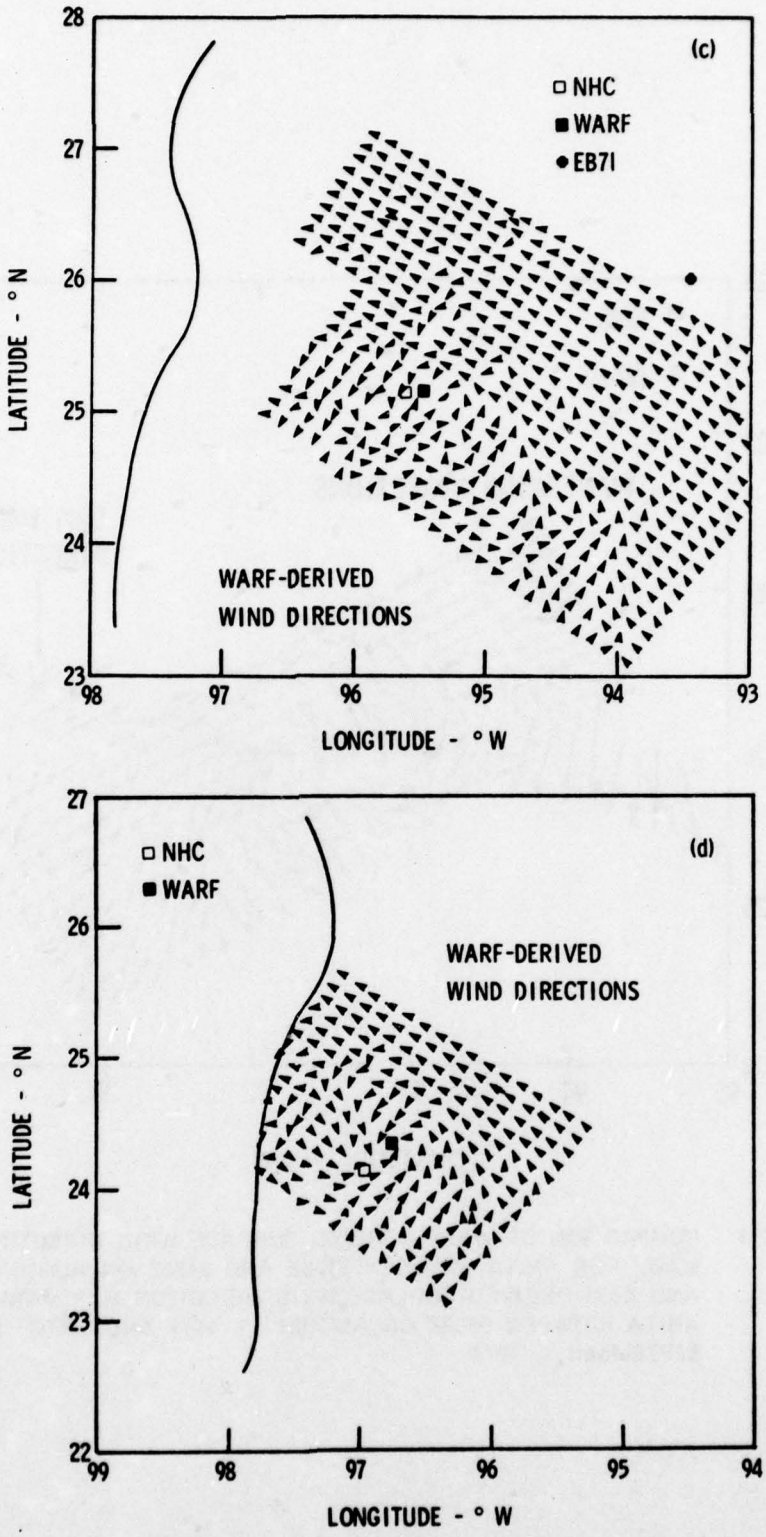


FIGURE 3 (Continued)

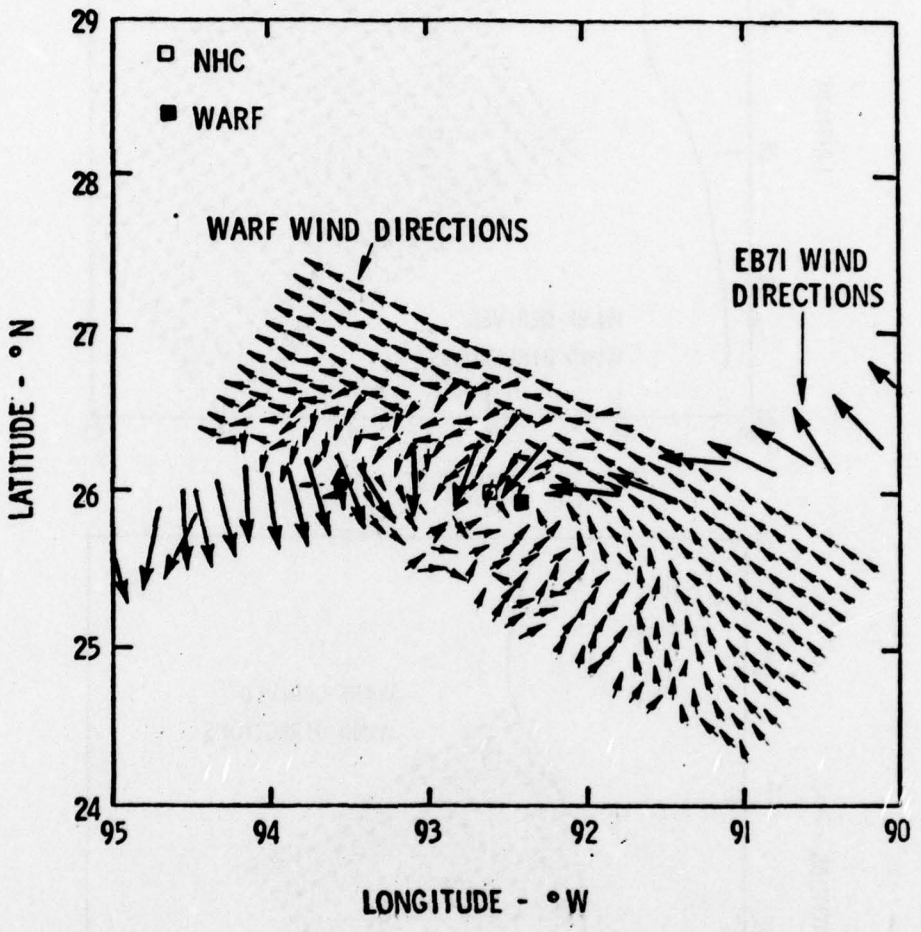


FIGURE 4 COMPARISON OF WARF-DERIVED SURFACE WIND DIRECTION MAP MADE FOR ANITA BETWEEN 2125Z AND 2155Z ON AUGUST 31, 1977 AND EB71-DERIVED SURFACE WIND DIRECTION MAP MADE FOR ANITA BETWEEN 0600Z ON AUGUST 31, 1977 AND 1800Z ON SEPTEMBER 1, 1977

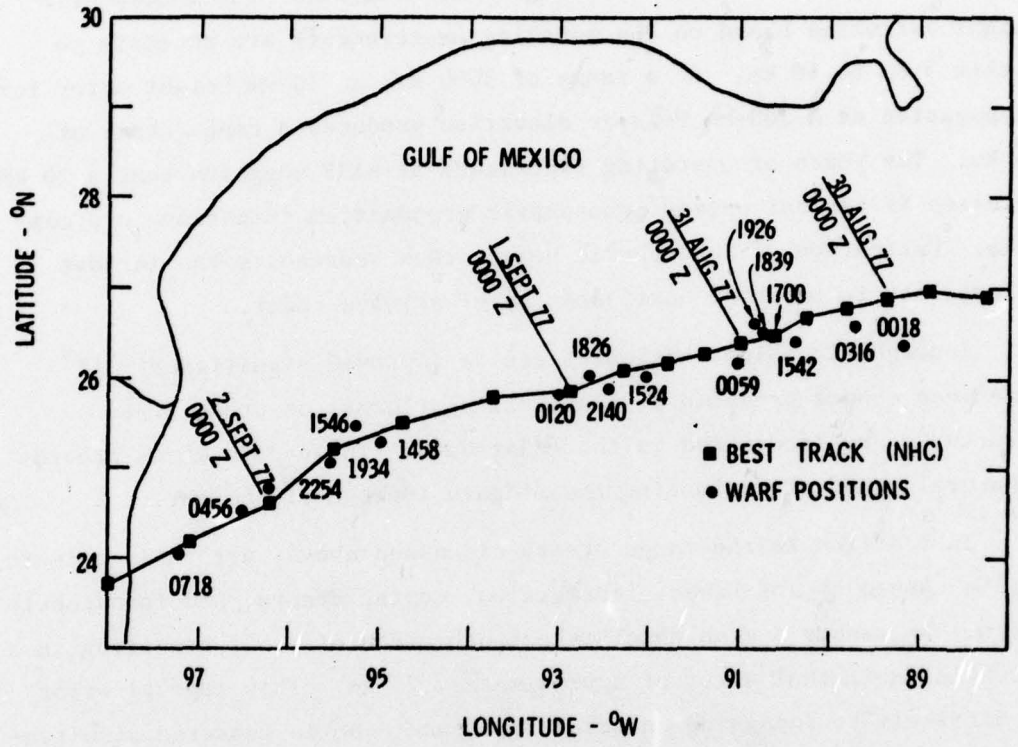


FIGURE 5 COMPARISON OF THE WARF-DERIVED POSITIONS WITH THE NHC-DERIVED TRACK OF HURRICANE ANITA

## A. Absolute Position Accuracy of WARF

The absolute position accuracy of the WARF radar depends in part on the precision of midpath ionospheric height estimates. However, direct measurements of midpath ionospheric height are generally impractical to make. We use overhead vertical-incidence soundings to estimate ionospheric height. In the absence of a reference echo, we can obtain an absolute range accuracy of approximately 20 km using only the vertical-incidence ionospheric height measurements. The ionospheric height estimates based on the sounding measurements are accurate to within 5 km to 10 km. At a range of 3000 km, a 10-km height error for propagation at a 300-km F-layer elevation produces a range error of $\pm 6$ km. Ten years of operating experience at WARF suggests that a 20 km accuracy is typical unless ionospheric propagation conditions are complex. Estimation of ionospheric height thus represents the largest uncertainty in tracking hurricanes by HF skywave radar.

Ionospheric height estimates can be improved significantly if reference echoes produced by land, oil platforms, or other fixed structures are identified in the radar data. These references provide a natural means of estimating the midpath ionospheric height.

In addition to the range errors discussed above, errors in azimuth may be caused by instrument imprecision, coning errors, and ionospheric tilts. We assume a mean absolute azimuth error of $0.5^{\circ}$, resulting in a potential azimuthal error of approximately 25 km. This type of error is difficult to recognize unless a reference echo is measured simultaneously by the radar.

## B. Accuracy of Radar-Derived Surface Wind Maps

The location of the storm center by radar is not strongly influenced by the accuracy of the directional model. Reasonable estimates of s, and subsequently $\theta$, are sufficient to produce an internally consistent map from which to locate the storm center. The primary sources of error in constructing a radar-derived surface-wind distribution map are the directional ambiguity inherent in Eq. (3), the influence of ocean scattering patch dimensions, and the density of the radar measurements near the storm center.

The method of resolving the left/right ambiguity is described in Maresca and Carlson [1977]. Near the center, the effect of the ambibuity in azimuth is negligible because the power ratio of the approaching to receding waves changes sign. The ambiguity is more difficult to resolve in range because the wind direction is approximately perpendicular to the radar beam. An iterative technique is used to select a center beginning in the outer regions of the storm where the ambiguity is easily resolved. Nevertheless, the final selection of a center is somewhat subjective. After several maps are compiled, the pattern that develops in the surface wind circulation simplifies the selection. The error caused by the ambiguity is difficult to isolate and quantify. Further comparisons of surface wind-direction measurements made simultaneously by WARF and by other sensors will help quantify the overall accuracy of the radar-derived wind maps.

The dimensions of the ocean scattering patch used in these measurements was 15 km in range by 25 km in azimuth. The effect of the size of the scattering patch on the wind speed and direction estimates throughout different regions of the hurricane was investigated in Maresca and Carlson [1977]. The simulations suggested that only in the eye region (±20 km of the center) where a $180^{o}$ shift in wind direction is possible over the scattering patch does the potential for large errors exist. Outside the eye, from the region of maximum winds outward, the errors are minimal.

The measurement density or spatial coverage of the radar affects the accuracy of the hurricane position estimate. The measurements made during Caroline and Kate were not as dense as those made for Eloise, Anita, and Babe. As a result, the storm centers for Caroline and Kate were less clearly defined than for the other hurricanes. The reliability of the position estimate improved with an increase in the number and density of the measurements. Experience dictates the importance of completely mapping the entire wind pattern near the eye for reliable position estimates based on surface wind circulation.

## C. Accuracy of Hurricane Position Based on Surface Wind Circulation

The radar-derived surface-wind-direction maps are internally consistent with respect to absolute position. Comparison of corresponding

NHC- and WARF-derived estimates of hurricane position for the five hurricanes shows agreement ranging from 5 km to 50 km, based upon surface-wind field measurements. Hurricanes are highly variable in time and space. It is difficult to accurately model a "universal" hurricane from which the model surface-wind direction would provide an accurate position estimate for every hurricane. The storms are frequently asymmetric and must be analyzed individually, according to their specific characteristics. An extensive analysis of the radar, buoy, and satellite wind fields has not yet been undertaken to find better ways of interpreting the radar data. A more extensive comparison of individual radar- and buoy-measured wind direction values will lead to an improved empirical model.

## SUMMARY

The tracking experiments conducted to date are limited to 5 different hurricanes. Only the Hurricane Anita data set was sufficient to develop a smooth radar-derived track spanning several days to compare to the NHC track. Agreement between the NHC Best Track and the WARF-measured track was within ±19 km. The WARF radar can be used independently or in conjunction with other sensors to estimate hurricane position.

The radar can reduce the chances of large errors caused by incorrectly identifying the hurricane eye in the satellite cloud photographs, can confirm that the cloud-level position estimate is representative of the surface position, can provide data when the cirrus clouds completely obscure the storm center to photographic analysis, and can provide additional surface analysis during the early development stages when the center may be diffuse or when several centers may be simultaneously observed. This additional data should be especially helpful for analyzing storms of weak to moderate strength. The radar position estimates can be made during both day and night periods.

ACKNOWLEDGMENTS

This research was supported by the Air Force Office of Scientific Research. We extend our appreciation to Mr. and Mrs. P. Duhon for maintaining a temporary field site during our experiments. We gratefully acknowledge the efforts of C. Powell, G. Glassmeyer, W. Preuss, and G. Tomlin in helping to collect the data at WARF.

## REFERENCES


Ahearn, J. L., S. R. Curley, J. M. Headrick and D. B. Trizna, "Tests of remote skywave measurement of ocean surface conditions," Proc. IEEE, 62(G), 681-687, 1974.

Barnum, J. R., J. W. Maresca, Jr., and S. M. Serebreny, "High resolution mapping of oceanic wind fields with skywave radar," IEEE Trans. on Antennas and Propagation, AP-25(1), 128-132, 1977.

Ewing, J. A., "Some measurements of the directional wave spectrum," J. Marine Res., 27, 163-171, 1969

Lipa, B. J., "Derivation of directional ocean-wave spectra by integral inversion of second-order radar echoes," Radio Science, 12, 425-434, 1977a.

Lipa, B. J., "Inversion of second-order radar echoes from the sea," J. Geophys. Res., 83, 959-962, 1977b.

Long, A. E., D. B. Trizna, "Mapping of North Atlantic winds by HF radar sea backscatter interpretation," IEEE Trans. on Antennas and Prop., AP-2[illegible], 680-685, 1973.

Longuet-Higgins, M. S., D. E. Cartwright, and N. D. Smith, "Observations of the directional spectrum of sea waves using motions of a floating buoy," Ocean Wave Spectra, 111-136, Prentice-Hall, Englewood Cliffs, New Jersey, 1963.

Maresca, J. W. Jr. and J. R. Barnum, "Remote measurement of the track of Hurricane Caroline by an OTH-B radar," (Abstract), paper presented at the 1975 Fall Annual Meeting of AGU, 1975.

Maresca, J. W. Jr., "Interpretation and collection of HF skywave radar sea backscatter obtained during hurricanes," (Abstract), paper presented at the 1976 Fall Annual Meeting of American Geophysical Union, San Francisco, California, December 1976.

Maresca, J. W. Jr. and C. T. Carlson, "Tracking and monitoring of hurricanes by HF skywave radar over the Gulf of Mexico," Technical Report 1, SRI International, Menlo Park, California, 1977.

Maresca, J. W. Jr. and C. T. Carlson, "HF skywave radar measurement of hurricane-generated ocean wave spectra," Proceedings of the Sixteenth Conference on Coastal Engineering, Hamburg, Germany, August 27-September 3, 1978.

Maresca, J. W. Jr. and J. R. Barnum, "Remote measurement of the position and surface circulation of Hurricane Eloise by skywave radar," Mon. Weather Rev., 1978.

Maresca, J. W. Jr., "High-frequency skywave measurements of waves and currents associated with tropical and extratropical storms," Ocean Wave Climate,(eds. M. D. Earle and A. Malahoff), Plenum Publishing Corporation, New York, 1978.

Maresca, J. W. Jr. and T. M. Georges, "HF skywave radar measurement of the ocean wave spectrum," submitted to J. Geophys. Res.

Mitsuyasu, H., F. Tasai, T. Suhara, S. Mizuno, M. Ohkusu, T. Honda, and K. Rikiishi, "Observations of the directional spectrum of ocean waves using a clover leaf buoy," J. Phys. Oceanog., 5, 4, 750-760, 1975.

Regier, L. A., "Observations of the power and directional spectrum of oceanic surface waves," Ph.D. Thesis, University of California, San Diego, California, 1975.

Sheets, R. C., and P. Grieman, "An Evaluation of the accuracy of tropical cyclone intensities and locations determined from satellite pictures, NOAA Technical Memorandum ERL WMPO-20, U.S. Department of Commerce, National Oceanic and Atmospheric Administration, Environmental Research Laboratories, February 1975.

Stanford Research Institute, "SRI Remote Measurements Laboratory Research Capabilities,"brochure, Menlo Park, California, August 1977.

Stewart, R. H., and J. R. Barnum, "Radio measurements of oceanic winds at long ranges: an evaluation," Radio Science, 10, 853-857, 1975.

Tyler, G. L., C. C. teague, R. H. Stewart, A. M. Peterson, W. H. Munk, and J. W. Joy, "Wave directional spectra from synthetic aperture observations of radio scatter," Deep-Sea Res., Vol. 21, No. 12, pp. 989-1016, 1974.

# APPENDIX C

## HF SKYWAVE RADAR TRACK OF TROPICAL STORM DEBRA

by

J. W. Maresca, Jr.
C. T. Carlson

To be Submitted to
Monthly Weather Review
1978

This work was performed by SRI International, Menlo Park, California, and was sponsored by the Air Force Office of Scientific Research.



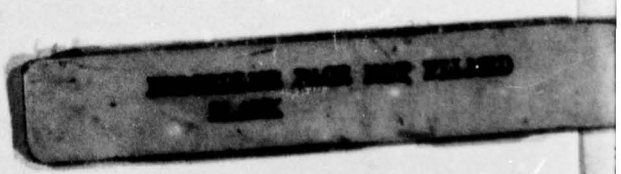

# HF SKYWAVE RADAR TRACK OF TROPICAL STORM DEBRA

J. W. Maresca, Jr. and C. T. Carlson
SRI International, Menlo Park, CA

Tropical storm Debra was tracked over a two day period using the Wide Aperture Research Facility (WARF) HF skywave radar. Tracking began at 1800Z on 27 August 1978 while Debra was only a depression and continued through landfall at about 0000Z on 29 August 1978. Seven position estimates were made from radar-derived surface wind direction maps. At about 1800Z on 28 August 1978 Debra intensified to a tropical storm, and the WARF radar position estimates were compared to reconnaissance aircraft, the Galveston microwave Doppler radar, and satellite position estimates for two different time periods. Agreement was 25±15 km, 22±10 km and 63±10 km, respectively.

# HF SKYWAVE RADAR TRACK OF TROPICAL STORM DEBRA

J. W. Maresca, Jr. and C. T. Carlson

SRI International
Menlo Park, California 94025

## I INTRODUCTION

The surface wind and wave fields of hurricanes can be monitored remotely using a high-resolution HF skywave radar. Propagation of the radio waves via the ionosphere permits propagation to distances greater than 3000 km. We conducted experiments at the SRI-operated Wide Aperture Research Facility (WARF) HF skywave radar that demonstrated the feasibility of tracking tropical storms and mapping the intensity of the winds and waves in all regions of the storm.[1-6] The surface wind direction maps can be routinely produced. A track can be developed by locating the center of the storm from each wind direction map. A track was developed for hurricane Anita[5] from 17 wind-direction maps. The WARF radar-determined positions were compared to interpolated positions along the official track developed by the National Hurricane Center (NHC), and the relative agreement was within 19 km.

Between 1800Z on 27 August 1978 and 0100Z on 29 August 1978, the WARF skywave radar was used to track tropical storm Debra. Debra intensified from a weak tropical depression to a tropical storm during this time. The purpose of this paper is to show the results of long-range radar tracking of a weak storm that has a large and poorly-defined center. All of the Debra measurements were made at distances greater than 2800 km from the radar via the F layer. The radar position estimates were computed from seven WARF-derived surface wind direction maps, and were compared to satellite, reconnaissance aircraft, and the Galveston shore-based radar position fixes. All position fixes were compared to the aircraft position fixes at approximately 2100Z and

2400Z on 28 August 1978. The mean differences between the aircraft positions and the WARF-radar, satellite, and Galveston radar were 25±15 km, 44±6 km, and 7±3 km, respectively.

## II THE MEASUREMENTS

A storm center is determined from the WARF-maps of the surface wind direction field. The WARF wind direction estimates are derived from the predominant direction of ocean waves over a rectangular area approximately 15 km x 25 km. The sea backscatter is range and Doppler processed for coherent integration times of 12.8 s to produce a sea-echo Doppler spectrum. Wind direction is estimated from the ratio of the upwind to downwind first-order echoes of the Doppler spectrum. A surface wind map is produced from 500 to 1000 individual wind direction estimates. The time required to map the wind direction field for Debra was approximately 45 min. However, this time can be reduced to 10 min under operational situations, because the WARF usually requires less than 10 min to collect and analyze all the data required to identify a storm center.

The accuracy of locating the storm center from the WARF-derived wind maps is dependent on the absolute position accuracy of the radar, the accuracy of the wind direction maps, and the uncertainties in determining the storm center from the surface wind circulation. The location of the wind map is dependent on, among other things, the height and tilt of the ionosphere. Estimates of the ionospheric height can be made from overhead vertical-incidence soundings. In some instances, these soundings are not representative of the actual propagation conditions at midpath. Uncertainties in properly estimating the midpath ionospheric height can result in errors of ±20 km or more. We improved the accuracy of our estimates of the ionospheric height for Debra over those made for hurricane Anita by recording backscatter along the coast both before and after the data for each wind map was collected. The ionospheric height was calculated from the known location of the land and this height was used to locate the wind maps.

Ionospheric motions and irregularities and multiple-path propagation may contaminate the radar measured sea-echo Doppler spectrum and may require more radar measurements to obtain high quality data at each measurement location. These additional radar measurements increase the time required to produce a wind map. Severe contamination may prevent the collection of data at specific locations. The wind direction measurement, however, is not extremely sensitive to this contamination, and more than 95% of the data recorded for Debra from sequential radar scans were used in this analysis. Moreover, the ionosphere was severely disturbed during most of this tracking experiment. In addition, a strong sporadic-E layer prevented propagation to the Gulf of Mexico between 1730Z and 2030Z on 28 August 1978. This was the first time in all six hurricanes that were tracked with WARF since 1975 that the propagation conditions prevented data collection. Nonetheless, the WARF measurements of Debra were taken during both day and night, and wind maps were made every 3 to 5 hours during our experiment.

## III WARF-DERIVED TRACKS

Four of the seven WARF wind maps made for Debra are shown in Figure 1. The maps are representative of the development of the storm from a weak depression to a tropical storm. Debra did not intensify to a tropical storm until 1800Z on 28 August 1978. The WARF position estimates and the official National Hurricane Center (NHC) track are shown in Figure 2. There are large differences between the WARF position estimates and interpolated positions on the official track between 1800Z on 27 August 1978 and 0300Z on 28 August 1978. WARF positions are about 125 km west of the NHC positions. Part of this difference can be explained by the inability by all sensors to precisely locate the storm from its large asymmetrical center. The WARF wind map shown in Figure 1a is representative of the four WARF wind maps taken at this time.

The potential sources of error in the WARF-derived positions are associated with the absolute position (range and azimuth) accuracy of

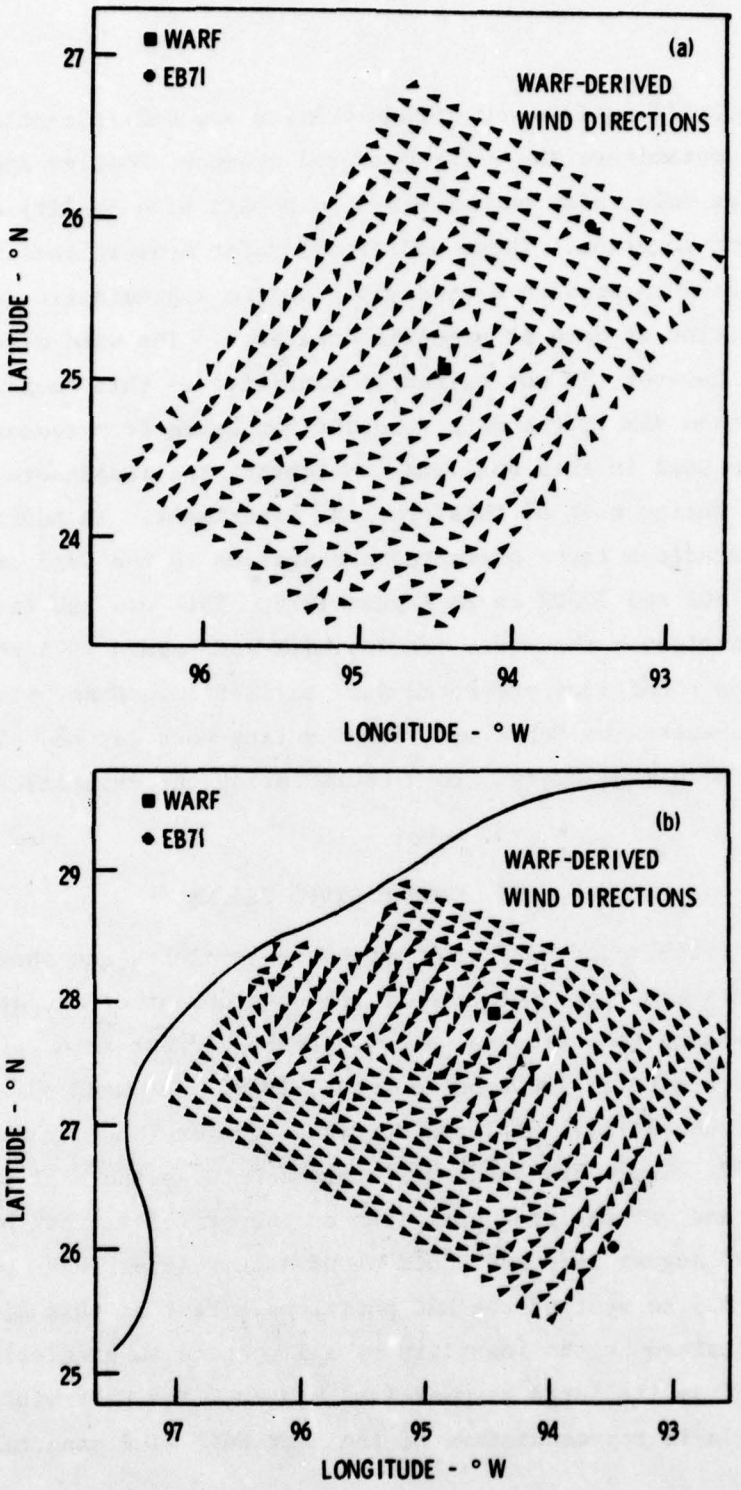


FIGURE 1 WARF-DERIVED SURFACE WIND MAPS FOR DEBRA MADE AT (a) 1801Z ON AUGUST 27, 1978, (b) 1600Z ON AUGUST 28, 1978, (c) 2049Z ON AUGUST 28, 1978, AND (d) 0017Z ON AUGUST 29, 1978

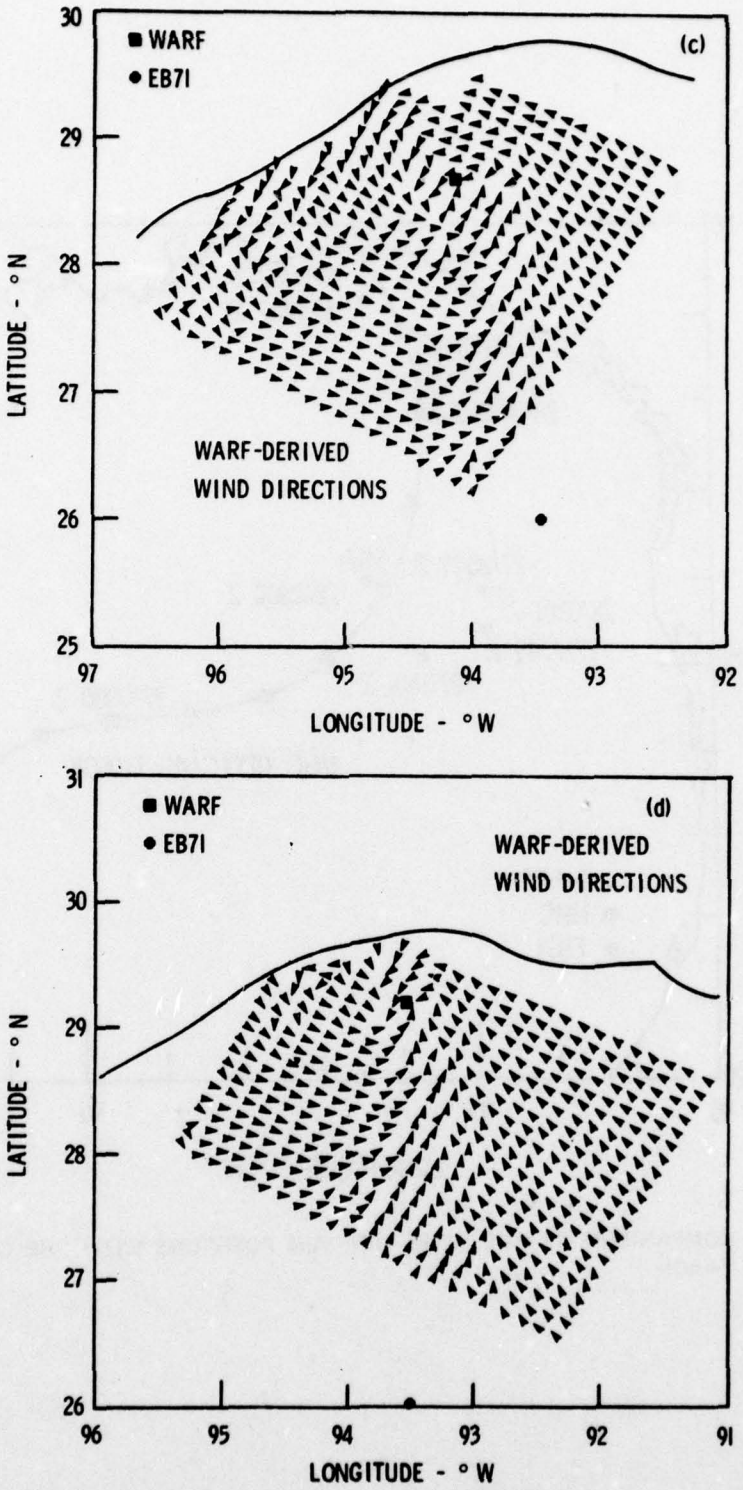


FIGURE 1 (Continued)

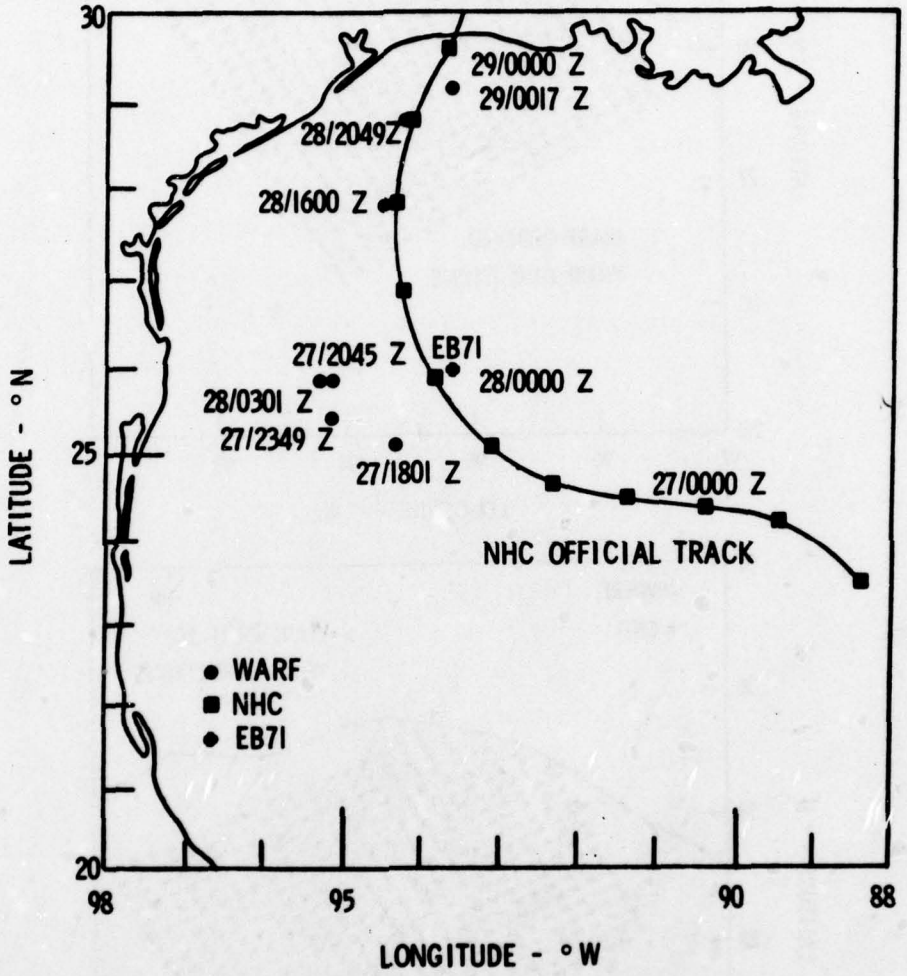


FIGURE 2 COMPARISON OF THE WARF-DERIVED POSITIONS WITH THE OFFICIAL NHC TRACK

the radar and the location of a storm center from the wind map. The absolute range position error is a function of the midpath ionospheric height. Overhead vertical-incidence soundings taken at WARF generally provide reasonable estimates of the ionospheric height at midpath. Sometimes large position errors can result if the radar signals are actually propagating from a different ionospheric layer than the one determined from the vertical-incidence soundings. We minimized this source of error by taking radar measurements along the Mexican-United States coastline. The land-echo can be easily distinguished from the sea-echo. Since the coast is approximately perpendicular to the radar beam, the location of the land-sea boundary can be identified in range but not in azimuth. Using this method, we could accurately calculate the ionospheric height at midpath, and increase the accuracy and reliability of the range position estimates. The absolute range position estimate is no more than 10 km. Azimuth errors, caused by ionosperic tilting, are also possible. No attempt was made to correct for this type or error. Generally, azimuth errors are no larger than 25 km. The surface circulation is well identified. Positive identification of the westerly flow north of the storm and the easterly flow south of the storm indicate that the storm could be as large as 120 km along an axis running northeast. We placed the storm center along an axis running parallel and halfway to these winds. It is usually more difficult to identify the storm center in range because of the left-right ambiguity associated with each wind direction measurement. However, the northerly flow emanating from the NW corner of the map and the southeasterly flow emanating from the SE corner of the map are unmistakable. The size of the storm center, based solely on the WARF wind direction, is 120 km x 120 km. We could only justify the selection of a storm center 50 km further out in range based on surface circulation and another 20 km based on the absolute position error. However, we would still be more than 50 km west of the official track position. The consistency of the four WARF positions and the high quality of the radar-wind maps suggest that the official track should be adjusted westward.

The WARF-wind maps compiled between 1000Z on 28 August 1978 and 0017Z on 29 August 1978 are shown in Figure 1(b) through (d). The storm intensified during this period. The center is asymmetrical with the longest axis elongated along an east-west axis. A reconnaissance aircraft flight through the center at 1700Z on 28 August 1978 measured the center as 75 km x 150 km. Peak surface winds of 21 m/s were estimated from the aircraft.

In Table 1 we compared the WARF position estimates to the position estimates made from the reconnaissance aircraft, shore-based Doppler microwave radar, and satellite cloud photography. The position estimates from all four sensors are shown in Figure 3. We computed the deviation of the reconnaissance aircraft position estimates of the storm location and the WARF, satellite, and Galveston radar positions for two time periods at approximately 2100Z and 2400Z on 28 August 1978. The deviations are given in Table 2 for 2100Z and 2400Z. As expected, the agreement between the Galveston radar and the aircraft was the best. The WARF position estimates were generally south of the aircraft fixes and the satellite positions were generally north of the aircraft fixes. In general there is poor agreement between all four sensors and the official best track position at 2100Z. An analysis and discussion of the deviation of the satellite and aircraft reconnaissance positions from the official track is given in Sheets and Grieman.[7] The average deviation of the satellite positions from the official track for data analyzed from three different satellites is about 65 km but this average deviation decreases for intense storms. The average deviation of the aircraft reconnaissance fixes from the official best track is approximately 25 km. Averaging the satellite and skywave radar measurements results in improved position accuracy and takes advantage of the strengths of both of these remote sensing tools. We averaged the WARF and satellite position estimates and compared these positions to the aircraft positions; agreement was within 20±5 km.

Table 1

DEVIATION OF THE WARF RADAR POSITION ESTIMATE FROM THE RECONNAISSANCE AIRCRAFT, MICROWAVE DOPPLER RADAR, AND SATELLITE POSITION ESTIMATES FOR TROPICAL STORM DEBRA AT 2100Z AND 2400Z AUGUST 28, 1978.

| Time (GMT) | Sensor | Deviation (km) |
|---|---|---|
| 2100 | Aircraft | 10 |
| | Doppler radar | 13 |
| | Satellite | 53 |
| 2400 | Aircraft | 40 |
| | Doppler radar | 32 |
| | Satellite | 73 |

Table 2

DEVIATION OF THE WARF RADAR, MICROWAVE DOPPLER RADAR, SATELLITE CLOUD PHOTOGRAPH, WARF-SATELLITE POSITION ESTIMATES FROM THE RECONNAISSANCE AIRCRAFT POSITION ESTIMATES FOR TROPICAL STORM DEBRA AT 2100Z AND 2400Z AUGUST 28, 1978.

| Time (GMT) | Sensor | Deviation (km) |
|---|---|---|
| 2100 | WARF | 10 |
| | Satellite | 50 |
| | Doppler radar | 4 |
| | WARF + satellite | 25 |
| 2400 | WARF | 40 |
| | Satellite | 38 |
| | Doppler radar | 10 |
| | WARF + satellite | 15 |

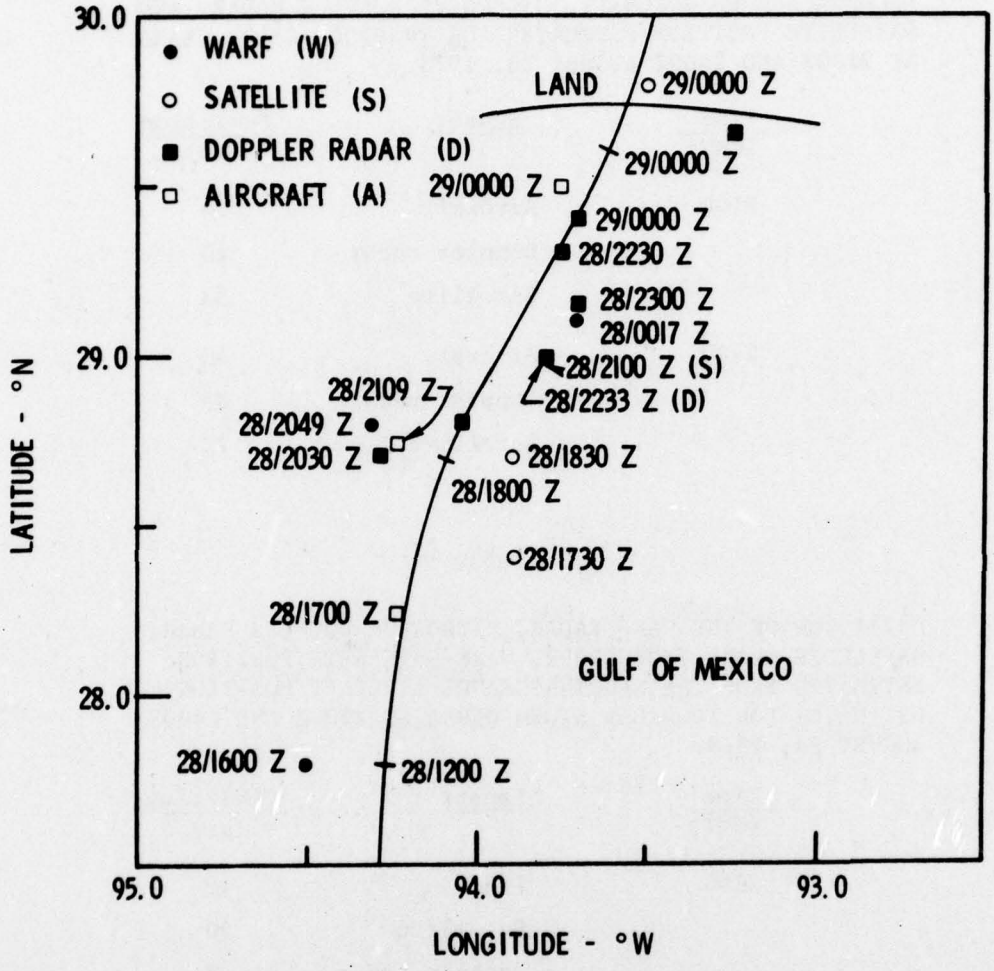


FIGURE 3 COMPARISON OF THE WARF-DERIVED POSITIONS WITH THE RECONNAISSANCE AIRCRAFT-, SHORE-BASED MICROWAVE DOPPLER RADAR-, AND SATELLITE-DERIVED POSITIONS

## IV CONCLUSION

We have compared the WARF radar measurements to the official NHC track and to position fixes determined by other conventional sensors. We attribute the large difference between the WARF position fixes and the NHC track before 1800Z on 28 August 1978 to an eastward bias in the NHC track caused by the large, poorly-defined storm center. The agreement between the WARF position fixes and the reconnaissance aircraft position fixes after 1800Z was within 25±15 km. This is quite reasonable considering the large size of the storm center associated with tropical storm Debra.

The capability to produce accurate surface wind direction maps at the time and location specified by the radar operator is an advantage of skywave radar over other available remote sensing techniques. As with early satellite cloud photographs, much information can be learned as the data base becomes larger. HF skywave radar is proving itself a valuable and reliable remote sensing tool to monitor tropical storms.

## ACKNOWLEDGMENTS

This research was supported by the Air Force Office of Scientific Research. We extend our appreciation to Mr. and Mrs. P. Duhon for maintaining a temporary field site during our experiments. We gratefully acknowledge the efforts of C. Powell, G. Glassmeyer, W. Preuss, and L. Robinson in helping to collect the data at WARF.

## REFERENCES


1 J. W. Maresca, Jr. and C. T. Carlson, "Tracking and Monitoring Hurricanes by HF Skywave Radar over the Gulf of Mexico," Technical Report 1, SRI International, Menlo Park, California (1977).

2 J. W. Maresca, Jr. and C. T. Carlson, "Tracking and Monitoring Hurricanes by HF Skywave Radar over the Gulf of Mexico," Final Report, SRI International, Menlo Park, California (1978).

3 J. W. Maresca, Jr. and J. R. Barnum, "Remote Measurements of the Position and Surface Circulation of Hurricane Eloise by Skywave Radar," accepted by Monthly Weather Review.

4 J. W. Maresca, Jr., "High Frequency Skywave Radar Measurements of Waves and Currents Associated with Tropical and Extra-Tropical Storms," Ocean Wave Climate, eds. M. D. Earle and A. Malahoff (Plenum Publishing Company, New York, 1978).

5 J. W. Maresca, Jr. and C. T. Carlson, "Tracking Hurricane Anita by HF Skywave Radar," submitted to J. Geophys. Res.

6 J. W. Maresca, Jr. and C. T. Carlson, HF Skywave Radar Estimates of Hurricane Winds and Waves," Proceedings of the Sixteenth Conference on Coastal Engineering, Hamburg, Germany (August 1978).

7 R. C. Sheets and P. Grieman, "An Evaluation of the Accuracy of Tropical Cyclones Intensities and Locations Determined from Satellite Pictures," NOAA Technical Memorandum ERL WMPO-20, U.S. Department of Commerce, National Oceanic and Atmospheric Administration, (1975).

APPENDIX D

# HF SKYWAVE RADAR MEASUREMENT OF HURRICANE WINDS AND WAVES

by

J. W. Maresca, Jr.
C. T. Carlson

Proceedings of the Sixteenth
Conference on Coastal Engineering
New York
1978

This work was performed by SRI International, Menlo Park, California, and was sponsored by the Air Force Office of Scientific Research. This paper will also be submitted to Science.

# HF SKYWAVE RADAR MEASUREMENT OF HURRICANE WINDS AND WAVES

Joseph W. Maresca, Jr. and Christopher T. Carlson*

## I. INTRODUCTION

We measured significant wave height, and surface wind speed and direction for the first two Gulf of Mexico hurricanes of the 1977 season by using a high frequency (HF) skywave radar. The radar measurements were made from California by using the SRI-operated Wide Aperture Research Facility (WARF). We recorded sea backscatter for hurricanes Anita and Babe, at distances more than 3000 km from the WARF, by means of single F-layer ionospheric reflection. We compiled real-time maps of the surface wind direction field within a radial distance of 200 km of the storm center, then estimated the hurricane position from these radar wind maps, and developed a track for Anita over a 4-day period between 30 August and 2 September 1977 as the storm moved westward across the Gulf of Mexico. The radar track was computed from 17 independent position estimates made before Anita crossed the Mexican coast, and was subsequently compared to the official track produced by National Hurricane Center (NHC). Agreement between the WARF position estimates and coincident temporal positions on the NHC smooth track was ±19 km. At approximately 0000Z on 1 September 1977, Anita passed within 50 km of the National Data Buoy Office (NDBO) open ocean moored buoy EB-71, and provided us with the opportunity to compare WARF estimates of the significant wave height, and surface wind speed and direction in all four quadrants of the storm with those made at the buoy. Agreement between the WARF and EB-71 measurements was within 10%.

Two days after Anita crossed land, tropical storm Babe--a weaker, short-lived storm--developed. WARF estimates of the significant wave height, and surface wind speed and direction were made for selected regions of the storm.[1] No in situ wave measurements were available for comparison to the WARF measurements. WARF estimates of the wind speed were compared to wind speed measurements made at nearby oil platforms, and surface wind speeds computed from flight level winds (305 m) measured by a NOAA reconnaissance aircraft. Agreement was again within 10%. The purpose of this paper is to describe the capability of remotely monitoring hurricanes and other open ocean storms by using an HF skywave radar. We will describe the important aspects of the WARF skywave radar, the sea-echo Doppler spectra, the method of analysis used to estimate the wave and wind parameters, and the accuracy of these radar-derived quantities.

*SRI International, Menlo Park, California 94025.

## II. WARF SKYWAVE RADAR

The Wide Aperture Research Facility (WARF)[2] is a high-resolution, experimental,high-frequency skywave radar located in central California. The radar is bistatic and operates in the HF band between 6 and 30 MHz. Ocean areas are illuminated by a 20-kW swept-frequency continuous-wave (SFCW) signal from a transmitter site located at Lost Hills, California. The energy reflected from the surface beam is received 185 km to the north at Los Banos, California. The receiving antenna array is 2.5-km long and consists of a double linear array of 256 whip antennas producing a nominal $1/2^{o}$ azimuthal beamwidth at 15 MHz. The signal propagates to and from remote ocean patches by means of one or more ionospheric "reflections."

The WARF coverage area is shown in Figure 1. The radar can be directed either east or west, and can be electronically steered in azimuth $\pm 32^{o}$ from boresight anywhere within the coverage area in $1/4^{o}$ increments. Position accuracy is a function of midpath ionospheric height estimates whose uncertainty in the midpath height results in a nominal position accuracy of approximately 20 km. At any one location, the accuracy between consecutive measurements in range and azimuth is an order of magnitude better. WARF has multiple-beam capability, and sea backscatter is usually received simultaneously at four adjacent ocean areas from four different beams separated by $1/4^{o}$. The size of the ocean scattering patch is a function of the beamwidth, the range, the range cell separation, and the number of range cells averaged together. The size of the minimum scattering patch at a range of approximately 2000 km is 3 km in range by 15 km in azimuth.

## III. IONOSPHERIC PROPAGATION

The ionosphere consists of ions produced in the earth's atmosphere, primarily by solar radiation. Radio-wave propagation by means of ionospheric reflection occurs primarily between elevations of 100 km and 500 km. A graph of electron density as a function of height may show peaks in the ionospheric profile. These peaks are defined as layers and are designated by $E_s$ (sporadic-E), E, F1, and F2. They correspond to peak electron densities located at about 110, 120, 200, and 300 km above the earth, respectively. Ionospheric conditions are transient in time and space, and they depend on the stability and strength of the electron density profile.

The minimum radar range for one hop ionospheric propagation is approximately 1000 km; the maximum radar range is approximately 3000 km. The ionosphere will support propagation to a specific range over a limited frequency band. The achievable range depends on the time of day, geographical region, and ionospheric height. We use two different types of real-time ionospheric soundings at WARF to manage the ionospheric propagation. An oblique-incidence sounding, shown in Figure 2, is primarily used to determine: the relative signal strength; the radio

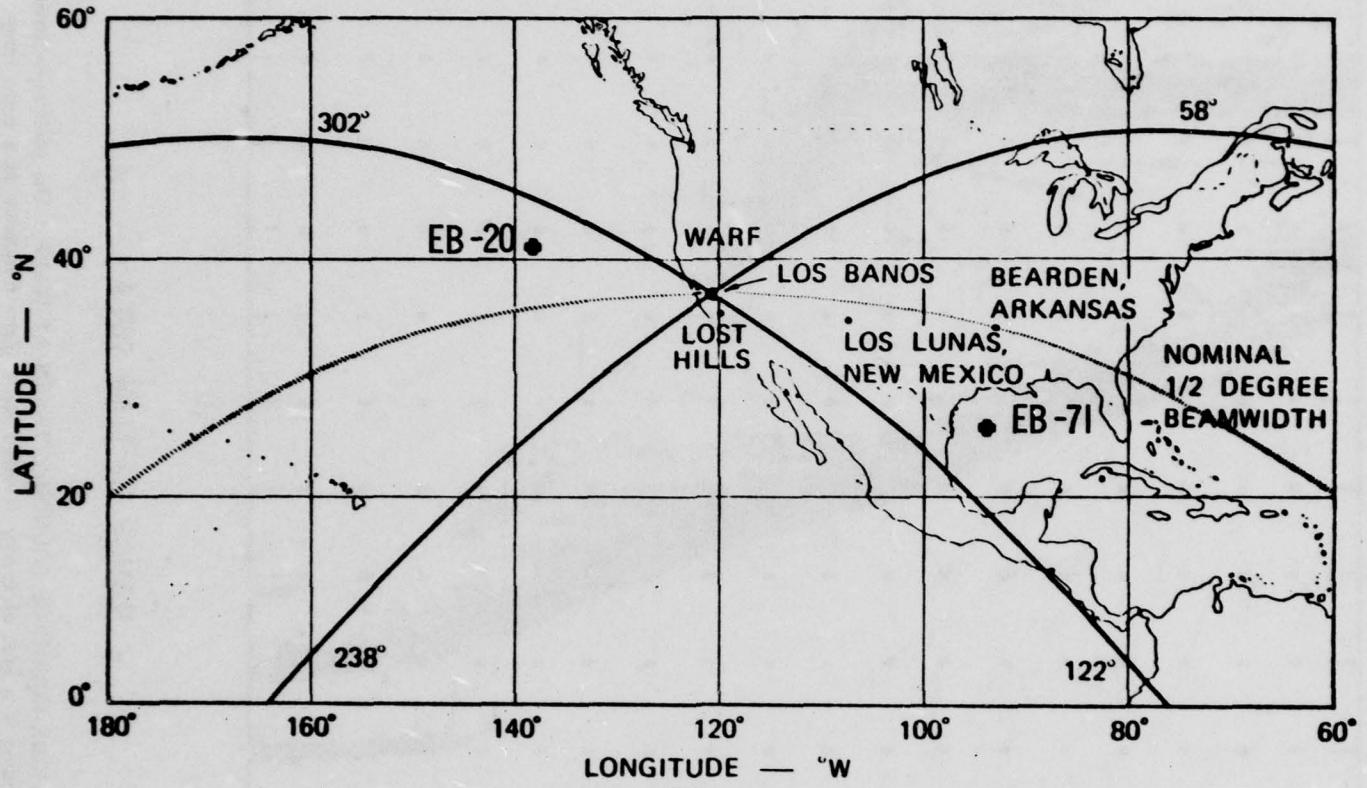


FIGURE 1 COVERAGE AREA OF THE WARF HF SKYWAVE RADAR. All Anita measurements were made west of 88°W in the Gulf of Mexico.

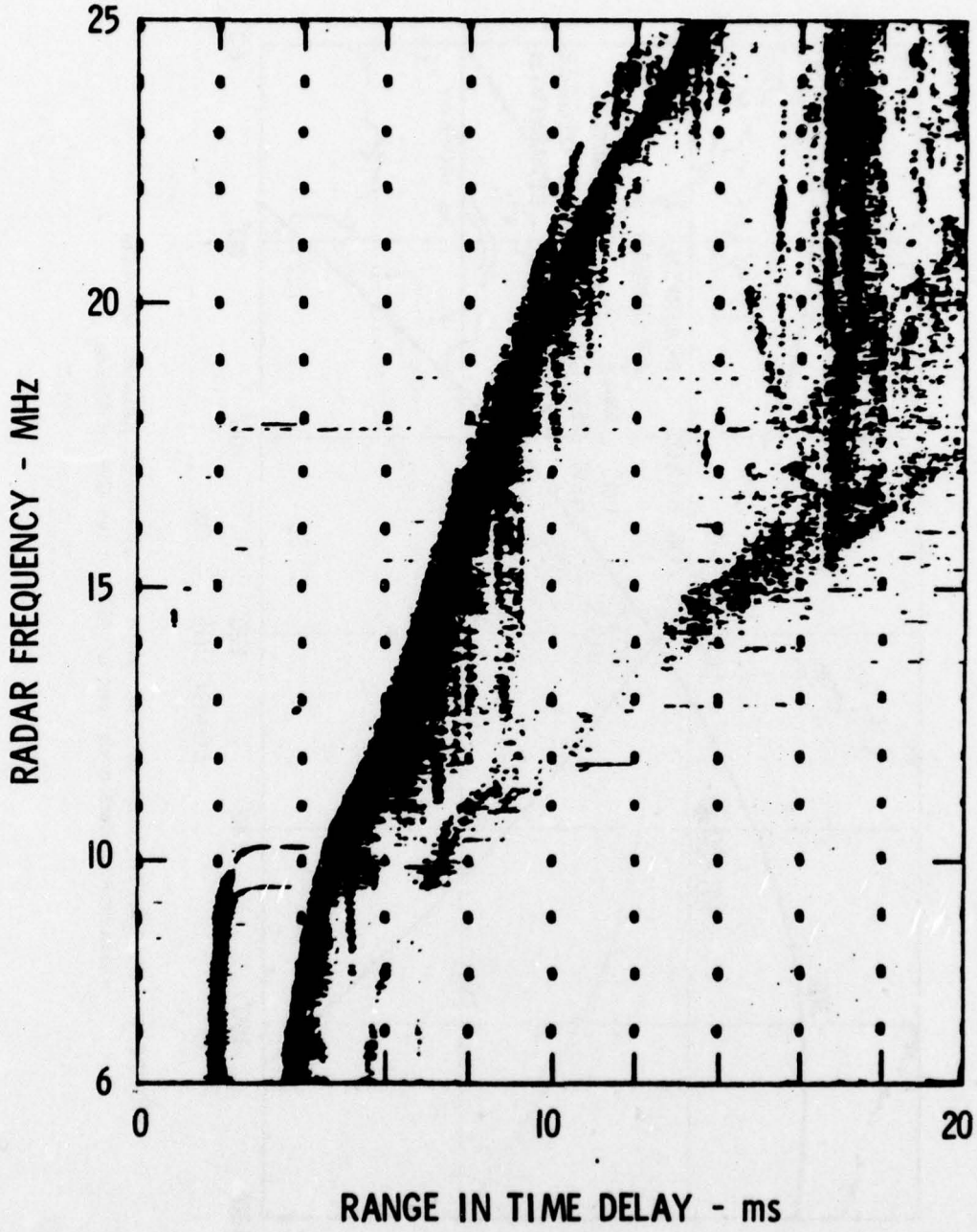


FIGURE 2 OBLIQUE-INCIDENCE SOUNDING TAKEN AT WARF. The oblique-incidence sounding is a plot of energy received for a given frequency at a given range.

frequencies that will propagate to a particular range; and certain types of ionospheric disturbances such as traveling waves, and focusing or defocusing of energy. A vertical-incidence sounding, shown in Figure 3, taken between the WARF transmitting and receiving arrays is primarily used to measure the overhead ionospheric mode structure and height of each ionospheric layer. A frequency surveillance spectrum analyzer is used to select interference-free frequency bands.

## IV. SEA ECHO DOPPLER SPECTRUM

The sea backscatter received at the WARF is coherently processed in range and Doppler to produce a sea-echo Doppler spectrum. We usually process 21 independent Doppler spectra spaced at 3-km range intervals. These spectra are obtained simultaneously at each of four adjacent radar beams. A total of 84 independent Doppler spectra are obtained for each coherent time period. We compute an average spectrum from a subset of these Doppler spectra, depending on the type of measurement and the time and space scales associated with the ocean surface features. An example of a mean sea-echo Doppler spectrum produced by averaging 112 spectra obtained from four consecutive 102.4 s coherent time periods, over a scattering patch consisting of 21 range cells and 3 adjacent beams, is shown in Figure 4.

The sea-echo Doppler spectrum shown in Figure 4 is characterized by two dominant first-order echoes surrounded by a second-order continuum. Crombie[4] interpreted the first-order echoes in terms of simple Bragg scattering that represented a resonant response between radio waves of wave number $k_o$ and ocean waves of wave number $k = 2\,k_o$. The radar measures the relative power and Doppler of the ocean waves traveling radially toward or away from the radar. The power ratio of the two first-order echoes are indicative of the wave direction of the waves of wave number k. Because k is usually large ($k > 0.5$), it is assumed that the wind direction is identical to the direction of these waves.

The wave-height spectrum is derived from the second-order structure surrounding the first-order echoes. For hurricanes, the power in the second-order echoes is large. As the total wave energy increases, the amplitude of the second-order echoes increases as illustrated in Figure 5. Barrick[5,6] derived theoretical expressions that accurately model the HF scattering process to second order. For a specific directional wave spectrum, the model computes the Doppler spectrum. The effects of the wind direction, wave directionality and the wave frequency spectrum on the modeled Doppler spectrum have been extensively studied through the use of this model.

## V. HURRICANE DATA SAMPLING

Data sampling during a hurricane is divided into two tasks to optimize the sampling time and the data quality. The spectral resolution,

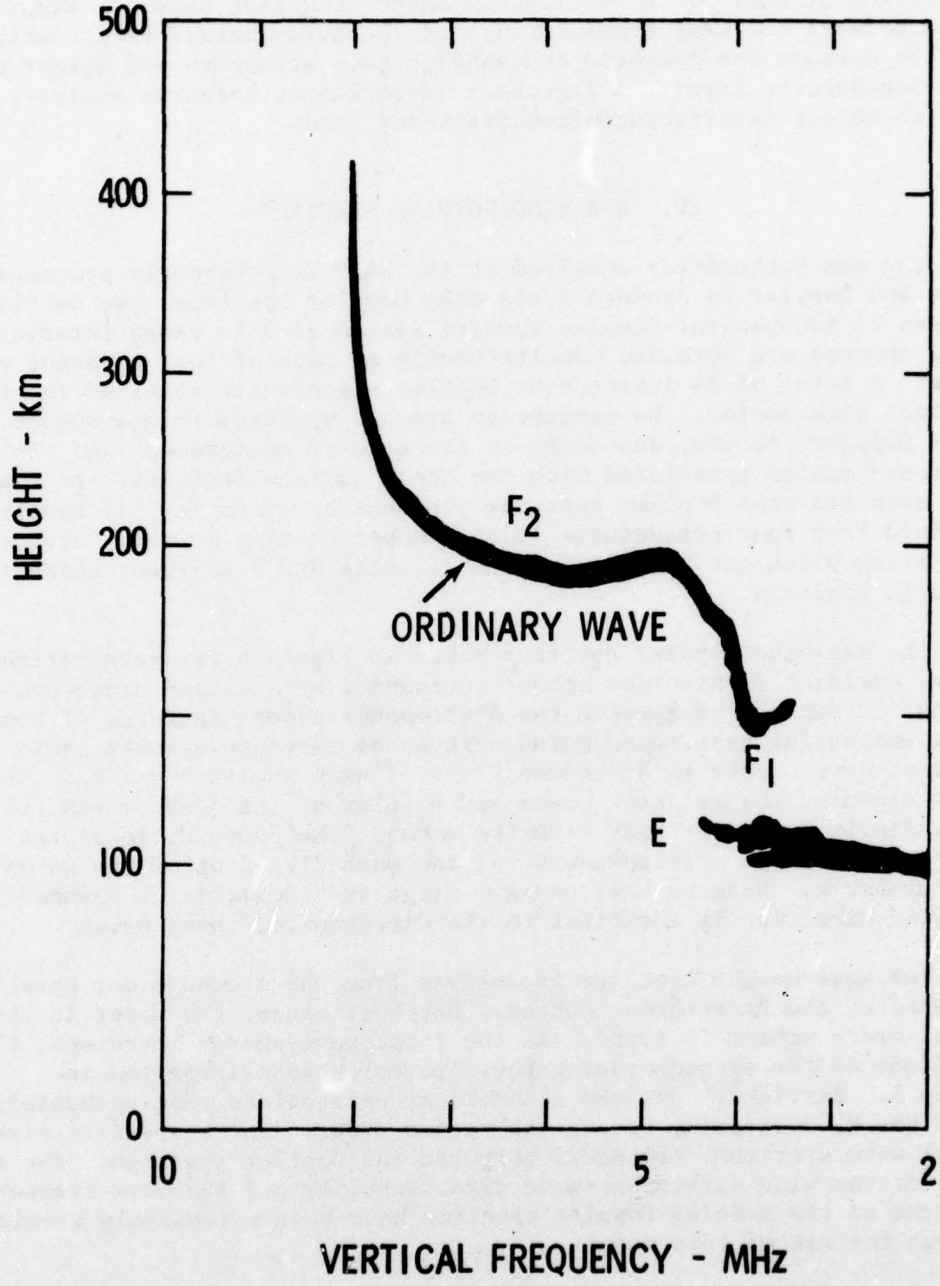


FIGURE 3 VERTICAL-INCIDENCE IONOSPHERIC SOUNDING TAKEN AT WARF. The vertical-incidence sounding is a plot of overhead energy for different frequencies.

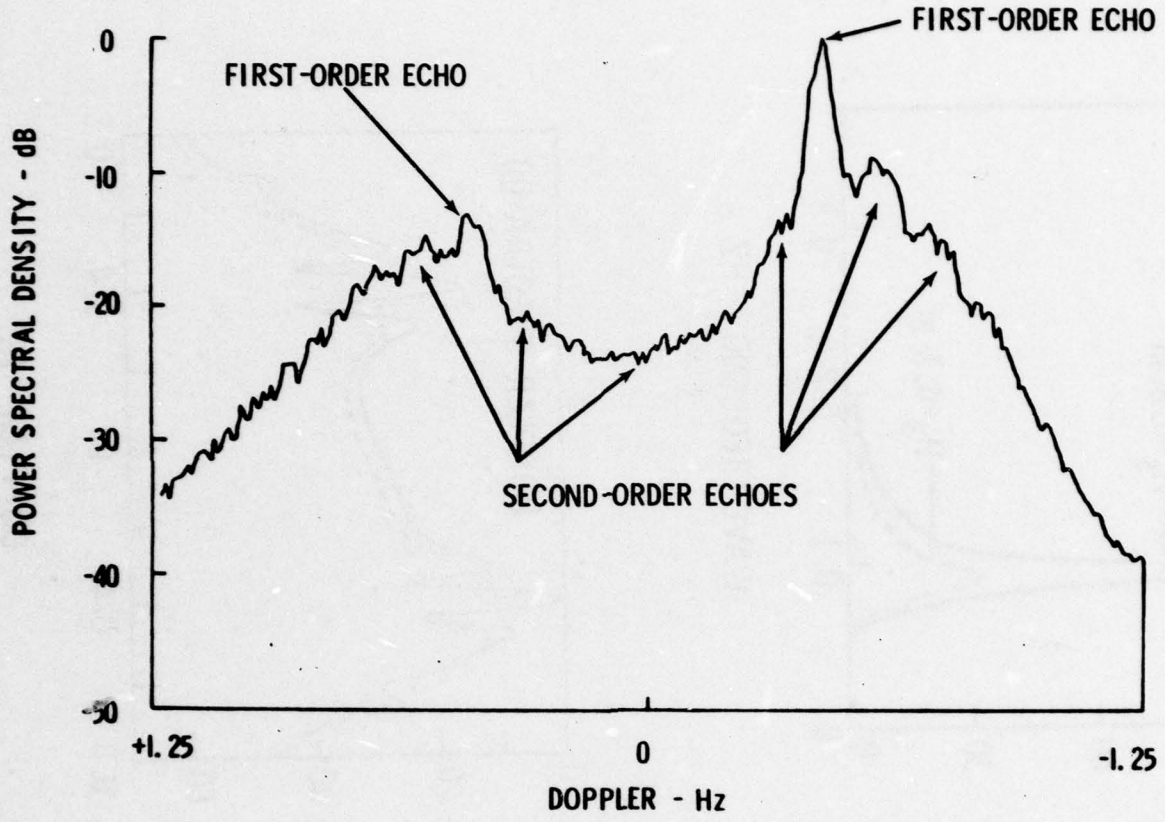


FIGURE 4 AVERAGE SEA ECHO DOPPLER SPECTRUM RECORDED WITHIN 35 km OF THE CENTER OF HURRICANE ANITA AT 2343Z ON AUGUST 31, 1977

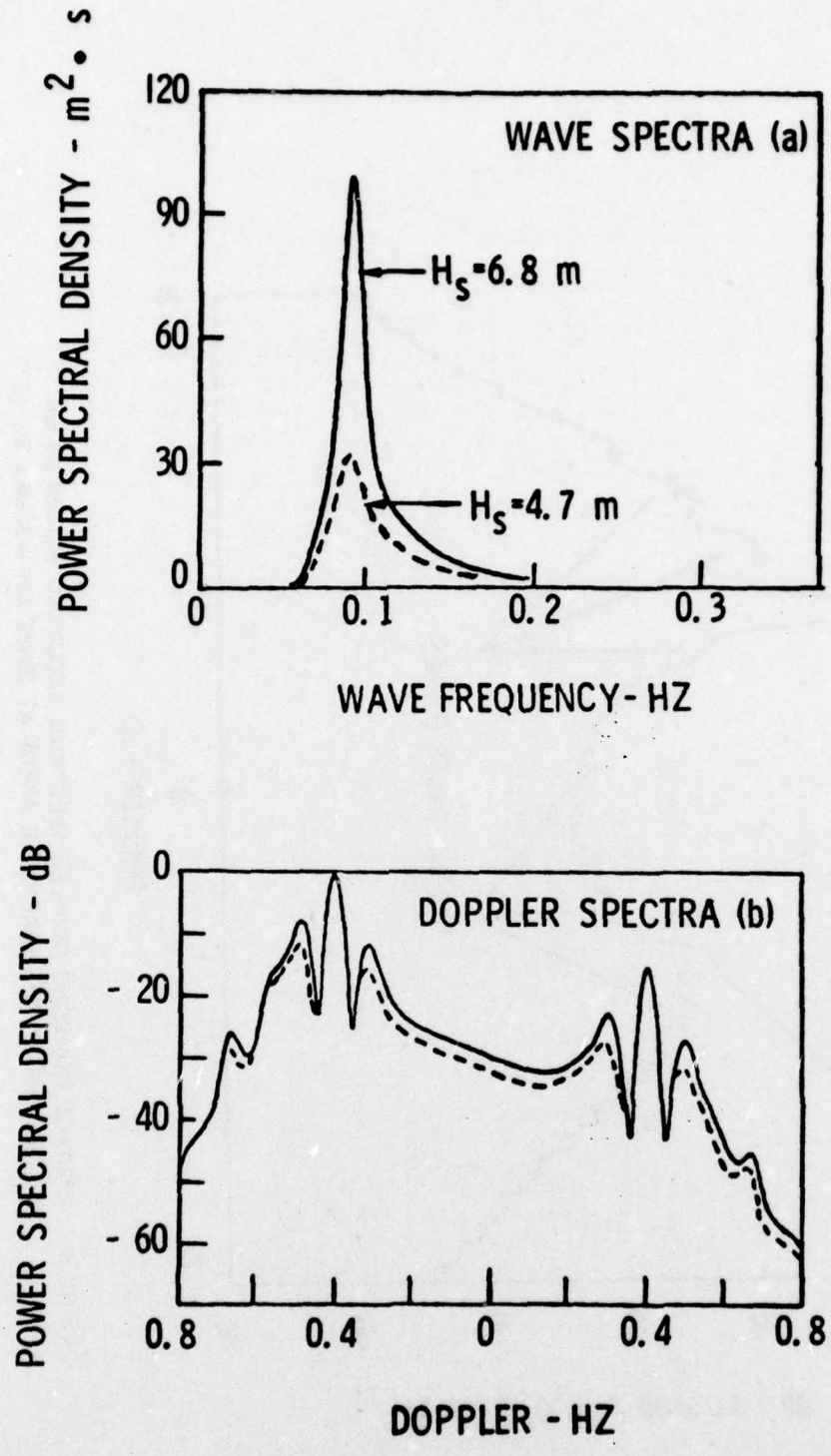


FIGURE 5 EXAMPLE OF TWO SYNTHETIC DOPPLER SPECTRA (b) PRODUCED FROM TWO INPUT WAVE SPECTRA (a) WITH THE SAME DIRECTIONAL DISTRIBUTION AND RADAR-TO-WIND DIRECTION, BUT DIFFERENT TOTAL WAVE ENERGY (0.02 Hz resolution)

directly related to the coherent integration time, can be much coarser for first-order measurements than for second-order measurements. Wind direction estimates are computed from the first-order echoes, and can be computed considerably more rapidly than wave height and wind speed estimates, which are computed from the second-order echoes. Usually, the longer the coherent integration time, the greater the influence the ionosphere has on the quality of the data.

The quality of the recorded sea backscatter depends on the ionospheric conditions over short periods--on the order of minutes. High-quality sea backscatter is obtained if the radio waves propagate by means of a strong, single, stable, coherent ionospheric layer. Sometimes the signals may be received at the same time from two or more different paths (multipath). In this case, the second or succeeding signals will be reflected from different parts of the ocean and different parts of the ionosphere, and will contaminate the sea echo received from the first path. If the ionosphere is changing in time or space during the coherent radar dwell (time period), further degradation of the data will occur. The ability to predict the ionospheric conditions would enable the radar operator to minimize the contaminating effects of the ionosphere, improve the quality of sea backscatter, and reduce the sampling time. The ionospheric soundings provide some data quality information. The vertical and oblique incidence soundings are taken every 10 minutes; a complete sounding requires approximately 3 minutes. The coherent radar measurements made at WARF require between 10 and 100 seconds to complete. Because the time required to complete a sounding is greater than the time required to record the sea backscatter data, assessment of the data quality is difficult for rapidly changing ionospheres. Therefore, real-time output of the data from the WARF site minicomputer is used to verify data quality.

The wind direction measurement is not extremely sensitive to ionospheric contamination caused by multipath or smearing because only the amplitude of the two strong first-order echoes must be measured. A coherent integration time of 12.8 seconds (0.078-Hz resolution) is sufficient to resolve the peaks of the first-order echoes. We can map the wind-direction field in a hurricane by scanning in range and azimuth. It is possible to routinely map the surface-wind-direction field of a hurricane and this can be accomplished in about 10 minutes. Once the surface-wind-direction map is made, the storm center can be identified for tracking purposes, and regions of interest can be selected for more extensive monitoring of wind speed and wave height anywhere within the storm.

The significant wave height and wind speed measurements are sensitive to ionospheric contamination. This contamination is the largest source of error in these measurements. A coherent integration time of 102.4 seconds (0.01-Hz resolution) is required to resolve the second-order echoes. The ionosphere does not generally support coherent integration time periods of this length. Multipath and ionospheric smearing can seriously degrade the weaker second-order echoes. Because of this

contamination, we are not able to routinely estimate wave height for each 102.4-second time period as we are able to calculate wind direction for each 12.8-second time period. A sampling strategy that combines careful propagation management through selection of frequencies, which result in a stable, coherent, single propagation path, and signal processing that minimizes the contaminating effects of the ionosphere are used to obtain a data set suitable for analysis. Recent work by SRI and NOAA[7] has resulted in improved methods of collecting high-quality data by sorting the data according to a spectral sharpness index. The effect of ionospheric contamination, however, is less severe for data recorded during large waves generated during a hurricane. The amplitude of the second-order echoes containing the wave height information may be stronger than the contamination effects, and thus, wave height can be calculated despite the contamination.

For the Anita and Babe wind direction measurements, we divided the data into 16 groups and analyzed three consecutive 12.8-second coherent radar dwells. Each wind direction estimate was calculated from a minimum of 15 Doppler spectra. At a range of 3000 km, the size of each scattering patch was 15 km x 25 km. It would be desirable to compute wave height and wind speed from a similar data set, but this is not generally possible. Longer coherent time periods and more independent samples of the spectra are required to obtain a high quality sample. We could collect the data over a small scattering patch by averaging over a long time, or we could increase the scattering patch size and average in space. Averaging in space is preferable because it reduces the total time required to obtain a mean Doppler spectrum. For the Anita and Babe wave height and wind speed measurements, we analyzed the data from three of the adjacent azimuth cells and 21 contiguous range cells. The total scattering patch was 63 km x 50 km. Several consecutive integration periods are required to record the data.

## VI. WIND DIRECTION MEASUREMENT

HF skywave radar has been used to map the surface-wind fields associated with large weather systems[8] and tropical storms.[9] The radar measured surface-wind directions are derived from the predominant direction of ocean gravity waves, approximately 10-m long. The waves satisfying the first-order Bragg scattering condition, $k = 2k_o$, are assumed to be tightly coupled to the wind for time scales on the order of tens of minutes. This assumption is reasonable for the high wind speed conditions associated with hurricanes. Available directional wave spectra measurements[10-12] indicate that the dominant wave direction is representative of the predominant wind direction. For open ocean conditions, agreement between the WARF radar and shipboard anemometer measurements of wind direction is $\pm 16^{\circ}$.[13] For hurricane winds, the agreement between coincident wind direction measurements made by the NOAA National Data Buoy Office (NDBO) data buoys and the WARF radar is better than $10^{\circ}$.[1,9]

The radar measures the relative power between the approaching and receding waves that satisfies the Bragg scattering condition. If a cosine directional distribution[10]

$$G(\theta) = \cos^{s}\theta/2 \qquad (1)$$

is assumed, then the relative power of the approaching and receding waves measured by the radar is sufficient to estimate $\theta$ with an ambiguity about the beam direction. This left-right ambiguity is resolved by the predictable cyclonic surface circulation within the hurricane. The shape of $G(\theta)$ is controlled by the spreading parameter, s, where $\theta$ is the angle between the radar beam and the wind direction. For open ocean conditions, we have estimated s from several models.[11,13] For the maximum hurricane winds, the values of s estimated from these models are too low. Based upon previous hurricane analyses and spot measurements of wind direction at NDBO data buoys, we used values of s between 1.0 and 2.0. No attempts were made to account for variations in s as a function of location within the hurricane.

## VII. SIGNIFICANT WAVE HEIGHT

Barrick[6] derived an integral expression that predicts the Doppler spectrum for a specific directional wave spectrum input. Recent efforts have succeeded in inverting this integral expression to compute the input rms wave height,[14,15] one-dimensional wave frequency spectrum,[16-19] and the directional distribution.[17-19] Barrick's[14,16] expressions have been used to analyze skywave radar data recorded for a Pacific Ocean storm[15] and tropical storms.[1,20]

We used a power law derived from simulated data by Maresca and Georges[15] to compute rms wave height by relating the ratio of the total second-order and first-order power to the rms wave height:

$$k_o h = aR_2^b \qquad (2)$$

where $0.2 \leq k_o h \leq 1.0$, h is the rms wave height; $k_o$ is the radar wave number; $R_2$ is the ratio of the total second- to total first-order power; and $a = 0.8$ and $b = 0.6$ are constants. This average expression was derived from theoretical simulations of the Doppler spectra for different radar-to-wind directions, directional distributions, functional forms of the wave-frequency spectrum, and operating radar frequencies. Equation (2) is accurate to within 10%. Discussion of the errors can be found in Maresca and Carlson,[1] and Maresca and Georges.[15]

## VIII. WIND SPEED

Historically, wave models have been developed to predict wave height and the wave spectrum from an input wind field. The accuracy of these models is dependent upon the accuracy of the input winds. Hasselmann et al.[21] proposed a one-dimensional parametric wind-wave model for fetch limited growing wind-sea conditions. Ross and Cardone[22-25] empirically derived a power-law expression for hurricanes based on the form proposed by Hasselmann that relates the nondimensional wave energy, $\tilde{E}$, by using wind, wave, and fetch measured during hurricanes Ava, Camille, and Eloise. For hurricanes,

$$\tilde{E} = 2.5 \times 10^{-5} \tilde{R}^{0.45} \tag{3}$$

where $\tilde{E} = Eg^2/W^4$; $\tilde{R} = rg/W^2$; $E = h^2$; and $H_s = 4h$. In $\tilde{E}$ and $\tilde{R}$, E is the total wave energy; h is the rms wave height; $H_s$ is the significant wave height; r is the radial distance from the eye to the measurement point that accounts for fetch; g is the gravitational acceleration; and W is the wind speed. Solving for wind speed in Eq. (3), we obtain

$$W = \left( \frac{h^2 g^2}{2.5 \times 10^{-5} (rg)^{0.45}} \right)^{0.323} . \tag{4}$$

The wind-wave model used to derive Eq. (4) is applicable for slow moving storms in which $W > 15$ m/s and $\tilde{R} < 3 \times 10^4$. For the unusual cases where the storms move very fast or very slow, Ross and Cardone[24] showed that significant differences in the modeled and measured wave heights occur.

We used Eq. (4) to calculate wind speed for both Anita and Babe and compared our results with the wind speeds measured at NDBO buoys, oil platforms, and by reconnaissance aircraft. The radial fetch (r) was measured from the WARF-derived wind maps, and the wave height (h) was computed using Eq. (2). The radar-derived W is not an instantaneous wind speed estimate; it is a smooth temporal and spatial average of the winds. Our radar-derived W was compared to the 15-minute wind speed averages made at NDBO moored data buoys.

## IX. ANITA MEASUREMENTS

Hurricane Anita formed as a tropical depression in the Gulf of Mexico at about 1200Z on 29 August 1977. Anita developed into a tropical storm at approximately 0600Z on 30 August 1977, and about 12 hours later intensified into the first Gulf of Mexico hurricane of the 1977 season. As Anita moved west across the Gulf, winds in excess of 75 m/s were recorded. Five days of skywave data beginning 29 August 1977, were recorded prior to Anita's landfall, 2 September 1977, approximately 48 km south of Brownsville, Texas. Twenty-one radar wind maps were compiled at WARF. The first 4 wind maps were not used in the

radar-derived track presented here because the radar showed two distinct centers during this early period. On 30 August 1977, the storm intensified and developed one center. The wind maps were updated 3 to 5 times per day during both daytime and nighttime periods and were used to develop the WARF-derived track. Figure 6 shows the radar-derived positions in relation to the official NHC smooth track produced from reconnaissance aircraft measurements, visible and infrared satellite cloud photographs, and shore-based microwave Doppler radar. The relative agreement between the WARF position estimates and the interpolated temporal position estimates along the smooth track is ±19 km.

There are two potential sources of error associated with the WARF hurricane position fixes: the absolute position error of the radar consisting of range and azimuth errors, and the errors associated with locating the storm center from the radar wind direction measurements. We estimate the range errors of the radar caused by errors in determining the ionospheric height at midpath to be 20 km. If a coastal scan is included as part of collecting the wind map data, the land echo can be used as a reference to more accurately determine the ionospheric height, and therefore, reduce this error. We estimate the error in azimuth caused by ionospheric tilting to be 20 km. These range and azimuth errors can be reduced significantly by installing an HF repeater along the coast which receives signals and transmits them back with a known frequency shift. When we assume similar mean ionospheric conditions within 200 km of the storm center, the entire wind map can be translated in azimuth and range to correct for the absolute position error. The location of the wind direction measurement with respect to the storm center is generally not affected by these position errors. The error associated with determining the storm center from the radar maps is about 20 km. The error is caused by the left/right ambiguity in the wind direction measurement. The average maximum error from these two potential sources of error is about 40 km. In comparing the WARF position fixes to the NHC track we found relative differences of between 5 and 50 km, and these relative differences can be attributed to the sources of error just discussed.

Anita passed 50 km south of NDBO buoy EB-71 at about 0000Z on 1 September 1977. Two WARF-derived wind maps were made at 2140Z on 30 August 1977 and 0120Z on 1 September 1977, which brackets this time period. One of these wind maps is shown in Figure 7. Also shown on Figure 7 are surface wind direction fields derived from data recorded by NDBO buoy EB-71. These buoy-measured wind directions were recorded at 2-hour intervals during the period ±18 hours of Anita's passing EB-71. The buoy-derived wind field was computed by a time-space conversion that assumed uniform wind direction and lateral storm motion during this period. We compared the buoy-derived wind directions to the WARF-derived wind directions; agreement was within 19°. Agreement between the WARF-derived wind direction estimate coincident in time and space with the buoy wind direction estimate was 1°.

Between 2314Z on 31 August 1977 and 0020Z on 1 September 1977, WARF measurements were made at five locations surrounding the center of the

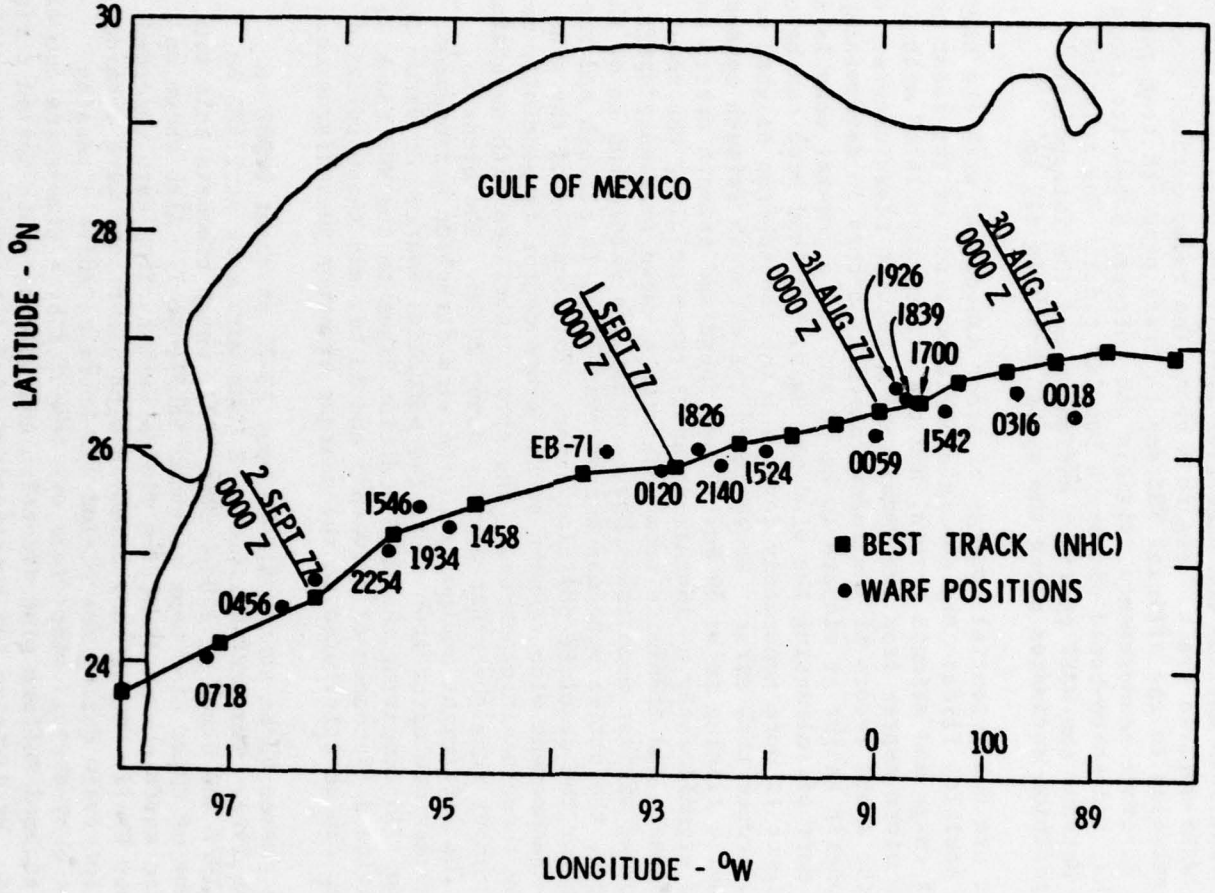


FIGURE 6 WARF-MEASURED TRACK OF HURRICANE ANITA PRODUCED FROM THE RADAR WIND MAPS

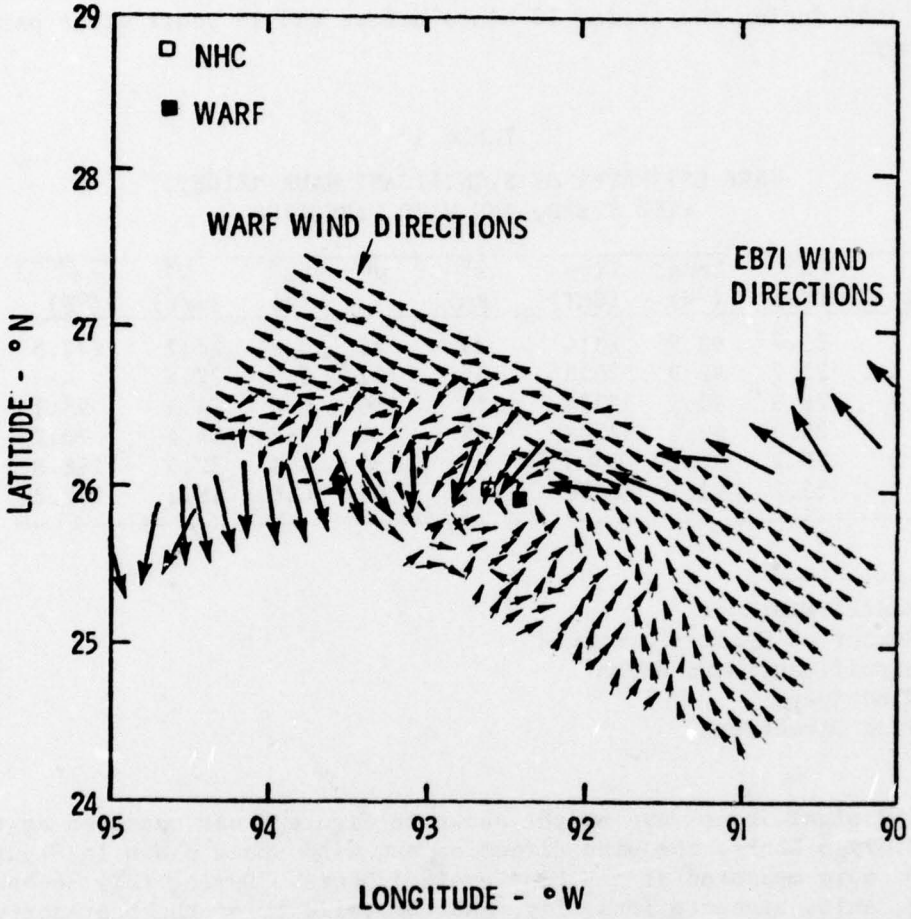


FIGURE 7 WARF-DERIVED WIND DIRECTION MAP MADE FOR ANITA AT 2140Z ON AUGUST 31, 1977

storm. The location of each measurement relative to the storm center was interpolated from the two wind maps. We computed the wind direction by using Eq. (1), wind speed by using Eq. (4), and wave height by using Eq. (2) at each location (see Table 1), and compared these measurements to a buoy-derived wind and wave field. The maps of the spatial distribution of the wind direction, wind speed, and wave height were compiled from NDBO EB-71 data buoy measurements. Each parameter was plotted in relation to the storm center; they are shown in Figures 8, 9, and 10. We assumed that Anita moved uniformly with no change in the meteorological conditions during the period 18 hours before and 18 hours after passing the buoy.

Table 1

WARF ESTIMATES OF SIGNIFICANT WAVE HEIGHT, WIND SPEED, AND WIND DIRECTION

| Point | Lat ($^{o}$N) | Long ($^{o}$W) | Time (GMT) | r* (km) | N* | $H_s$* (m) | W* (m/s) | $\phi$* ($^{o}$N) |
|---|---|---|---|---|---|---|---|---|
| A | 25.7 | 92.9 | 2314 | 35 | 80 | 5.8 | 26.7 | 277.5 |
| A | 25.7 | 92.9 | 2343 | 35 | 112 | 5.2 | 22.8 | - |
| B | 26.3 | 92.1 | 2324 | 75 | 80 | 6.0 | 24.4 | 95.1 |
| C | 26.3 | 93.1 | 2358 | 65 | 35 | 5.8 | 24.4 | 70.2 |
| D | 25.7 | 92.1 | 0003 | 65 | 134 | 5.1 | 22.5 | 168.8 |
| E | 25.2 | 91.1 | 0020 | 180 | 49 | 4.6 | 18.1 | 137.2 |

*
r = Radial Distance
N = Number of Spectra Averaged
$H_s$= Significant Wave Height
W = Wind Speed
$\phi$ = Wind Direction

The significant wave height shown in Figure 8 was measured at the buoy every 3 hours; the wind direction and wind speed shown in Figures 9 and 10 were measured at the buoy every 2 hours. During this 36-hour period, Anita began to intensify, and the validity of the buoy-derived wind and wave fields are suspect. Exact comparison of the EB-71 and WARF measurements are difficult because of the differences in the time, location, and area of ocean monitored. On Figure 8 we also included the wave forecast for significant wave height computed by Cardone et al.[25] for comparison.

The WARF estimates made at Point B (26.3$^{o}$N, 92.1$^{o}$W) were in close proximity to the buoy-derived estimates located at (26.2$^{o}$N, 92.1$^{o}$W). The remaining WARF wind and wave height estimates were too far away from the buoy-derived quantities for direct comparison, but the agreement between the WARF- and buoy-derived wind and wave fields was reasonable.

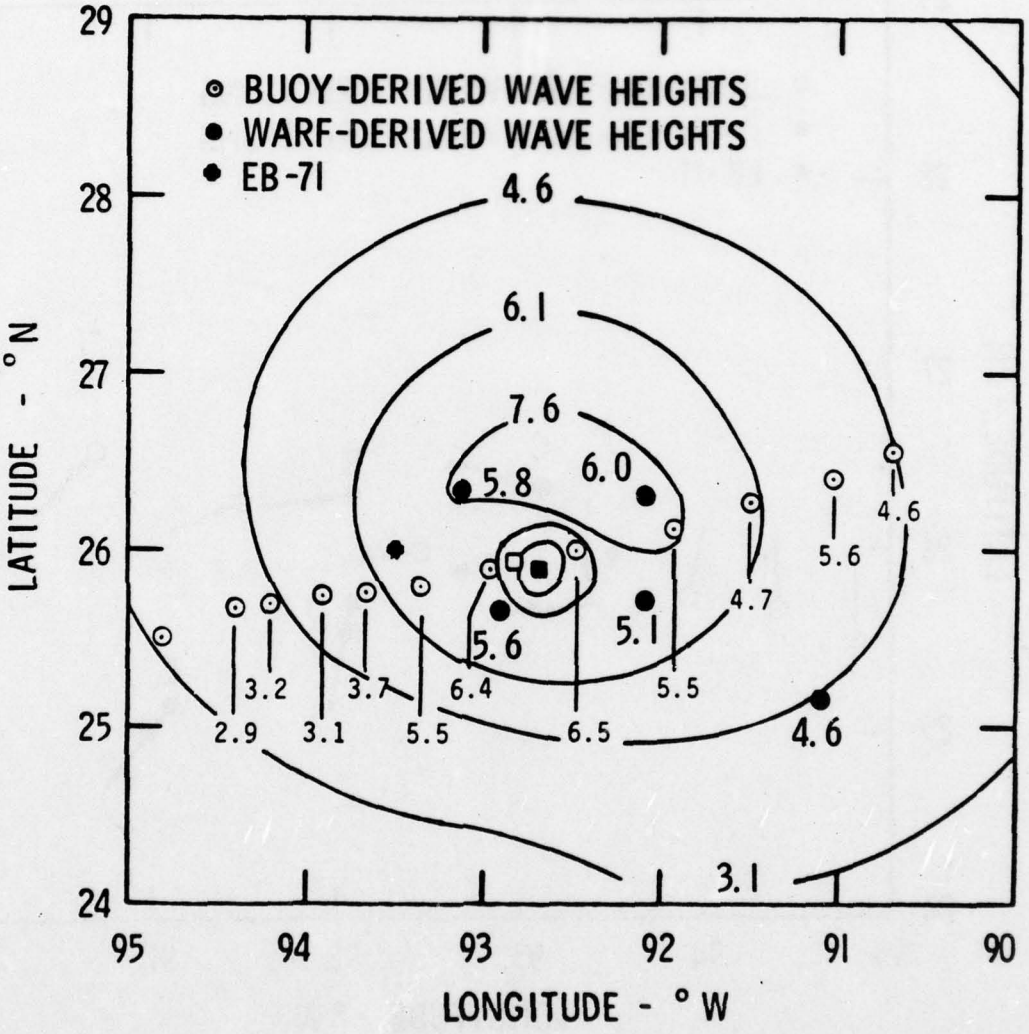


FIGURE 8 COMPARISON OF THE WARF-DERIVED SIGNIFICANT WAVE HEIGHTS (m) MEASURED BETWEEN 2314Z ON AUGUST 31, 1977 AND 0020Z ON SEPTEMBER 1, 1977 AND THE EB71-DERIVED SIGNIFICANT WAVE HEIGHTS MADE BETWEEN 0600Z ON AUGUST 31, 1977 AND 1800Z ON SEPTEMBER 1, 1977. The wave height contours are reproduced from Figure 9 of Reference 25. The letter designations are given on Figure 9.

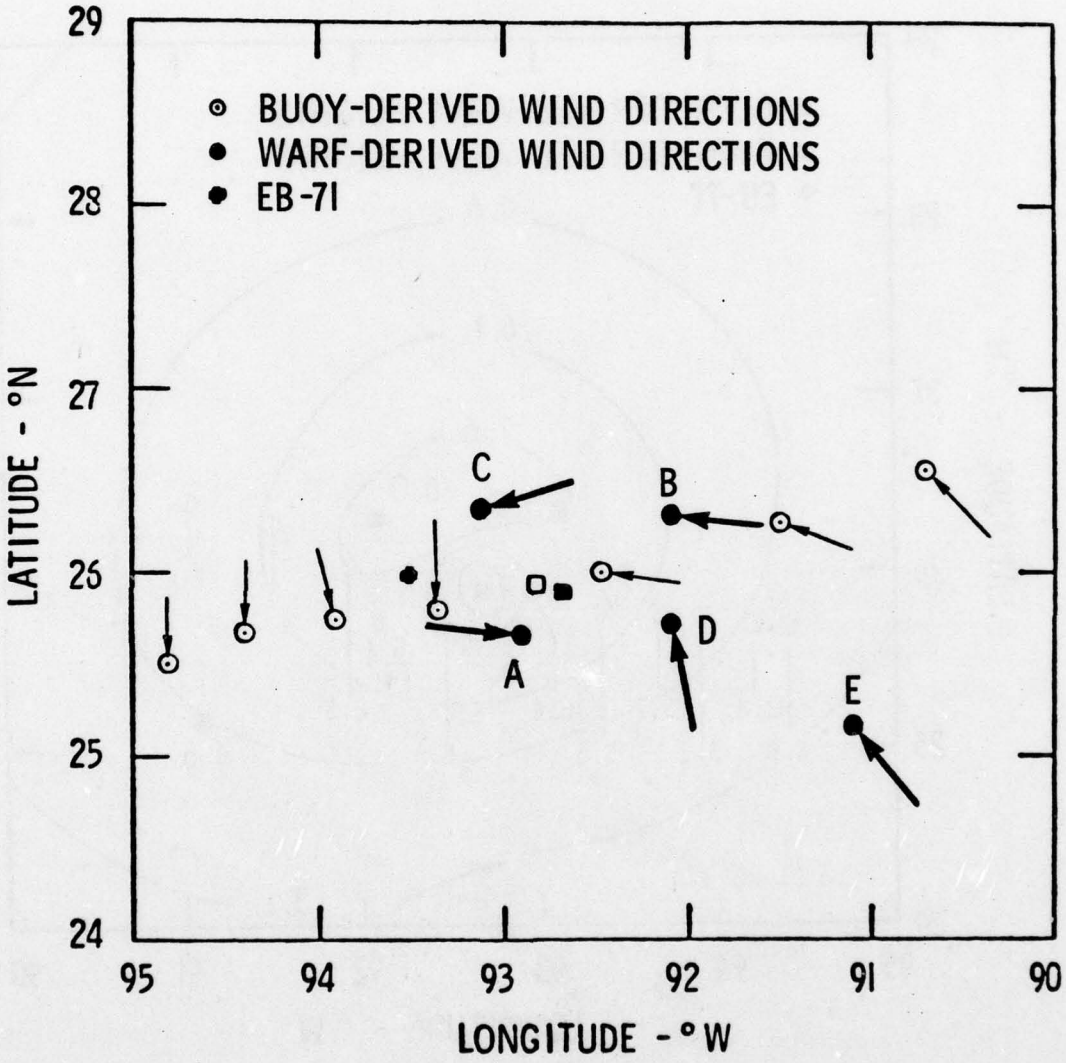


FIGURE 9 COMPARISON OF THE WARF-DERIVED WIND DIRECTIONS (⟵) MADE BETWEEN 2314Z ON AUGUST 31, 1977 AND 0020Z ON SEPTEMBER 1, 1977 AND THE EB71-DERIVED WIND DIRECTIONS (⟶) MADE BETWEEN 0600Z ON AUGUST 31, 1977 AND 1800Z ON SEPTEMBER 1, 1977

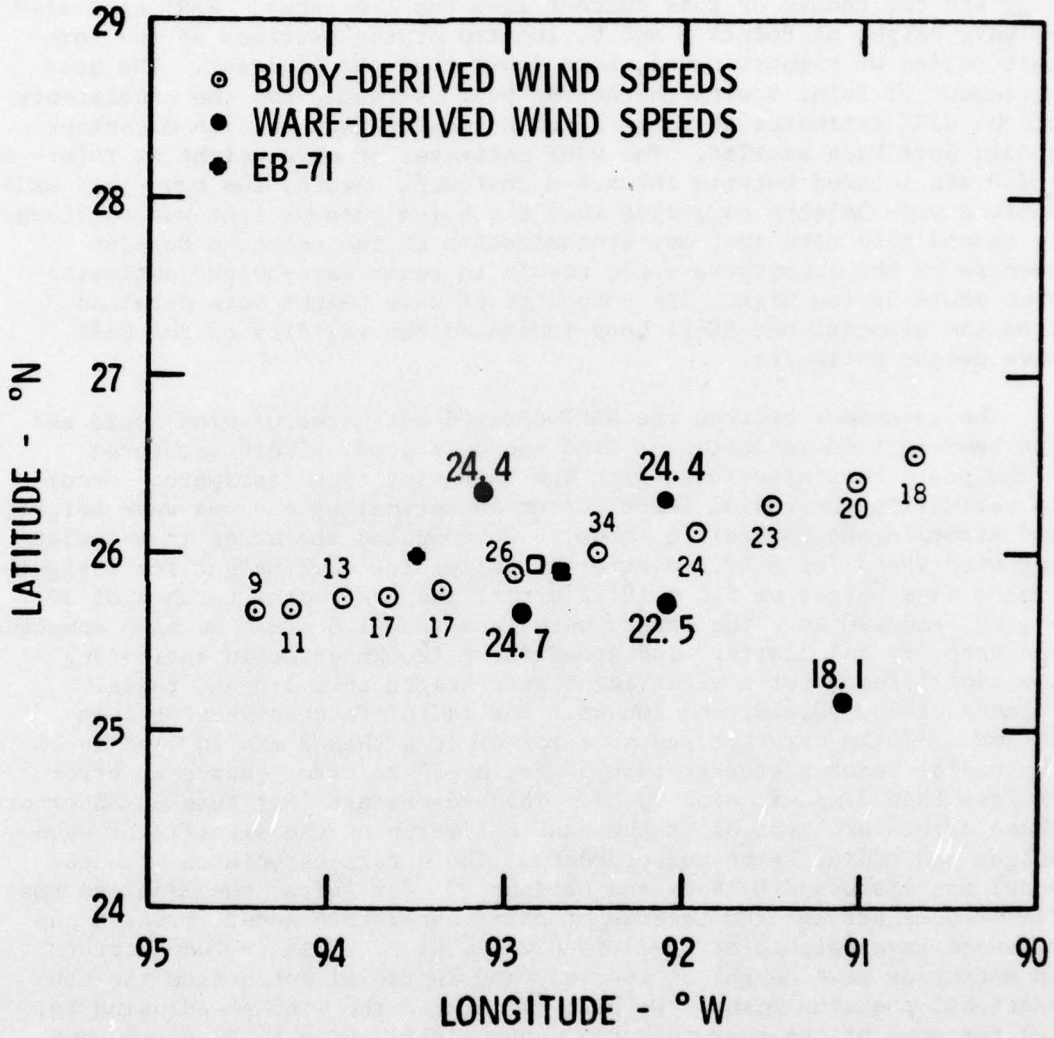


FIGURE 10 COMPARISON OF THE WARF-DERIVED WIND SPEEDS (m/s) MEASURED BETWEEN 2314Z ON AUGUST 31, 1977 AND 0020Z ON SEPTEMBER 1, 1977 AND THE EB71-DERIVED WIND SPEEDS (m/s) MEASURED BETWEEN 0600Z ON AUGUST 31, 1977 AND 1800Z ON SEPTEMBER 1, 1977

The wave forecast was compared to both the buoy- and WARF-derived wave heights. We found good agreement between the forecast, buoy, and WARF estimates of wave height along the 4.6-m contour east of the hurricane. The buoy estimate west of the hurricane along the 4.6-m contour line suggests the radius of this contour line was too large. WARF estimates of wave height at Points B and C, located at the extremes of the forecast region of highest waves, were lower than the hindcast. The good agreement of Point B with the nearby buoy estimate, and the consistency of the WARF estimates at Point B and C suggest that the 7.6-m contour should have been smaller. The WARF estimates of wave height at Points A and D are located between the 6.1-m contours. Again, the buoy- and WARF-derived wave heights suggested that the 6.1-m contour line was too large. We should also note that any contamination of the sea-echo Doppler spectra by the ionosphere would result in radar wave-height estimates that would be too high. The composite of wave height data obtained from the hindcast and EB-71 buoy indicated the validity of the WARF wave height estimates.

The agreement between the WARF-derived estimates of wind speed and the buoy-derived estimates of wind speed is good. There are three principal errors associated with the WARF wind speed estimate: error in estimating the radial fetch, error in estimating the rms wave height, and error in the parametric model. We computed the error in calculating wind speed for a ±0.5-m error in estimating wave height for a significant wave height of 5.5 m (9.1% error) and for radial fetches of 30, 50, 70, and 100 km. The errors were less than 1.6 m/s. We also computed the error in calculating wind speed for a ±20-km error in estimating the radial fetch for a significant wave height of 5.5 m and radial fetches of 30, 50, 70, and 100 km. For radial fetches greater than 30 km, a +20-km error causes an error of less than 2 m/s in wind speed. For radial fetches greater than 50 km, a -20-km error causes an error of less than 2 m/s in wind speed. This represents less than an 8% error. These errors are typical of the WARF estimates of the significant wave height and radial fetch measurements. The errors associated with the model are discussed by Ross and Cardone.[24] For Anita, the mean and rms differences between the Cardone et al.[25] parametric model forecast and measured wave heights at EB-71 is 0.21 ±0.83 m. This includes errors in measuring wave height at the buoy and in radial fetch from the conventional position fixes. We also calculated the wind speed using Eq. (4) for some of the buoy-measured wave heights shown in Figure 8, and compared the calculated wind speed measurements to wind speeds measured at the buoy (Table 2). The data is indicative of the accuracy we could expect from the WARF estimates of wind speed using Eq. (4). For these data, we believe the largest sources of error in the comparison were the uncertainty in the radial distance to each point caused by compiling the map over a 36-hour period, and the assumption of a symmetrical distribution of the winds.

Table 2

COMPARISON OF WIND SPEED VALUES CALCULATED FROM EQ. (4) DERIVED FROM EB-71 SIGNIFICANT WAVE HEIGHT MEASUREMENTS

| Lat (°N) | Long (°W) | $H_s$* (m) | r* (km) | $W_c$* (m/s) | $W_m$* (m/s) | Difference (m/s) |
|---|---|---|---|---|---|---|
| 25.5 | 94.8 | 2.5 | 217 | 11.9 | 7.6 | +4.3 |
| 25.7 | 94.4 | 2.9 | 174 | 13.5 | 9.0 | +4.5 |
| 25.7 | 93.9 | 3.1 | 124 | 14.9 | 13.3 | +1.6 |
| 25.8 | 93.4 | 5.5 | 69 | 23.4 | 17.4 | +6.0 |
| 26.0 | 92.5 | 6.5 | 24 | 30.4 | 34.1 | -3.7 |
| 26.3 | 91.5 | 4.7 | 126 | 19.4 | 23.1 | -3.7 |
| 26.6 | 90.7 | 4.6 | 212 | 17.7 | 18.1 | -0.4 |

*
$H_s$ = Significant Wave Height
r = Radial Distance
$W_c$ = Computed Wind Speed
$W_m$ = Measured Wind Speed

## X. BABE DATA

We recorded skywave data for Babe from 2000Z on 4 September 1977 until its landfall on 5 September 1977. Wind direction maps were made at 2253Z on 4 September 1977 and 1507Z on 5 September 1977. Babe was already onshore before the second map was made. We analyzed a sea echo Doppler spectrum near the peak winds for wind speed. This spectrum was recorded at a radius of 50 km from the hurricane center (27.9°N, 91.6°W). The WARF estimate of significant wave height was 3.6 m. The wind speed was computed by using Eq. (4), and was compared to wind speeds measured at several offshore oil platforms at 2100Z and from aircraft reconnaissance at 1800Z. Winds measured from aircraft at an altitude of 305 m were reduced to the equivalent 10 m wind for comparison to the radar data. We reduced the aircraft winds to the surface using a simple ratio relating upper level gradient wind to the surface wind, indicated by Elsberry et al.[26] calculations. Using the two layer Cardone[27] marine boundary layer model, Elsberry et al.[26] computed the ratio of the wind at the top of the upper layer to the wind at the top of the surface layer for different regions of the hurricane, different surface roughness and different ratios of heat conductivity to eddy viscosity. For moderate to high wind speeds, the top of the surface layer is approximately 20 m. This wind ratio ranges from about 0.5 to 0.85. The lower value represents regions near the peak winds. We assumed the 305-m aircraft wind was representative of the wind at the top of the upper layer and reduced it to 20 m using a ratio of 0.6. The corrected 20-m wind is 18.5 m/s. We realize the error associated with this calculation can

be large. We computed the 19.5-m WARF wind speed for comparison by assuming a logarithmic profile in the surface boundary layer of the form

$$W(z) = \frac{W_*}{k} \ln\left(\frac{z}{z_o}\right) \tag{5}$$

where $W(z)$ is the wind speed at a height of $z$, $W_* = C_D W^2$ is the friction velocity, $C_D$ is the drag coefficient, $k \cong 0.4$ is Von Karman's constant, and $z_o$ is the surface roughness. We estimated $z_o = 0.00392$ m for hurricane conditions using the wind speeds measured during Eloise[28] at NDBO buoy EB-10 at 10 m, and a constant drag coefficient of 0.0026 proposed by Wu[29] for high wind speeds to calculate $W^*$. We found good agreement between our 19.5-m computed wind speed using Eq. (5) for Eloise and the 19.5-m Eloise wind speed computed by Ross and Cardone.[24] Using $z_o = 0.00392$ m and $C_D = 0.0026$ m,we computed the 19.5-m WARF Babe wind speed to be 18.3 m/s. We also computed the maximum wind speed, $W_{max}$, and the maximum sustained wind speed, $W_s$, for a storm moving at 5.1 m/s from the following expressions[30] relating the central pressure and radius of the storm to wind speed at 10 m:

$$W_{max} = 0.868\ [6.45(P_n - P_o)^{1/2} - 0.296\ rf] \tag{6}$$

and

$$W_s = 0.865\ W_{max} + 0.5\ V_F \tag{7}$$

where $W_{max}$ and $W_s$ are in m/s, $P_n$ is the normal pressure of 1013 mbars, $P_o$ is the central pressure in mb, r is the radius in km, f is the coriolis parameter in radians/hour, and $V_F$ is the forward motion of the storm in m/s. The maximum wind recorded from the aircraft at 1800Z were located approximately 60 km from the center and the central pressure was reported as 1000 mb. We calculated $W_{max} = 16.4$ m/s and $W_s = 16.8$ m/s. We summarize these wind speed estimates in Table 3. Because none of the wind speed estimates were coincident in time or space with the WARF estimate and the assumptions inherent in deriving these quantities we only compared the results qualitatively. The WARF wind speed estimate is quite reasonable.

## XI. SUMMARY

Spatially-averaged hurricane wind speed, wind direction, and wave height estimates made at the WARF for Anita and Babe were compared to point measurements made at NDBO buoys and oil platforms and by reconnaissance aircraft. Agreement was within the nominal measurement accuracy of all the sensors. The WARF data set is not limited to the results presented in this paper. Other analyses of the radar data that were not obtained in the vicinity of the buoy are also available. These

experiments indicated that during a hurricane, HF skywave radar can provide operational surface data that are as accurate as the more recognized in situ measurements. The supportive surface data supplied by the WARF radar would prove particularly useful for tracking during early formative stages of hurricanes when multiple centers may be observed or when cirrus shielding may obscure visual location by satellite cloud photography. The high resolution, large coverage area, real-time steering, and continuous monitoring capabilities are unique to skywave radar. The hurricane data obtained from skywave radar complements data obtained from satellites, aircraft, and buoys.

Table 3

BABE WIND SPEED ESTIMATES MADE ON 4 SEPTEMBER 1977

| Sensor | Observation (GMT) | Bearing From Hurricane Center ($^{o}$N) | Radial Distance From Hurricane Center (km) | Wind Speed (m/s) |
|---|---|---|---|---|
| WARF (10 m) | 2253 | 340 | 60 | 18.2 |
| WARF (19.5 m) | 2253 | 340 | 60 | 18.3 |
| Aircraft (305 m) | 1800 | 25 | 60 | 30.8 |
| Aircraft (19.5 m) | 1800 | 25 | 60 | 18.5 |
| Oil Platform (19.5 m) | 2100 | 320 | 100 | 15.4 |
| Oil Platform (19.5 m) | 2100 | 0 | 35 | 11.3 |
| $W_{CM}$[a] (9.1 m) | - | - | 60 | 16.4 |
| $W_{CS}$[b] (9.1 m) | - | - | 60 | 16.8 |

[a]Computed maximum wind speed from Eq. (3-35) in Reference 30.

[b]Computed maximum sustained wind speed from Eq. (3-34) in Reference 30.

Acknowledgments. This work was supported by the Air Force of Scientific Research (AFOSR) under Contract No. F49620-76-C-0023. We gratefully acknowledge the help of G. Glassmeyer, W. Preuss, G. Tomlin, and C. Powell of SRI in collecting data at WARF; D. Westover for writing the real-time sampling software; and B. Richards and J. King for typing the manuscript.

## REFERENCES


1. J. W. Maresca, Jr. and C. T. Carlson, "Tracking and Monitoring Hurricanes by HF Skywave Radar over the Gulf of Mexico," Technical Report 1, SRI International, Menlo Park, California (1977).
2. "SRI Remote Measurements Laboratory Research Capabilities," brochure, Stanford Research Institute, Menlo Park, California (1977).
3. K. Davies, Ionospheric Radio Propagation, NBS Monograph 80, U.S. Government Printing Office, Washington, D.C. (1965).
4. D. D. Crombie, "Doppler Spectrum of Sea Echo at 13.56 Mc/s," Nature, Vol. 175, pp. 681-682 (1955).
5. D. E. Barrick, "First-order Theory and Analysis of MF/HF/VHF Scatter From the Sea," IEEE Trans. Antennas and Propagation, AP-20, pp. 2-10 (1972).
6. D. E. Barrick, "Remote Sensing of Sea State by Radar," Remote Sensing of the Troposphere, V. E. Derr, ed., U.S. Government Printing Office, Washington, D.C. (1972).
7. T. M. Georges and J. W. Maresca, Jr., "The Effect of Radar Beamwidth on the Quality of Sea Echo Doppler Spectra Measured with HF Skywave Radar," accepted by Radio Science.
8. J. R. Barnum, J. W. Maresca, Jr., and S. M. Serebreny, "High-Resolution Mapping of Oceanic Wind Fields with Skywave Radar," IEEE Trans. on Antennas and Propagation, AP-25, pp. 128-132 (1977).
9. J. W. Maresca, Jr. and J. R. Barnum, "Remote Measurements of the Position and Surface Circulation of Hurricane Eloise by Skywave Radar," accepted by Monthly Weather Review.
10. M. S. Longuet-Higgins, D. E. Cartwright, and N. D. Smith, "Observations of the Directional Spectrum of Sea Waves Using Motions of a Floating Buoy," Ocean Wave Spectra, pp. 111-136,(Prentice-Hall: Englewood Cliffs, New Jersey, 1963).
11. H. Mitsuyasu, F. Tasai, T. Suhara, S. Mizuno, M. Ohkusu, T. Honda, and K. Rikiishi, "Observations of the Directional Spectrum of Ocean Waves Using a Clover Leaf Buoy," J. Phys. Oceanog., Vol. 5, No. 4, pp. 750-760 (1975).
12. J. A. Ewing, "Some Measurements of the Directional Wave Spectrum," J. Marine Research, Vol. 27, pp. 163-171 (1969).
13. R. H. Stewart and J. R. Barnum, "Radio Measurements of Oceanic Winds at Long Ranges: An Evaluation," Radio Science, Vol. 10, pp. 853-857 (1975).
14. D. E. Barrick, "Extraction of Wave Parameters from Measured HF Sea-Echo Doppler Spectra, Radio Science, Vol. 12, pp. 415-424 (1977).
15. J. W. Maresca, Jr. and T. M. Georges, "HF Skywave Radar Measurement of the Ocean Wave Spectrum," submitted to J. Geophys. Research.
16. D. E. Barrick, "The Ocean Waveheight Nondirectional Spectrum from Inversion of the HF Sea-echo Doppler Spectrum," Remote Sensing of Environment, Vol. 6, pp. 201-277 (1977).
17. B. J. Lipa, "Derivation of Directional Ocean-wave Spectra by Integral Inversion of Second-order Radar Echoes," Radio Science, Vol. 12, pp. 425-434 (1977).
18. B. J. Lipa, "Inversion of Second-order Radar Echoes from the Sea," J. Geophys. Research, Vol. 83, pp. 959-962 (1977).

19. D. E. Barrick and B. J. Lipa, "Ocean Surface Features Observed by HF Coastal Ground-wave Radars: A Progress Review," Ocean Wave Climate, eds. M. D. Earle and A. Malahoff (Plenum Publishing Company, New York 1978).
20. J. W. Maresca, Jr., "High Frequency Skywave Radar Measurements of Waves and Currents Associated with Tropical and Extra-Tropical Storms," Ocean Wave Climate, eds. M. D. Earle and A. Malahoff (Plenum Publishing Company, New York 1978).
21. K. Hasselmann, D. B. Ross, P. Muller, and W. Sell, "A Parametric Wave Prediction Model," J. Phys. Oceanog., Vol. 6, pp. 200-228 (1976).
22. D. B. Ross, "A Simplified Model for Forecasting Hurricane Generated Waves" (Abstract), Bull. Am. Meteorol. Soc., presented at Conference on Atmospheric and Oceanic Waves, Seattle, Washington, March 29-April 2, 1976 American Meteorological Society (1976).
23. V. J. Cardone and D. B. Ross, "State of Art Wave Predictions and Data Requirements," Ocean Wave Climate, eds. M. D. Earle and A. Malahoff (Plenum Publishing Company, New York 1978).
24. D. B. Ross and V. J. Cardone, "A Comparison of Parametric and Spectral Hurricane Wave Prediction Products," to be published in the Proceedings of "NATO Symposium on Turbulent Fluxes Through the Sea Surface, Wave Dynamics and Prediction," Marseilles, France, September 12-16, 1977 (Plenum Publishing Company, New York 1978).
25. V. J. Cardone, D. B. Ross, and M. R. Ahrens, "An Experiment in Forecasting Hurricane Generated Sea States," Proceedings of the 11th Technical Conference on Hurricanes and Tropical Meteorology, Miami, Florida (December 13-16, 1977).
26. R. L. Elsberry, N. A. S. Pearson, L. B. Corgnati, Jr., "A Quasi-Empirical Model of the Hurricane Boundary Layer," J. Geophys. Research, Vol. 79, pp. 3033-3040 (1974).
27. V. J. Cardone, "Specification of the Wind Distribution in the Marine Boundary Layer for Wave Forecasting," Report TR 69-1 Geophys. Sci. Lab., New York University NTIS No. AD702490 (1969).
28. G. W. Whithee and A. Johnson, Jr., "Data Report: Buoy Observations During Hurricane Eloise, September 19-October 11, 1975," Environmental Sciences Division, Data Buoy Office, National Oceanic and Atmospheric Administration, Bay St. Louis, Mississippi (1975).
29. J. Wu, "Wind Stress and Surface Roughness at Air-Sea Interface," J. Geophys. Research, Vol. 74, pp. 444-455 (1969).
30. U.S. Army Coastal Engineering Research Center, Shore Protection Manual, Vol. 1, U.S. Government Printing Office, Washington, D.C. (1973).

APPENDIX E

# HIGH-FREQUENCY SKYWAVE RADAR MEASUREMENTS OF WAVES AND CURRENTS ASSOCIATED WITH TROPICAL AND EXTRA-TROPICAL STORMS

by

J. W. Maresca, Jr.

Ocean Wave Climate
Plenum Publishing Corporation
New York
1978

This work was performed by SRI International, Menlo Park, California, and was sponsored in part by the Air Force Office of Scientific Research and the National Atmospheric and Oceanic Administration.

# HIGH FREQUENCY SKYWAVE RADAR MEASUREMENTS OF WAVES AND CURRENTS ASSOCIATED WITH TROPICAL AND EXTRA-TROPICAL STORMS

Joseph W. Maresca, Jr.
SRI International

## ABSTRACT

The capability of HF skywave radar to measure surface winds, waves, and currents at distances up to 3000 km for tropical and extratropical storm conditions is summarized. Significant wave height and wave spectral estimates made using the Wide Aperture Research Facility skywave radar were compared to similar measurements obtained by National Data Buoy Office buoys EB20 (41°N, 138°W) and EB71 (26°N, 93.5°W). Agreement to within 10% was found for wave heights under varying conditions, ranging from less than 1 m to hurricane wave conditions greater than 5 m.

## I INTRODUCTION

High-frequency (HF) skywave radar estimates of the surface wind speed and direction, surface current, significant wave height, and wave spectrum can be made over several million square kilometers of ocean by remotely measuring the Doppler spectrum of the sea-echo signal. Measurements made at the SRI-operated Wide Aperture Research Facility (WARF) HF skywave radar demonstrate that the skywave radar can track large extratropical storms, and small intense tropical storms and hurricanes; the radar can also provide detailed surface maps of the winds, waves, and currents within a storm. The large coverage area of the WARF skywave radar is possible because the HF radio waves are transmitted to, and returned from, ocean areas by means of one or more ionospheric "reflections." For one ionospheric reflection, ocean areas up to 3000 km away from the radar can be monitored. The purpose of this paper is to summarize the capabilities of HF skywave radar that utilizes ionospheric

reflection, with special emphasis on the measurement of significant wave height and the one-dimensional wave-frequency spectrum.

The skywave radar estimates of the surface wave parameters are obtained from the HF sea-echo Doppler spectrum. An example of the sea-echo spectrum recorded at WARF for 51.2 s of coherent integration is shown in Figure 1. The spectrum consists of two strong first-order echoes produced by the resonant interaction of ocean waves of wave number k and radio waves of wave number $k_o$. For near grazing angles,

$$k \cong 2k_o.$$

In addition, a second-order continuum that is sensitive to changes in the directional ocean wave spectrum surrounds the first-order echoes. Barrick (1972a,b) has derived theoretical expressions that accurately describe the HF scattering process. These expressions have been mathematically inverted to recover parts of the directional wave spectrum directly from the Doppler spectrum.

Barrick and Lipa (1978) summarize the theory of HF scattering from ocean waves; the methods for computing the wave height, the wave spectrum, and the surface current; and the results of several experiments conducted to validate these methods through the use of HF groundwave radar. In this paper, experiments conducted at the WARF skywave radar to determine the accuracy of these methods, including a simple method of mapping wind direction, are described. The WARF radar measurements have been compared to in situ point measurements made from National Data Buoy Office (NDBO) data buoys or research vessels. The relative agreement between the radar and in situ measurements have been found to be within the measurement accuracy of the in situ instrument.

## II WARF SKYWAVE RADAR

WARF is a bistatic HF skywave radar located in central California. The radar is operated in the HF band between 6 and 30 MHz. A 20-kW swept-frequency continuous-wave (SFCW) signal is transmitted from the transmitter site at Lost Hills, California; after round-trip ionospheric

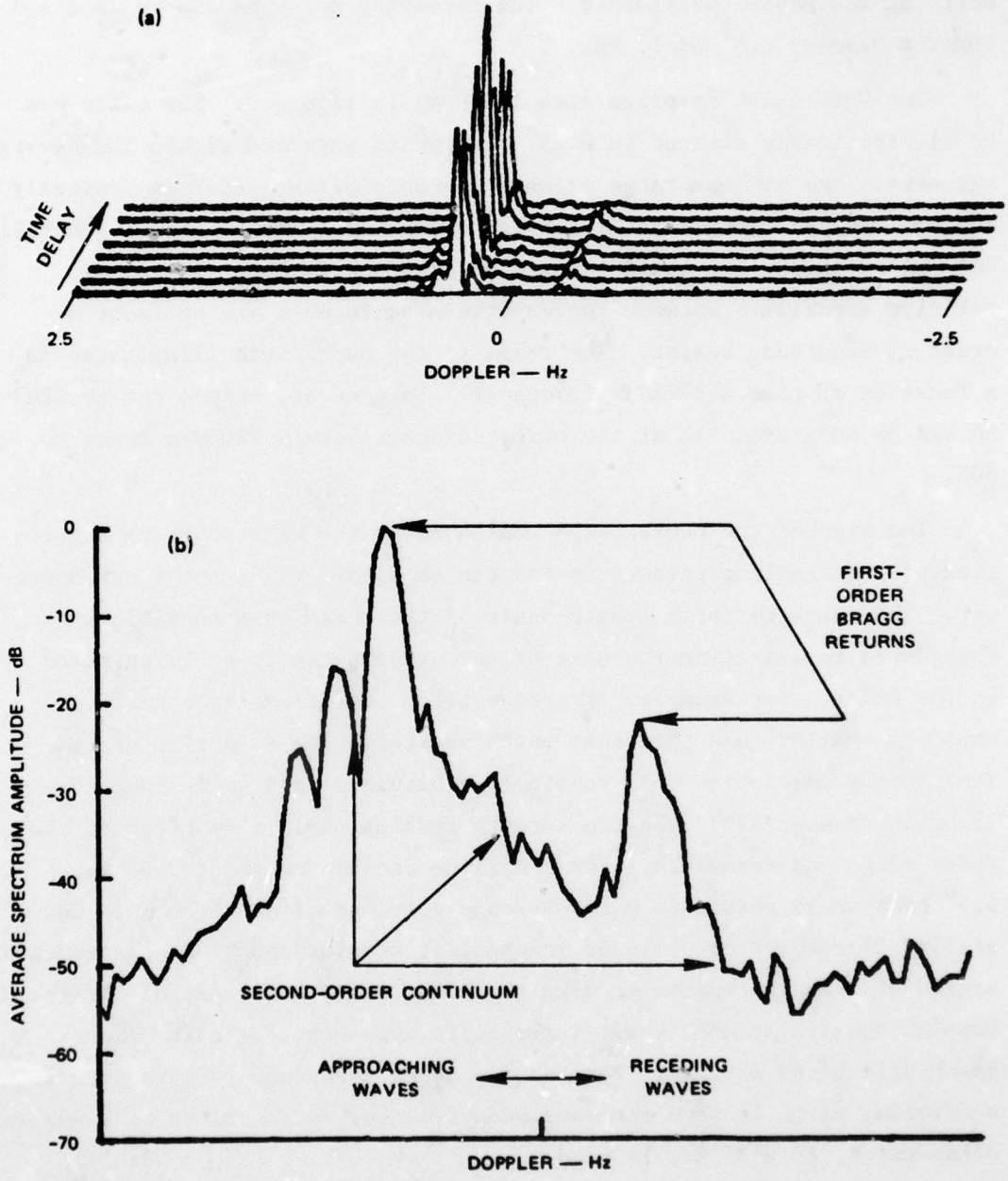


FIGURE 1 RANGE-DOPPLER-PROCESSED SEA-ECHO DOPPLER SPECTRUM. The mean Doppler spectrum is an average of Doppler spectra recorded at different range lines separated by 3 km. The first-order echoes produced by a resonant interaction between the radio waves and the ocean waves is sensitive to changes in the wind-direction field. The second-order sideband structure surrounding the stronger Bragg line is sensitive to changes in the directional ocean wave spectrum.

AD-A064 972 SRI INTERNATIONAL MENLO PARK CA F/G 4/2
TRACKING AND MONITORING HURRICANES BY HF SKYWAVE RADAR OVER THE--ETC(U)
NOV 78 J W MARESCA, C T CARLSON F49620-76-C-0023
UNCLASSIFIED AFOSR-TR-79-0042 NL

2 OF 2
AD
AD A064 972

END
DATE FILMED
4 -79
DDC

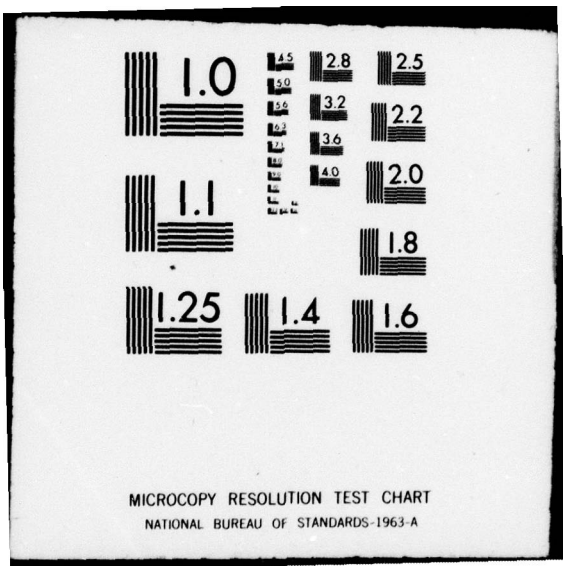
1.0
1.1
1.25
1.4
1.6
1.8
2.0
2.2
2.5
2.8
3.2
3.6
4.0
4.5
5.0
5.6
6.3
MICROCOPY RESOLUTION TEST CHART
NATIONAL BUREAU OF STANDARDS-1963-A

propagation, the signal is received at the receiving site 185 km to the north at Los Banos, California. The receiving array is 2.5-km long and forms a beam of $0.5^{o}$ at 15 MHz.

The WARF radar coverage area is shown in Figure 2. The radar can be electronically steered in $0.25^{o}$ increments anywhere within the coverage area. The minimum range or skip distance of the radar is typically 800 km, and the maximum range for one ionospheric reflection is generally 3000 km or less. The nominal position accuracy is about 20 km, and relative accuracies between consecutive measurements are at least an order of magnitude better. The range to the ocean path illuminated is a function of time and radar frequency. In general, ranges out to 2200 km can be monitored 95% of the time; coverage beyond 2200 km drops to 50%.

The size of the ocean patch monitored by the WARF radar is a function of the sampling parameters and can be specified by the radar operator. The characteristic length-scale of the ocean wave conditions is considered in selecting the size of the ocean patch to be illuminated by the radar. For example, the ocean patch monitored for a hurricane would be smaller than the ocean patch monitored for a Pacific storm. The minimum resolution cell routinely achievable is 3 km in range by 15 km in cross-range. The cross-range resolution is a function of the radar range and beamwidth. For a maximum one-hop range of 3000 km, a $0.5^{o}$ beam would result in a cross-range distance of about 26 km. Generally, 21 resolution cells or independent Doppler spectrum measurements spaced at 3-km increments make up the illuminated ocean patch. If the Doppler spectra at each range interval is averaged, the size of ocean patch will be 63 x 25 km. For Pacific Ocean measurements, the 63 x 25 km scattering patch is used for wave measurements; for hurricanes, a smaller ocean patch, 15 x 25 km, is used.

## III SURFACE WIND DIRECTION MAPS

The capability and technique for mapping the surface wind direction field for large weather systems over the ocean has previously been

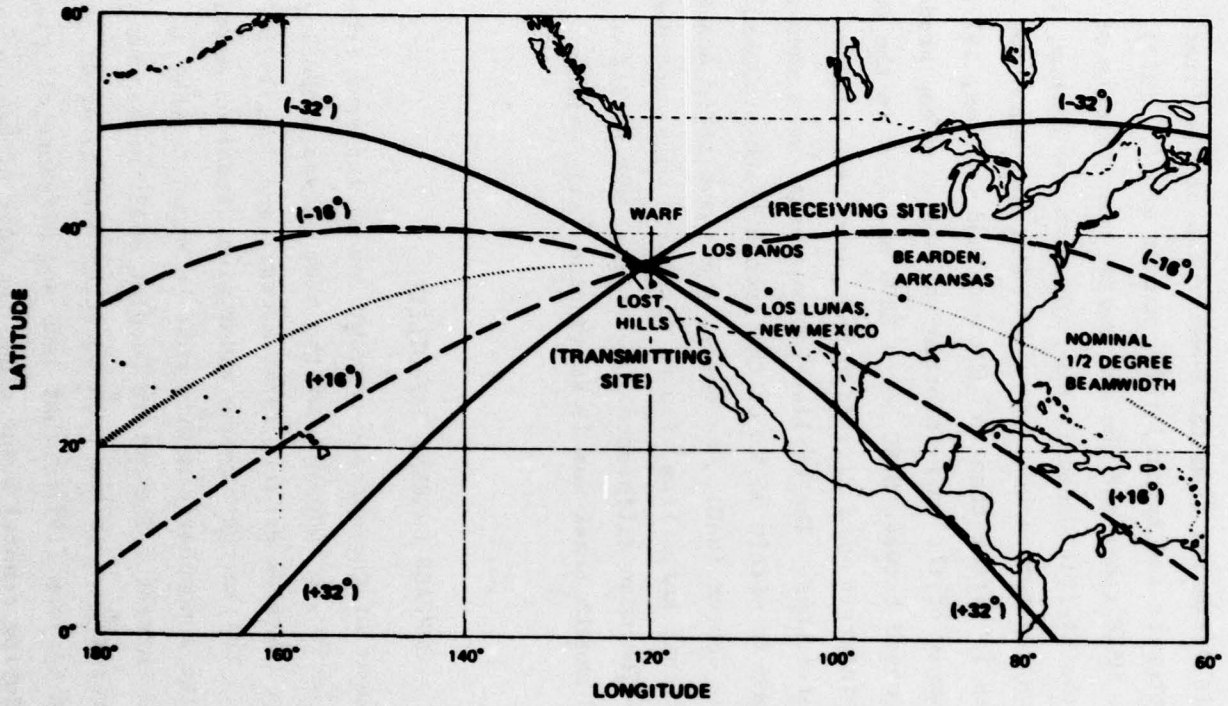


FIGURE 2 WIDE APERTURE RESEARCH FACILITY COVERAGE MAP

demonstrated (Long and Trizna, 1973; Barnum et al., 1977). This mapping technique has also been applied directly to tropical storm and hurricane wind fields (Maresca and Barnum, 1978; Maresca and Carlson, 1977).

Wind direction is estimated from the power ratio of the first-order echo returns (Stewart and Barnum, 1975; Barnum et al., 1977). Agreement between the WARF radar and the anemometer measurements of wind direction over the Pacific Ocean is $\pm 16^{\circ}$ (Stewart and Barnum, 1975). For hurricane winds, agreement between the WARF radar and NDBO buoy wind direction measurements is better than $10^{\circ}$ (Maresca and Carlson, 1977b). Figure 3 shows an example of the WARF-inferred surface wind map produced as Hurricane Eloise passed between NDBO buoys EB04 and EB10 in the Gulf of Mexico. The WARF-inferred wind direction maps have been used to locate the center of hurricanes. The earliest measurements were made on Eloise, and they agreed to within 35 km of the smooth track produced by the National Hurricane Center (NHC). Recently, a skywave radar track was compiled for Hurricane Anita from 17 wind direction maps recorded over a 4-day period. The mean difference between the WARF position estimates and the NHC smooth track was 19 km (Maresca and Carlson, 1978b).

## IV SURFACE CURRENT CAPABILITY

The radial component of the surface current can be inferred from the measured phase velocity, or Doppler, of the ocean waves producing the first-order echoes (Barrick et al., 1974; Stewart and Joy, 1975; Barrick et al., 1977). Unlike the skywave radar wind direction measurement, the effects of the ionospheric motion must be known to make a skywave measurement of current. The entire Doppler spectrum can be shifted by ionospheric motion. It has been shown by Maresca et al. (1976) and Maresca and Carlson (1977b) that land and offshore oil platform echoes received during coastal scans along the Gulf of Mexico are sufficient to remove the effects of the ionosphere from the data. The analysis of the ocean surface would then be identical to the groundwave radar analysis. The requirement of a reference would generally limit

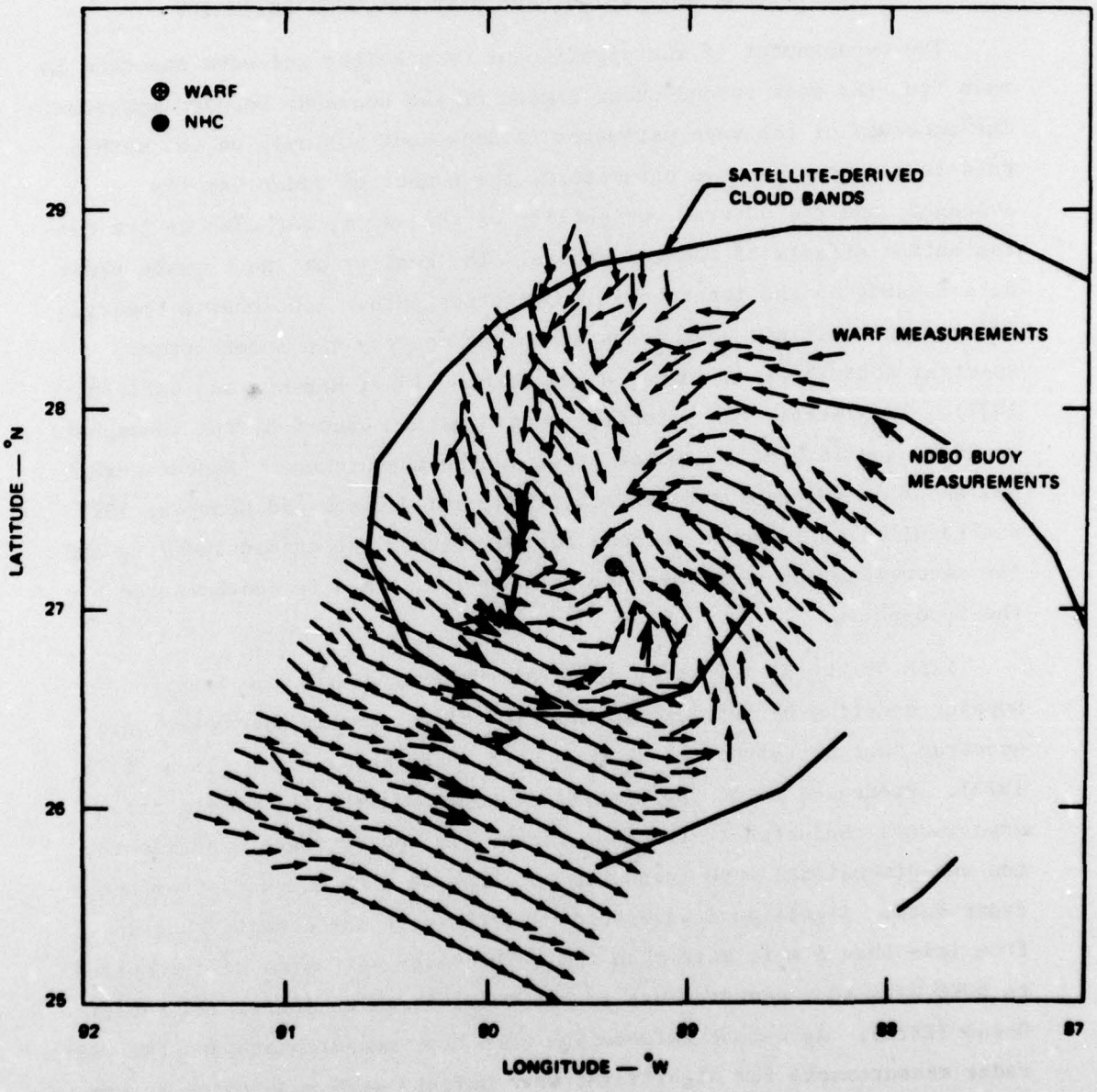


FIGURE 3 COMPARISON OF WARF-INFERRED SURFACE WIND DIRECTIONS WITH NDBO DATA BUOY WIND DIRECTIONS FOR HURRICANE ELOISE. Agreement is within 10°.

the measurement to coastal regions. The expected accuracy of the surface current estimates is about 10 cm/s.

## V SIGNIFICANT WAVE HEIGHT AND WAVE SPECTRUM ESTIMATES

The measurement of the significant wave height and wave spectrum is made from the weak second-order region of the sea-echo Doppler spectrum. The accuracy of the wave estimates is dependent not only on the method used to compute the wave parameters, the number of radar samples averaged, and the natural variability of the waves, but also on the contamination effects of the ionosphere. The quality of the skywave radar data depends on the ionospheric propagation path. Ionospheric smearing effects and multiple-path propagation can destroy the second-order spectral contributions (Maresca and Barnum, 1977; Maresca and Carlson, 1977). In general, the potential contamination caused by the ionosphere would be the largest source of error in the measurement. Recent work by SRI and NOAA (Georges and Maresca, 1978; and Maresca and Georges, 1978) has resulted in improved methods for collecting uncontaminated data and for recovering the wave spectra, even when the data is contaminated by the ionosphere.

Each of the HF inversion formulas summarized from the measured Doppler spectrum by Barrick and Lipa (1978) to compute the ocean wave spectrum must be tested for skywave data (Barrick, 1977a,b; Lipa, 1977, 1978). Presented below are results of three wave-height verification experiments conducted at the WARF radar. In one of these experiments, the one-dimensional wave frequency spectrum is also computed from the radar data. Significant wave heights during the experiments ranged from less than 1 m to more than 5 m. The radar estimates were compared to NDBO data buoy measurements in the Gulf of Mexico (EB71) and Pacific Ocean (EB20). Agreement between the NDBO buoy measurements and the WARF radar measurements for significant wave heights were within the accuracy of the NDBO buoy measurements.

## VI WAVE SPECTRAL ESTIMATES FROM THE HF DOPPLER SPECTRUM

Barrick (1977a,b) derived the following approximate closed-form expression to compute the one-dimensional wave frequency spectrum, $S(\omega)$, and rms wave height, $h_*$, from the Doppler spectrum:

$$S(\omega_B|\nu-1|) = \frac{4\sigma_2(\omega_B\nu)/W(\nu)}{k_o^2 \int_0^{\infty} \sigma_1(\omega_B\nu)\,d(\omega_B\nu)} \qquad (1)$$

and

$$h_*^2 = \frac{2 \int_{-\infty}^{\infty} [\sigma_2(\omega_B\nu)/W(\nu)]\,d(\omega_B\nu)}{k_o^2 \int_{-\infty}^{\infty} \sigma_1(\omega_B\nu)\,d(\omega_B\nu)} \qquad (2)$$

where $\omega = (\omega_B|\nu-1|)$ is the radian ocean wave frequency; $\omega_B$ is the radian Bragg frequency; $\omega_D$ is the radian Doppler frequency; $\nu = \omega_D/\omega_B$; $\sigma_1(\omega_B\nu)$ and $\sigma_2(\omega_B\nu)$ are the first- and second-order power contribution to the Doppler spectrum expressed as radar cross section per mean surface area per radian per second of bandwidth; $k_o$ is the radian radio wave number; and $W(\nu)$ is a weighting function derived by Barrick (1977a)

The weighted second-order power contribution used in Eq. (1) is obtained by averaging the return from both sides of the stronger first-order echo. The rms wave height is obtained by dividing the total weighted second-order power surrounding both sides of the stronger first-order echo by the total first-order power. If one assumes that the process is Gaussian, the significant wave height, $H_s$ is $4h_*$.

The accuracy of these expressions can be evaluated by inverting theoretical Doppler spectra produced from known input directional wave spectra. The results indicate that Eqs. (1) and (2) tend to over-estimate wave height by a constant amount. Barrick (1977a) has shown that when the ratio of the actual wave height to the radar-measured wave height $h/h_*$, is plotted as a function of the parameter $k_o h_*$, $h/h_*$ is a constant for $k_o h > 0.20$. Maresca and Carlson (1977b) also showed the dependence of $h/h_*$ on radar frequency and wave directionality.

Barrick (1977a) has tested Eq. (2) by using surface wave HF radar data and in situ buoy measurements, and the agreement was found to be within 22%. The rms error is primarily dependent on the accuracy of the method used to compute wave height and the number of independent Doppler spectra averaged before computing the wave height. Each Doppler spectrum of the sea-echo signal in Barrick's test was an average of 9 samples. If the number of samples averaged had been increased, then better estimates of the sea echo would have resulted and the 22% error might have been reduced.

## VII WARF MEASUREMENTS OF SIGNIFICANT WAVE HEIGHT AND THE WAVE SPECTRUM

The results of three WARF wave height verification experiments conducted on 2 June 1977, 23 August 1977, and 1 September 1977 are reported here to demonstrate the accuracy of the skywave radar measurement technique over a range of seas and ionospheric conditions. The radar measurements were recorded in the vicinity of NDBO buoys EB71 ($26^{o}$N, $93.5^{o}$W) in the Gulf of Mexico and EB20 ($41^{o}$N, $138^{o}$W) in the Pacific Ocean. EB71 is located approximately 2900 km from WARF; EB20 is located about 1700 km from WARF. The Doppler spectra were produced from 102.4 s of coherent integration. Eq. (1) was used to compute the ocean wave spectrum, and Eq. (2) was used to compute the rms wave height. The significant wave height was computed by multiplying the rms wave height by 4.0. At least 40 independent samples of the Doppler spectra were averaged. The errors in the spectral estimates are proportional to $1/\sqrt{N}$, where N is the number of samples (Barrick and Snider, 1977). The sampling error based on 40 or more averages for all three experiments is 16% or less. The nominal accuracy of NDBO moored buoys measurement of significant wave height reported by the Data Quality Division of NDBO is ±0.3 m. The WARF measurements of significant wave height made for all three experiments agree to within ±0.3 m of the buoy measurements. The results of some NDBO calibration experiments are described in Steele and Johnson (1978).

A. June 2, 1977 Experiment

The placement of NDBO data buoy EB20 on station in the Pacific Ocean in 1977 provided the first opportunity to compare the WARF-estimates of significant wave height, $H_s$, with an independent in situ measurement. The Doppler spectra were taken on 2 June 1977 to the west of an atmospheric front. The front passed through EB20, travelling to the east. During a period of less than 6 hours, $H_s$ increased from 1.4 m to 3.0 m and remained constant at approximately 3 m for more than 6 hours. The significant wave height measured over a 12-hour period is given in Table 1.

The WARF radar measurement reported here was centered 125 km west of EB20 at 1819Z. Since the wave height and wave spectral measurements at EB20 remained constant (±0.1 m) from 1800 to 2400Z, we expected that the WARF measurement of the significant wave height should be about 3.0 m. We compared the WARF radar estimates of significant height computed from Eq. (2) and the one-dimensional wave frequency spectrum computed from Eq. (1) to those measurements made at EB20. The WARF estimate of $H_s$ is 3.0 m; the WARF measured wave spectrum is shown in Figure 4. We compared these estimates to those made at EB20 at 2100Z because the WARF measurement was located west of the buoy where the seas were probably slightly larger. However, the difference in the EB20 wave spectra measurements at 1800Z and 2100Z are negligible, and comparison of the EB20 and WARF measurements any time between 1800Z and 2100Z produces essentially identical results. The agreement between the significant wave heights measured at EB20 and WARF is within the ±0.3 m accuracy of the NDBO moored buoys. Further details of this experiment are available in Maresca and Carlson (1977a) and Maresca and Georges (1978b).

B. August 23, 1977 Experiment

The placement of the NDBO data buoy EB71 on station in 1977 provided the first opportunity to compare WARF estimates of significant wave height in the Gulf of Mexico with an in situ measurement. WARF measurements recorded at 2140Z on 23 August 1977 were centered on EB71. Wave conditions at EB71 remained fairly constant before, during, and after

Table 1

SIGNIFICANT WAVE HEIGHT
MEASURED AT EB20 JUNE 2, 1977

| Time (GMT) | Significant Wave Height (m) |
|---|---|
| 1200 | 1.4 |
| 1500 | 1.8 |
| 1800 | 3.0 |
| 2100 | 3.1 |
| 2400 | 2.9 |

Table 2

SIGNIFICANT WAVE HEIGHT
MEASURED AT EB71 AUGUST 23, 1977

| Time (GMT) | Significant Wave Height (m) |
|---|---|
| 1200 | 0.9 |
| 1500 | 0.9 |
| 1800 | 1.0 |
| 2100 | 0.9 |
| 2400 | 0.8 |

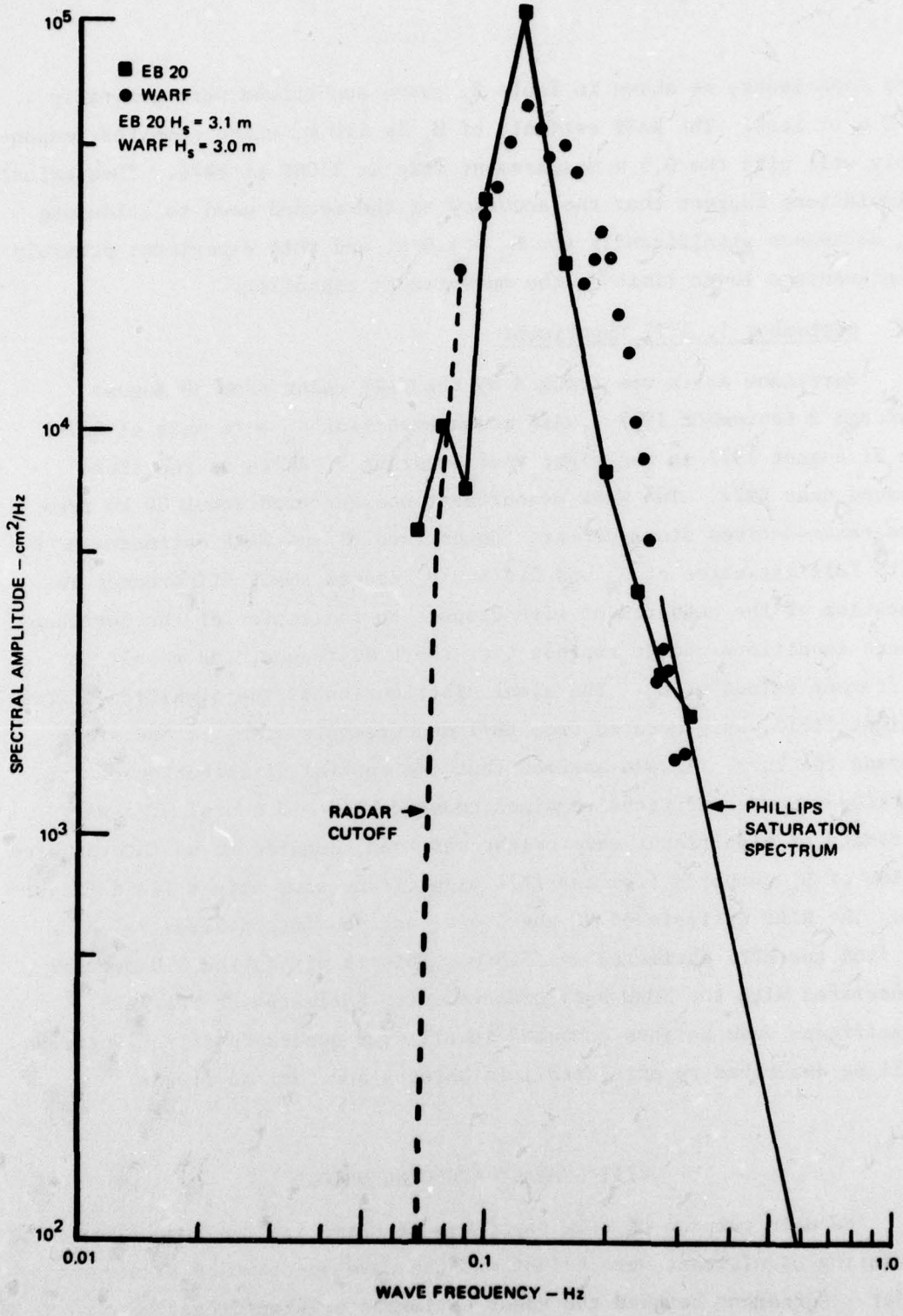


FIGURE 4 COMPARISON OF THE ONE-DIMENSIONAL WAVE FREQUENCY SPECTRUM DERIVED FROM WARF MEASUREMENTS OF THE DOPPLER SPECTRUM WITH THAT OF NDBO DATA BUOY EB20

the experiment, as shown in Table 2. Wave conditions were generally 1.0 m or less. The WARF estimate of $H_s$ is 1.0 m, which compares reasonably well with the 0.9 m measurement made at 2100Z at EB71. Theoretical simulations suggest that the accuracy of the method used to calculate $h_*$ decreases significantly for $H_s < 1.0$ m, and this experiment probably represents a lower limit on the measurement capability.

C. September 1, 1977 Experiment

Hurricane Anita was tracked by the WARF radar from 29 August through 2 September 1977. WARF measurements of $H_s$ were made at 2324Z on 31 August 1977 in the right rear quadrant of Anita as the storm passed near EB71. The WARF measurement was centered about 80 km from the radar-derived storm center. Comparison of the WARF estimates of $H_s$ with EB71 estimates of $H_s$ was difficult because small differences in location of the measurement with respect to the center of the hurricane, where conditions change rapidly over short distances, can result in different values of $H_s$. The areal distribution of the significant wave-height field was generated from EB71 measurements of $H_s$ as the storm passed the buoy. It was assumed that the spatial distribution of the hurricane wave conditions remained constant for ±12 hours. The WARF estimate of significant wave height was then compared to an interpolated value of $H_s$ computed from the EB71 significant wave height field (Figure 5). The WARF estimate of $H_s$ was 5.4 m, and the interpolated value of $H_s$ from the EB71 estimates was 5.5 m. This is within the 0.3 m error associated with the NDBO buoy measurement. Estimates of the WARF significant wave heights computed in all four quadrants of the hurricane will be described in more detail in Maresca and Carlson (1978a).

## VIII SUMMARY AND CONCLUSIONS

The main purpose of this paper was to summarize the capability of measuring significant wave height and the wave spectrum by HF skywave radar. Agreement between the radar estimates of significant wave height and NDBO data buoy measurements was within 10% for a wide range of wave conditions. Similar accuracy was found for the wave spectrum

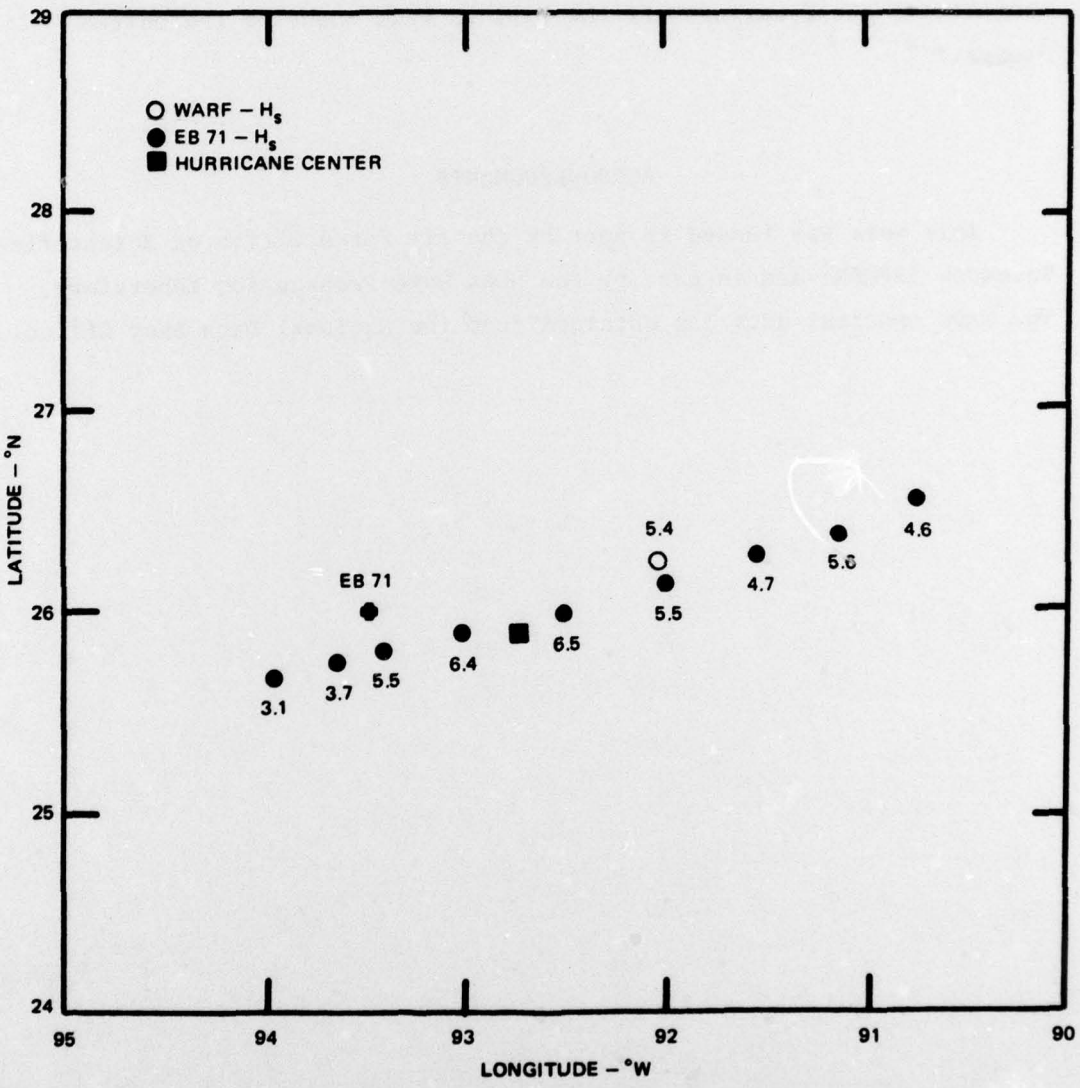


FIGURE 5 COMPARISON OF THE SIGNIFICANT WAVE HEIGHT MEASURED BY THE WARF SKYWAVE RADAR AND NDBO EB71. The EB71 significant wave height estimates were compiled from 24 hours of data and were plotted with respect to the hurricane center.

estimate. The demonstrated capability by skywave radar for continuously tracking and monitoring the surface winds and waves throughout all regions of a hurricane is unique. One skywave radar similar in design to WARF could routinely monitor the incident wave conditions along entire continental shelf regions off the east or west coast of the United States.

## ACKNOWLEDGMENTS

This work was funded in part by the Air Force Office of Scientific Research (AFOSR) and in part by the NOAA Wave Propagation Laboratory. The wave spectral data was obtained from the National Data Buoy Office.

## References


Barnum, J. R.., J. W. Maresca, Jr., and S. M. Serebreny, 1977. High-resolution mapping of oceanic wind fields with skywave radar, IEEE Trans. on Antennas and Propagation, AP-25, 128-132.

Barrick, D. E., 1972a. First-order theory and analysis of MF/HF/VHF scatter from the sea, IEEE Trans. on Antennas and Propagation, AP-20, 2-10.

Barrick, D. E., 1972b. Remote sensing of sea state by radar, in: Remote Sensing of the Troposphere, (ed. V. E. Derr), Chapter 12, U.S. Government Printing Office.

Barrick, D. E., J. M. Headrick, R. W. Bogle, and D. D. Crombie, 1974. Sea backscatter at HF: interpretation and utilization of the echo, Proceedings of the IEEE, 62, 673-680.

Barrick, D. E. and J. B. Snider, 1977. The statistics of HF sea-echo Doppler spectra, IEEE Trans. on Antennas and Propagation, AP-25, 19-28.

Barrick, D. E., M. W. Evans, and B. L. Weber, 1977. Ocean surface currents mapped by radar, Science, 198, 138-144.

Barrick, D. E., 1977a. Extraction of wave parameters from measured HF sea-echo Doppler spectra, Radio Science, 12, 415-424.

Barrick, D. E., 1977b. The ocean waveheight nondirectional spectrum from inversion of the HF sea-echo Doppler spectrum, Remote Sensing of Environment, 6, 201-227.

Barrick, D. E. and B. J. Lipa, 1978. Ocean surface features observed by HF coastal ground-wave radars: a progress review, Ocean Wave Climate, (eds. M. D. Earle and A. Malahoff), Plenum Publishing Company, New York.

Georges, T. M. and J. W. Maresca, Jr., 1978. The effect of radar beam-width on the quality of sea-echo Doppler spectra measured with HF skywave radar, in preparation.

Lipa, B. J., 1977. Derivation of directional ocean-wave spectra by integral inversion of second-order radar echoes, Radio Science, 12, 425-434.

Lipa, B. J., 1978. Inversion of second order radar echoes from the sea, J. Geophys. Research, 83, 959-962.

Long, A. E. and D. B. Trizna, 1973. Mapping of North Atlantic winds by HF radar sea backscatter interpretation, IEEE Trans. on Antennas and Propagation, AP-21, 680-685.

Maresca, J. W. Jr., J. R. Barnum, and K. L. Ford, 1976. HF skywave radar measurements of coastal and open ocean surface currents (Abstract), 1976 Annual Meeting of USNC/URSI University of Massachusetts, Amherst, Massachusetts, October 11-15, 1976.

Maresca, J. W. Jr. and J. R. Barnum, 1977. Measurement of oceanic wind speed from HF sea scatter by skywave radar, IEEE Trans. on Antennas and Propagation, AP-25, 132-136.

Maresca, J. W. Jr. and C. T. Carlson, 1977a. Remote measurement of the ocean wave frequency spectrum by HF skywave radar (Abstract), 1977 Fall Meeting American Geophysical Union, San Francisco, California, December 5-9, 1977.

Maresca, J. W. Jr. and C. T. Carlson, 1977b. Tracking and monitoring of hurricanes by HF skywave radar over the Gulf of Mexico, Technical Report 1, SRI International, Menlo Park, California.

Maresca, J. W. Jr. and J. R. Barnum, 1978. Remote measurements of the position and surface circulation of hurricane Eloise by skywave radar, Monthly Weather Review, in press.

Maresca, J. W. Jr. and C. T. Carlson, 1978a. HF skywave radar measurements of wave height for hurricane Anita, in preparation.

Maresca, J. W. Jr. and C. T. Carlson, 1978b. HF skywave radar track of hurricane Anita, in preparation.

Maresca, J. W. Jr. and T. M. Georges, 1978a. Estimating significant wave height from the HF Doppler spectrum of the sea echo received from two or more ionospheric paths, in preparation.

Maresca, J. W. Jr. and T. M. Georges, 1978b. HF skywave radar measurement of the ocean wave spectrum, in preparation.

Maresca, J. W. Jr. and T. M. Georges, 1978c. Ionospheric diagnostics and sea scatter propagation management, in preparation.

Steele, K. and A. Johnson, Jr., 1978. NDBO wave measurements, Ocean Wave Climate, (eds. M. D. Earle and A. Malahoff), Plenum Publishing Corporation, New York.

Stewart, R. H. and J. R. Barnum, 1975. Radio measurements of oceanic winds at long ranges: an evaluation, Radio Science, 10, 853-857.

Stewart, R. H. and J. W. Joy, 1974. HF radio measurements of surface currents, Deep-Sea Research, 21, 1039-1049.